Three-State Air Quality Modeling Study (3SAQS) -- Weather Research Forecast 2011 Meteorological Model Application/Evaluation

Prepared for:
Tom Moore
Western Regional Air --Partnership
c/o CIRA, Colorado State University
1375 Campus Delivery
Fort Collins, CO 80523-1375

Prepared by:
UNC-Chapel Hill
137 E. Franklin Street
Chapel Hill, NC 27514

ENVIRON International Corporation
773 San Marin Drive, Suite 2115
Novato, CA 94998

19020 33rd Avenue West, Suite 310
Lynnwood, WA 98036

August 4, 2014

UNC INSTITUTE FOR THE ENVIRONMENT

ENVIRON

CONTENTS

TABLES

FIGURES

EXECUTIVE SUMMARY

The Three-State Air Quality Study (3SAQS) is intended to facilitate air resource analyses for federal and state agencies in the states of Wyoming, Colorado, and Utah. The main focus of the study is on assessing the environmental impacts of emission sources in the region especially those related to oil and gas development and production. The 3SAQS is developing a regional photochemical grid model (PGM) modeling platforms for the states of Colorado, Wyoming, and Utah. The PGM modeling platforms will be used to assess the contributions of emissions to ozone, fine particulate matter ($PM_{2.5}$), visibility, sulfur and nitrogen deposition and potentially other air quality and air quality related values (AQRVs). This includes the quantification of the impacts of proposed oil and gas development projects within the 3SAQS region on current and future air quality and AQRVs throughout the region and in particular within National Parks and Wilderness Areas. The 3SAQS is setting up the CAMx and CMAQ PGMs for the 2011 calendar year using grid resolutions of 36, 12 and 4 km. Meteorological data are key inputs for PGM modeling. These data include wind speed and direction, temperature, water vapor concentrations (mixing ratio), sunlight intensity, clouds, precipitation, and vertical mixing. The meteorological inputs for PGM models are generated using prognostic meteorological models that solve the fundamental (primitive) equations of the atmosphere. The 3SAQS used the Weather Research Forecast (WRF Version 3.5.1) Advanced Research WRF (WRF-ARW) for the 2011 calendar year with a 36 km continental U.S. (CONUS), 12 km western U.S. (WESTUS), and 4 km three-state domain that covered the states of Colorado, Wyoming, and Utah and neighboring areas.

The 3SAQS 2011 WRF 36/12/4 km simulation was run in 5-day segments with a half day initialization. The annual WRF simulation used 16 processors per run segment. Each run segment took on average two wall clock days to complete. The 2011 annual WRF simulations were evaluated for surface wind, temperature, mixing ratio observations, and monthly accumulated precipitation from the PRISM analysis fields based on observations. In addition to the standard meteorological metrics for air quality, WRF performance includes targeted episodic evaluation for wintertime ozone episodes.

There were numerous WRF sensitivity simulations performed to help identify an optimal WRF configuration for the annual 2011 simulation. Sensitivity simulations were tested for wintertime (January) and summertime (July) periods. First-order sensitivities from a base configuration were simulated to help select the initial and boundary conditions (IC and BC), land-use land-cover data, land surface model, use of a surface drag parameterization scheme over complex terrain, and use of observation nudging with insight from the ROMANS II study. Evaluation of standard meteorological variables provided insight into the final WRF configuration selected. Most first-order tests revealed consistent bias over the three states with WRF being slightly warmer with an underestimation of wind speed. Specifically, precipitation bias was found to be very sensitive to observational nudging. Nudging too strongly produces too much precipitation without changing the performance vs. independent MESONET data. The precipitation overestimation bias was especially prevalent during the summer months in the intermountain west and was primarily due to overactive convective precipitation. However, the PRISM precipitation analysis fields based on observations are likely less reliable during summer convective precipitation events compared to winter synoptic storm events.

The 2011 WRF model performance for surface winds, temperature and mixing ratios was evaluated across the states of Colorado, Wyoming, and Utah as well as across the 4 km three-state and 12 km WESTUS domains. The WRF model performance statistics were compared against meteorological model

performance benchmarks that have been developed by analyzing meteorological model performance of ~30 "good" performing prognostic model simulations conducted to support air quality modeling. Most of these simulations were for urban ozone modeling of stagnation episodes in fairly flat locations. More recently, new sets of meteorological model performance benchmarks have been developed for more complex conditions (e.g., complex terrain and complex meteorological phenomena) that were also used to help assess WRF model performance.

Quantitative evaluation of surface winds, temperature, and water mixing ratio showed that WRF's representation of these fields in the 4 km simulation is generally very good. The monthly bias and error statistics rarely exceeded the model performance benchmarks when the fields were evaluated on a domain-wide and state-by-state basis. This evaluation revealed a number of minor biases in the WRF simulation that are worth noting. WRF appears to have some difficulty simulating the nighttime temperature inversion commonly observed in regions with mountainous terrain. This leads to too warm temperatures at night in Utah during the winter months and a cool bias during nighttime hours in other areas. It was also found that modeled temperatures are too warm immediately following sunrise in many locations. WRF consistently under-predicts wind speed by approximately 0.5 m/s throughout the entire year across much of the modeling domain. We also observed a distinct seasonal pattern in mixing ratio bias. Mixing ratio is generally over-predicted during the cooler months, peaking during the daytime hours. Conversely, mixing ratio is under-predicted across much of the 4 km domain during the warmer months.

The 3SAQS evaluation for the 4 km three-state and 12 km WESTUS domains also including precipitation. In general the WRF did a very good job in reproducing the spatial distribution and magnitudes of the PRISM monthly precipitation analysis fields during the winter, early spring and late fall. However, during the summer monsoon conditions, the WRF monthly precipitations exhibited more differences with the PRISM analysis fields with WRF estimating higher and more wide-spread convective precipitation events in the summer than indicated by PRISM analysis fields. This is likely due in part to the difficulty in capturing spotty transitional localized precipitation from convective cells in the precipitation observational network and son that they won't be fully represented in the PRISM analysis fields.

The WRF 2011 36/12/4 km simulation was also evaluated for winter ozone event periods using routine and special field study data from the Upper Green River Winter Ozone Study (UGRWOS). Although the initial 2011 WRF simulation was not configured to simulate meteorological conditions associated with winter ozone events (e.g., cold pooling), the evaluation for the winter high ozone periods will help setup a more focused winter ozone modeling analysis planned for later stages in the 3SAQS. WRF did reproduce the slow wind speeds, temperature inversions and dry conditions associated with winter ozone events, but exhibited high wind speed and direction error.

We conclude that the 3SAQS 2011 WRF application exhibited reasonably good model performance that was as good or better than other recent prognostic model applications used in air quality planning and it was therefore reasonable to proceed with their use as inputs for the 3SAQS regional photochemical grid modeling. We recommend that additional WRF sensitivity simulations with alternative options be evaluated before the WRF results are used to simulate winter ozone exceedance episodes.

1.0 INTRODUCTION

The University of North Carolina (UNC) at Chapel Hill and ENVIRON International Corporation (ENVIRON) are performing the Three State Air Quality Modeling Study (3SAQS). The 3SAQS includes cooperators from U.S. Environmental Protection Agency (EPA), United States Forest Service (USFS), Bureau of Land Management (BLM), National Park service (NPS), Fish and Wildlife Service (FWS), Region 8 of the U.S. Environmental Protection Agency (EPA) and the state air quality management agencies of Colorado, Utah, and Wyoming. The 3SAQS is intended to facilitate air resource analyses for federal and state agencies in the states of Wyoming, Colorado, and Utah. Funded by the Environmental Protection Agency (EPA), Bureau of Land Management (BLM), and the U.S. Forest Service (USFS) and with in-kind support from the National Park Service (NPS) and Colorado, Utah, and Wyoming state air agencies, the main focus of the study is on assessing the air quality impacts of emissions within the three-state region with particular emphasis on sources related to oil and gas development and production. To quantify the impacts of proposed oil and gas development projects on current and future air quality, including ozone visibility levels in the National Parks and Wilderness areas, a regional air quality modeling platform is being developed for photochemical grid models (PGMs) and the 2011 calendar year. An important component of the 2011 PGM modeling platform is the meteorological inputs, whose development and evaluation are described in this document.

1.1 Meteorological Modeling

Over the past decade, emergent requirements for numerical simulation of urban and regional scale air quality have led to intensified efforts to construct high-resolution emissions, meteorological and air quality data sets. The concomitant increase in computational throughput of low-cost modern scientific workstations has ushered in a new era of regional air quality modeling. It is now possible, for example, to exercise sophisticated mesoscale prognostic meteorological models and Eulerian and Lagrangian photochemical/aerosol models for multi-seasonal periods over near-continental scale domains in a matter of weeks with the application tailored to a specific air quality modeling project.

The tool used for this meteorological modeling study is the Weather Research and Forecasting (WRF) model[1][2], more specifically, the Advanced Research WRF dynamic core (WRF-ARW, henceforth simply called WRF). WRF is a next-generation mesoscale numerical weather prediction system designed to serve both operational forecasting and atmospheric research needs[3][4][5]. WRF contains separate modules to compute different physical processes such as surface energy budgets and soil interactions, turbulence, cloud microphysics, and atmospheric radiation. Within WRF, the user has many options for selecting the different schemes for each type of physical process. There is a WRF Preprocessing System

[1] Skamarock, W.C., J.B. Klemp, J. Dudhia, D.O. Gill, M. Barker, M.G. Duda, X.-Y. Huang, W. Wang, and J.G. Powers, 2008: A description of the Advanced Research WRF version 3. NCAR Technical Note NCAR/TN475+STR
[2] http://www.wrf-model.org/index.php
[3] Skamarock, W. C. 2004. Evaluating Mesoscale NWP Models Using Kinetic Energy Spectra. *Mon. Wea. Rev*., Volume 132, pp. 3019-3032. December. (http://www.mmm.ucar.edu/individual/skamarock/spectra_mwr_2004.pdf)
[4] Skamarock, W. C., J. B. Klemp, J. Dudhia, D. O. Gill, D. M. Barker, W. Wang and J. G. Powers. 2005. A Description of the Advanced Research WRF Version 2. National Center for Atmospheric Research (NCAR), Boulder, CO. June. (http://www.mmm.ucar.edu/wrf/users/docs/arw_v2.pdf)
[5] Skamarock, W. C. 2006. Positive-Definite and Monotonic Limiters for Unrestricted-Time-Step Transport Schemes. Mon. Wea. Rev., Volume 134, pp. 2241-2242. June. (http://www.mmm.ucar.edu/individual/skamarock/advect3d_mwr.pdf)

(WPS) that generates the initial and boundary conditions used by WRF, based on topographic datasets, land use information, and larger-scale atmospheric and oceanic models.

This report describes an application and performance evaluation of WRF for an atmospheric simulation for calendar year 2011 over a modeling domain that covers the continental United States at 36 km grid spacing (CONUS), the Western and Midwestern United States at 12 km grid spacing (WESTUS domain) and the three state domain 4 km resolution (3SD).

1.2 3SAQS WRF Meteorological Modeling

The 3SAQS study performed numerous first-order (one option removed from base configuration) WRF meteorological modeling simulations for the 36/12/4 km domains. These simulations were performed for only the first week of January and July of 2011 to help determine the best choice for input datasets and physics options for temperature, mixing ratio, and wind speed/direction performance. The preliminary model performance of input datasets included choice of Initial Condition and Boundary Condition (ICBC) from the North American Model (NAM) and ECMWF Interim Reanalysis Data (ERA-Interim) and land-use land-cover data from the 2006 National Land Cover Database (NLCD[6]) and US Geological Survey (USGS[7]). Evaluation revealed better overall performance for standard near surface meteorological fields using NAM ICBC and USGS land cover data. In particular, the newer NLCD land cover data requires additional attention when considering look-up values found in METGRID.TBL and VEGPARM.TBL. That is, although the NLCD represents a newer land cover data set than USGS, the WRF performance was worse because the parameters associated with the NLDC land cover categories (e.g., surface roughness, albedo, Bowen ratio, etc.) have not been as optimized as the USGS values. An additional test changed the land surface module (LSM) and planetary boundary layer (PBL) options from Noah[8]-YSU[9] (Yonsei University) to PX[10]-ACM2[11] (Pleim/Xiu-Asymetric-Convective Model version 2). Unfortunately, PX-ACM2 crashed for the summer case causing us to revert to Noah-YSU. However, we found Noah-YSU to outperform PX-ACM2 for the wintertime case and have reasonable performance during the summer relative to other recent prognostic model applications used in air quality planning. The above options of Noah-YSU with NAM ICBC and USGS land cover were then run for the entire months of January and July with additional sensitivities performed using observational nudging. Nudging too strong to observations generates too much precipitation in WRF and indicates careful attention is needed with observational nudging, especially over complex terrain. The best performing WRF configuration from the sensitivity simulations is presented in Chapter 2 (see Table 2-1) and was used for the annual WRF 2011 36/12/4 km simulation.

[6] Fry, J., Xian, G., Jin, S., Dewitz, J., Homer, C., Yang, L., Barnes, C., Herold, N., and Wickham, J., 2011, Completion of the 2006 National Land Cover Database for the Conterminous United States, *PE&RS*, Vol. 77(9):858-864

[7] Pielke, R.A., T.J. Lee, J.H. Copeland, J.L. Eastman, C.L. Ziegler, and C.A. Finley, 1997, Use of USGS-provided data to improve weather and climate simulations, *Ecol. Appl*., 7(1), 3-21.

[8] Chen, F., K. and J. Dudhia, 2001, Coupling an advanced land surface hydrology model with the Penn State-NCAR MM5 modeling system, Part I: Model implementation and sensitivity, *Mon. Weather Rev*., 12, 569-585.

[9] Hong, S.-Y, Y. Noh, and J. Dudhia, 2006, A new vertical diffusion package with explicit treatment of entrainment processes. Mon. Wea. Rev., 134, 2318-2341

[10] Gilliam, R. and J.E. Pleim, 2010, Performance Assessment of New Land-Surface and Planetary Boundary Layer Physics in the WRF-ARW. Journal of App. Meteor. And Climatol. 49 (4), 760-774.

[11] Pleim, J.E., 2007, A combined local and nonlocal closure model for the atmospheric boundary layer. Part I: Model description and testing. *J. Appl. Meteor. Climatol*., 46, 1383-1395.

2.0 METHODOLOGY

The methodology used in the 2011 WRF application for the 3SAQS was to apply the WRF model for the 2011 annual period using our assessment of the best physics options for the region and then evaluate the WRF results (e.g., wind speeds, wind directions, temperatures, and precipitation) with available meteorological observations.

2.1 WRF Model Inputs

A brief summary of the WRF input data preparation procedure used for this annual modeling exercise is provided below.

Model Selection: The publicly available version of WRF (version 3.5.1) was used in the modeling study. The WPS preprocessor programs including GEOGRID, UNGRIB, and METGRID were used to develop model inputs.

Horizontal Domain Definition: The WRF 36/12/4 km domains are defined with at least a 5 grid cell buffer in all directions from the CAMx/CMAQ air quality modeling domains to minimize any potential numeric noise along WRF domain boundaries affecting the air quality model meteorological inputs. Such numeric noise can occur near the boundaries of the WRF domain solution as the boundary conditions come into balance with the WRF numerical algorithms. The WRF horizontal domains are presented in Figure 2-1. The grid projection was Lambert Conformal with a pole of projection of 40 degrees North, -97 degrees East and standard parallels of 33 and 45 degrees.

Vertical Domain Definition: The WRF modeling was based on 37 vertical layers with an approximately 12 meter deep surface layer. The vertical domain is presented in both sigma and approximate height coordinates in Table 2-2.

Topographic Inputs: Topographic information for the WRF was developed using the standard WRF terrain databases. The 36 km CONUS domain was based on the 10 min. (18 km) global data. The 12 km WESTUS domain was based on the 2 min. (~4 km) data. The 4 km 3SD was based on the 30 sec. (~900 m) data

Vegetation Type and Land Use Inputs: Vegetation type and land use information was developed using the most recently released WRF databases provided with the WRF distribution. Standard WRF surface characteristics corresponding to each land use category were employed.

Atmospheric Data Inputs: The first guess fields were taken from the 12 km (Grid #218) North American Model (NAM) archives available from the National Climatic Data Center (NCDC) NOMADS server.

Time Integration: Third-order Runge-Kutta integration was used with a fixed time step of 90 seconds for 36 km CONUS domain, 30 seconds for 12 km WESTUS domain, and 10 seconds for the 4 km 3SD.

Diffusion Options: Horizontal Smagorinsky first-order closure with sixth-order numerical diffusion and suppressed up-gradient diffusion was used.

Lateral Boundary Conditions: Lateral boundary conditions were specified from the initialization dataset on the 36 km CONUS domain with continuous updates nested from the 36 km domain to the 12 km 3SD domain and continuous updates nested from the 12 km domain to the 4 km 3SD.

Top and Bottom Boundary Conditions: The top boundary condition was selected as an implicit Rayleigh dampening for the vertical velocity. Consistent with the model application for non-idealized cases, the bottom boundary condition was selected as physical, not free-slip.

Water Temperature Inputs: The water temperature data were taken from the NCEP RTG global one-twelfth degree analysis[12].

FDDA Data Assimilation: The WRF model was run with a combination of analysis and observation nudging (i.e., Four Dimensional Data assimilation [FDDA]). Analysis nudging was used on the 36-km and 12-km domain. For winds and temperature, analysis nudging coefficients of $5x10^{-4}$ and $3.0x10^{-4}$ were used on the 36-km and 12-km domains, respectively. For mixing ratio, an analysis nudging coefficient of $1.0x10^{-5}$ was used for both the 36-km and 12-km domains. The nudging used both surface and aloft nudging with nudging for temperature and mixing ratio not performed in the lower atmosphere (i.e., within the boundary layer). Observation nudging for winds and temperature was performed on the 4 km grid domain using the Meteorological Assimilation Data Ingest System (MADIS)[13] observation archive. The MADIS archive includes the National Climatic Data Center (NCDC)[14] observations and the National Data Buoy Center (NDBC) Coastal-Marine Automated Network C-MAN[15] stations. The observational nudging coefficients for winds and temperatures were $1.2x10^{-3}$ and $6.0x10^{-4}$, respectively and the radius of influence was set to 60-km.

Physics Options: The WRF model contains many different physics options. The physics options chosen for this application are presented in Table 2-1. These physics options were selected after performing several WRF sensitivity tests for portions of January and July 2011 and selecting the best performing configuration.

Application Methodology: The WRF model was executed in 5-day blocks initialized at 12Z every 5 days with a 90 second integration time step. Model results were output every 60 minutes and output files were split at 24 hour intervals. Twelve (12) hours of spin-up was included in each 5-day block before the data were used in the subsequent evaluation. The model was run at the 36 km, 12 km and 4 km grid resolution from December 16, 2010 through January 1, 2012 using two-way grid nesting with no feedback (i.e., the meteorological conditions are allowed to propagate from the coarser grid to the finer grid but not vice versa).

2.2 Evaluation Approach

The model evaluation approach was based on a combination of qualitative and quantitative analyses. The quantitative analysis was divided into monthly summaries of 2-m temperature, 2-m mixing ratio, and 10-m wind speed using the boreal seasons to help generalize the model bias and error relative to a

[12] Real-time, global, sea surface temperature (RTG-SST) analysis. http://polar.ncep.noaa.gov/sst/oper/Welcome.html
[13] Meteorological Assimilation Data Ingest System. http://madis.noaa.gov/
[14] National Climatic Data Center. http://lwf.ncdc.noaa.gov/oa/ncdc.html
[15] National Data Buoy Center. http://www.ndbc.noaa.gov/cman.php

set of standard model performance benchmarks. The evaluation focused on the 4 km three-state domain and the states of Colorado, Wyoming, and Utah and supplemented with select diurnal and time series analyses. The observed database for winds, temperature, and water mixing ratio used in this analysis was the National Oceanic and Atmospheric Administration (NOAA) Earth System Research Laboratory (ESRL) Meteorological Assimilation Data Ingest System (MADIS). The locations of the MADIS monitoring sites within the 4 km three-state modeling domain are shown in Figure 2-2. The qualitative approach was to compare spatial plots of model estimated monthly total precipitation with the monthly PRISM precipitation. An initial analysis of the WRF model performance for winter high ozone event periods was also examined. The WRF performance and focused sensitivity tests for the winter ozone events will be studied in more detail in later phases of the 3SAQS. In general, the evaluation was developed to summarize the meteorological model performance to inform downstream PGM activities with a description of the model errors, including potential physical reasons for these errors.

Table 2-1. Physics options used in the 3SAQS WRF Version 3.5.1 simulation of the 2011 calendar year.

WRF Treatment	Option Selected	Notes
Microphysics	Thompson	A scheme with ice, snow, and graupel processes suitable for high-resolution simulations.
Longwave Radiation	RRTMG	Rapid Radiative Transfer Model for GCMs includes random cloud overlap and improved efficiency over RRTM.
Shortwave Radiation	RRTMG	Same as above, but for shortwave radiation.
Land Surface Model (LSM)	NOAH	Two-layer scheme with vegetation and sub-grid tiling.
Planetary Boundary Layer (PBL) scheme	YSU	Yonsie University (Korea) Asymmetric Convective Model with non-local upward mixing and local downward mixing.
Cumulus parameterization	Kain-Fritsch in the 36 km and 12 km domains. None in the 4 km domain.	4 km can explicitly simulate cumulus convection so parameterization not needed.
Analysis nudging	Nudging applied to winds, temperature and moisture in the 36 km and 12 km domains	Temperature and moisture nudged above PBL only
Observation Nudging	Nudging applied to surface wind and temperature only in the 4 km domain	moisture observation nudging produces excessive rainfall
Initialization Dataset	12 km North American Model (NAM)	

Table 2-2. Vertical layer definition for WRF simulations.

WRF Meteorological Model				
WRF Layer	Sigma	Pressure (mb)	Height (m)	Thickness (m)
37	0.0000	50.00	19260	2055
36	0.0270	75.65	17205	1850
35	0.0600	107.00	15355	1725
34	0.1000	145.00	13630	1701
33	0.1500	192.50	11930	1389
32	0.2000	240.00	10541	1181
31	0.2500	287.50	9360	1032
30	0.3000	335.00	8328	920
29	0.3500	382.50	7408	832
28	0.4000	430.00	6576	760
27	0.4500	477.50	5816	701
26	0.5000	525.00	5115	652
25	0.5500	572.50	4463	609
24	0.6000	620.00	3854	461
23	0.6400	658.00	3393	440
22	0.6800	696.00	2954	421
21	0.7200	734.00	2533	403
20	0.7600	772.00	2130	388
19	0.8000	810.00	1742	373
18	0.8400	848.00	1369	271
17	0.8700	876.50	1098	177
16	0.8900	895.50	921	174
15	0.9100	914.50	747	171
14	0.9300	933.50	577	84
13	0.9400	943.00	492	84
12	0.9500	952.50	409	83
11	0.9600	962.00	326	82
10	0.9700	971.50	243	82
9	0.9800	981.00	162	41
8	0.9850	985.75	121	24
7	0.9880	988.60	97	24
6	0.9910	991.45	72	16
5	0.9930	993.35	56	16
4	0.9950	995.25	40	16
3	0.9970	997.15	24	12
2	0.9985	998.58	12	12
1	1.0000	1000	0	

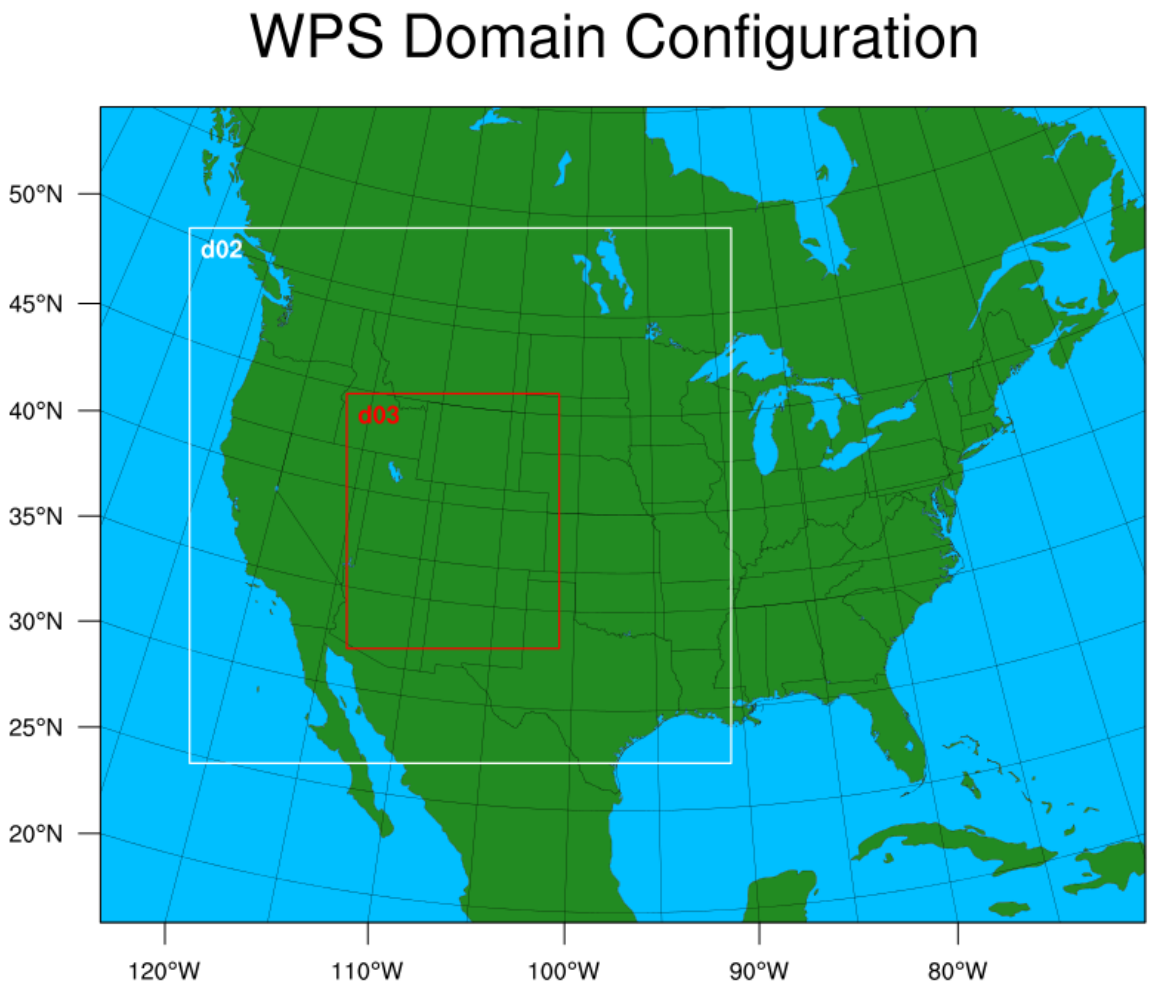

Figure 2-1. 36 km CONUS, 12 km WESTUS (d02), and 4 km 3SAQS (d03) WRF modeling domains.

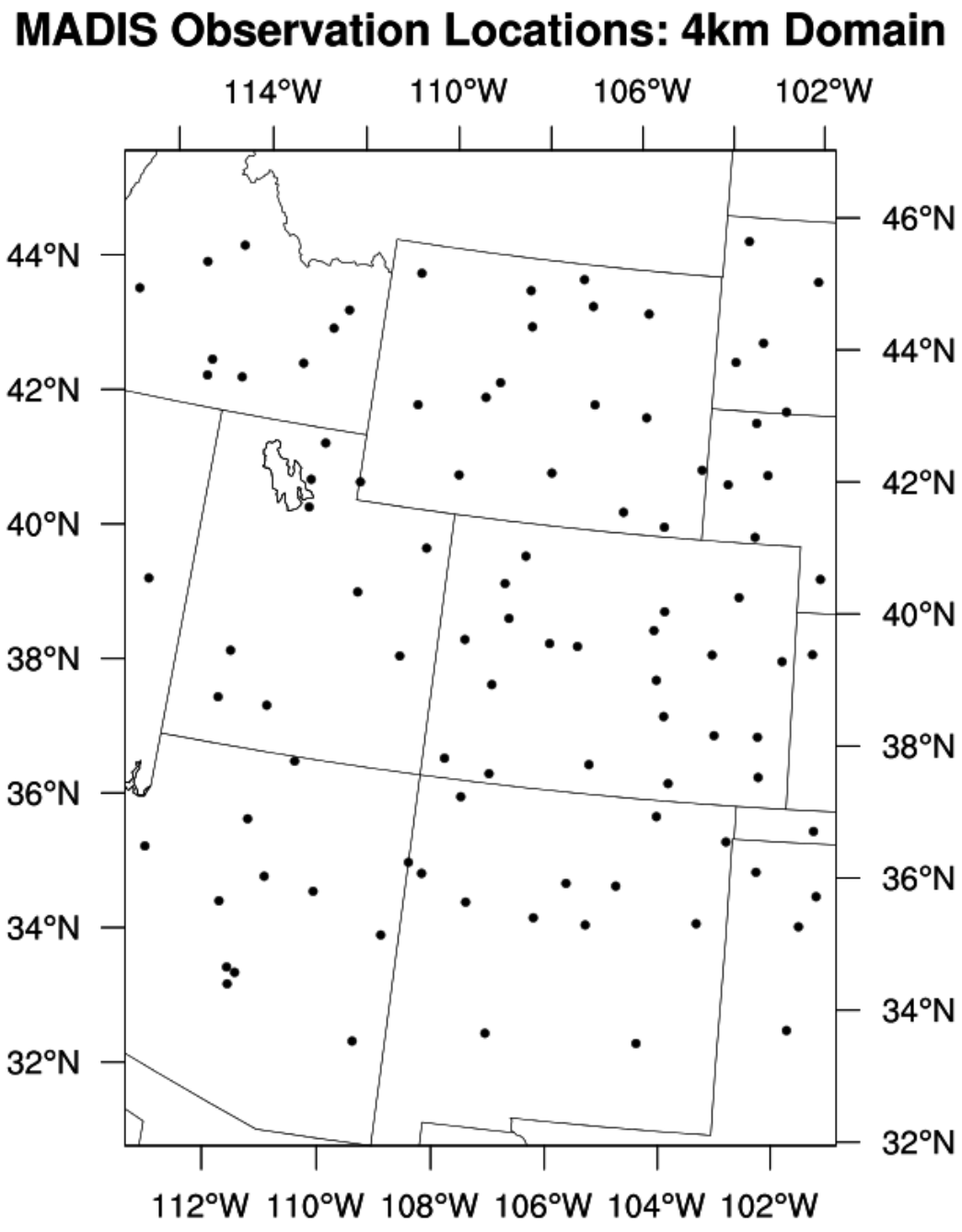

Figure 2-2. Locations of MADIS surface meteorological modeling sites with the WRF 4 km 3SAQS modeling domain.

3.0 WRF SURFACE MODEL PERFORMANCE EVALUATION RESULTS

3.1 Seasonal Quantitative Model Evaluation Results

Statistical model evaluation results are presented in this section. The quantitative model performance evaluation of WRF using surface meteorological measurements was performed using the publicly available AMET evaluation tool. AMET calculates statistical performance metrics for bias, error and correlation for surface winds, temperature and mixing ratio and can produce time series of predicted and observed meteorological variables and performance statistics. A full annual model evaluation is very difficult to summarize in a single document, especially a simulation that could be used for many different purposes. With this in mind, the evaluation only summarizes the meteorological model performance using bias and error model performance statistics metrics with select plots to enhance potential users understanding of model performance. However, we provide an online source so potential data users can independently judge the adequacy of the model simulation. Overall comparisons are offered herein to judge the model efficacy, but this review does not necessarily cover all potential user needs and applications.

To evaluate the performance of the WRF 2011 simulation for the U.S., a number of performance benchmarks for comparison were used. Emery and co-workers[16] derived and proposed a set of daily performance "benchmarks" for typical meteorological model performance for good performing models in air quality model applications. These performance benchmarks were based upon the evaluation of about 30 MM5 and RAMS meteorological simulations of limited duration (multi-day episodes) in support of air quality modeling study applications performed over several years. These were primary ozone model applications for cities in the eastern and Midwestern U.S. and Texas that were primarily simple (flat) terrain and simple (stationary high pressure causing stagnation) meteorological conditions. More recently these benchmarks have been used in annual meteorological modeling studies that include areas with complex terrain and more complicated meteorological conditions; therefore, they must be viewed as being applied as *guidelines* and not *bright-line* numbers. That is, the purpose of these benchmarks is not to give a passing or failing grade to any one particular meteorological model application, but rather to put its results into the proper context of other models and meteorological data sets. Recognizing that these simple conditions benchmarks may not be appropriate for more complex conditions, McNally[17] analyzed multiple annual runs that included complex terrain conditions and suggested an alternative set of benchmarks for temperature, namely a guideline of within ±1.0 K for bias and 3.0 K for error. As part of the Western Regional Air Partnership (WRAP) meteorological modeling of the western United States, including the Rocky Mountain Region as well as the complex conditions in Alaska, Kemball-Cook et al.[18] proposed model performance benchmarks for complex conditions. Based on these reviews, we have adopted "simple" and "complex" model performance benchmarks for surface temperature, mixing ratio

16 Emery, C., E. Tai, and G. Yarwood, 2001. "Enhanced Meteorological Modeling and Performance Evaluation for Two Texas Ozone Episodes." Prepared for the Texas Natural Resource Conservation Commission, prepared by ENVIRON International Corporation, Novato, CA. 31-August.
http://www.tceq.texas.gov/assets/public/implementation/air/am/contracts/reports/mm/EnhancedMetModelingAndPerformanceEvaluation.pdf

17 McNally, D. E., 2009. "12km MM5 Performance Goals." Presentation to the Ad-hoc Meteorology Group. 25-June.
http://www.epa.gov/scram001/adhoc/mcnally2009.pdf

18 Kemball-Cook, S., Y. Jia, C. Emery, and R. Morris, 2005. Alaska MM5 Modeling for the 2002 Annual Period to Support Visibility Modeling. Prepared for the Western Regional Air Partnership, by ENVIRON International Corp., Novato, CA.
http://pah.cert.ucr.edu/aqm/308/docs/alaska/Alaska_MM5_DraftReport_Sept05.pdf

(humidity) wind speed and wind direction bias and error as shown in Table 3-1. The equations for bias and error are given below.

$$\text{Bias} = \frac{1}{N}\sum_{i=1}^{N}\left(P_i - O_i\right)$$

$$\text{Error} = \frac{1}{N}\sum_{i=1}^{N}\left|P_i - O_i\right|$$

Table 3-1. Meteorological model performance benchmarks for simple and complex conditions.

Parameter	Simple	Complex
Temperature Bias	≤ ±0.5 K	≤ ±1.0 K
Temperature Error	≤ 2.0 K	≤ 3.0 K
Humidity Bias	≤ ±0.5 g/kg	≤ ±1.0 g/kg
Humidity Error	≤ 1.0 g/kg	≤ 2.0 g/kg
Wind Speed Bias	≤ ±0.5 m/s	≤ ±1.0 m/s
Wind Speed RMSE	≤ 2.0 m/s	≤ 3.0 m/s
Wind Direction Bias	≤ ±5 degrees	≤ ±10 degrees
Wind Direction Error	≤ 40 degrees	≤ 80 degrees

3.1.1 Winter 2011

Wintertime (December, January, and February) temperature bias and error statistics for the entire 4 km 3SAQS modeling domain and the states of Colorado, Wyoming, and Utah are presented in Table 3-2. WRF's wintertime temperature performance over the 4 km domain as a whole is generally good. There is a slight (0.1-0.3 K) cool bias in the winter months when all stations in the 4 km are aggregated, which is well within the temperature bias benchmark for both simple (≤±0.5 K) and complex (≤±1.0 K) conditions. The cool bias is generally being driven by stations in Colorado, Wyoming, and New Mexico. Utah, on the other hand, exhibits a significant warm bias in the winter months. Utah's warm bias is especially significant in the month of January, with a state-wide bias of +1.3 K, which exceeds the complex bias benchmark of ≤±1.0 K.

The January diurnal time series of temperature bias and error across all stations in the 4 km domain is shown in Figure 3-1. The late night and morning hours, roughly from 0600-1800 UTC, experience a domain-wide warm bias. There is a marked cool bias in the afternoon and evening hours, especially immediately following sunset. Figure 3-2 shows that temperatures are consistently too warm across Utah during nighttime hours, sometimes by as much as 5 K.

This diurnal pattern of temperature bias suggests that WRF may have some difficulty modeling temperature inversions over complex terrain. The inversion could be either too shallow and/or mixing out too quickly in the model, causing temperatures to be too warm at night. Lack of snow cover over Utah during these months may also contribute to the warm bias at night in those areas. Additional analysis is needed to confirm this.

Table 3-2. 2-m temperature monthly bias and mean absolute error (K) over the 4 km domain, Colorado, Wyoming, and Utah for the winter months of December, January, and February 2011. Values in red are beyond defined threshold values.

Bias / MAE (K)	DEC.	JAN.	FEB.
4-km Domain	-0.3 / 1.7	-0.1 / 1.9	-0.3 / 1.9
CO	0.0 / 0.4	-0.1 / 1.0	-0.2 /0.5
WY	-0.9 / 1.9	-0.5 / 2.1	-0.3 / 2.1
UT	0.6 / 1.7	**1.3** / 2.5	0.3 / 1.8

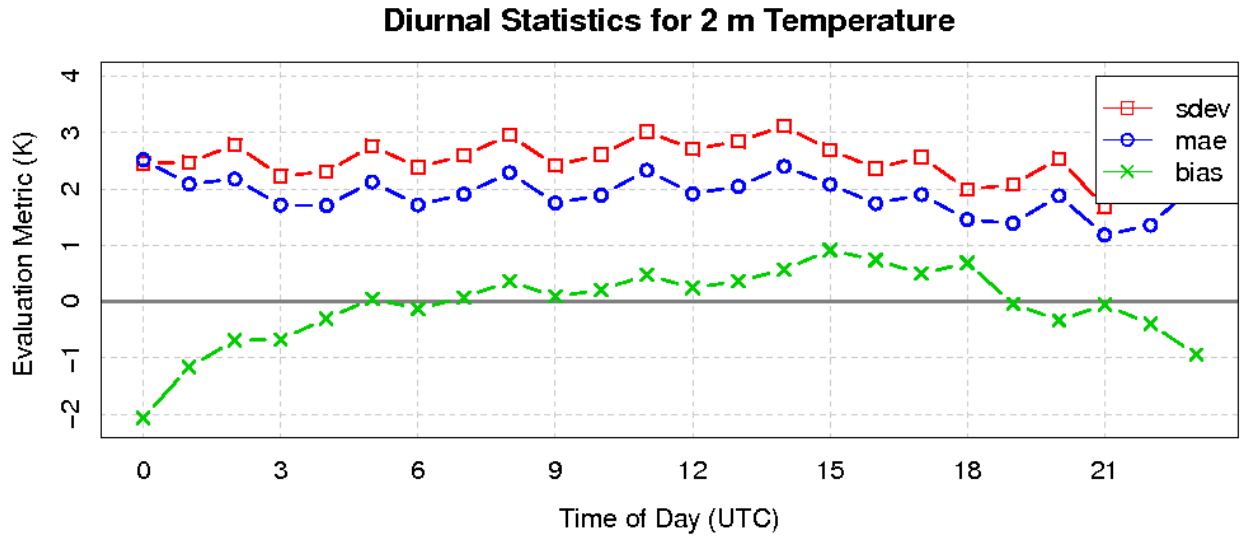

Figure 3-1.Diurnal average temperature time series of standard deviation, mean absolute error, and bias (K) for January 2011 over all stations in the 4 km domain.

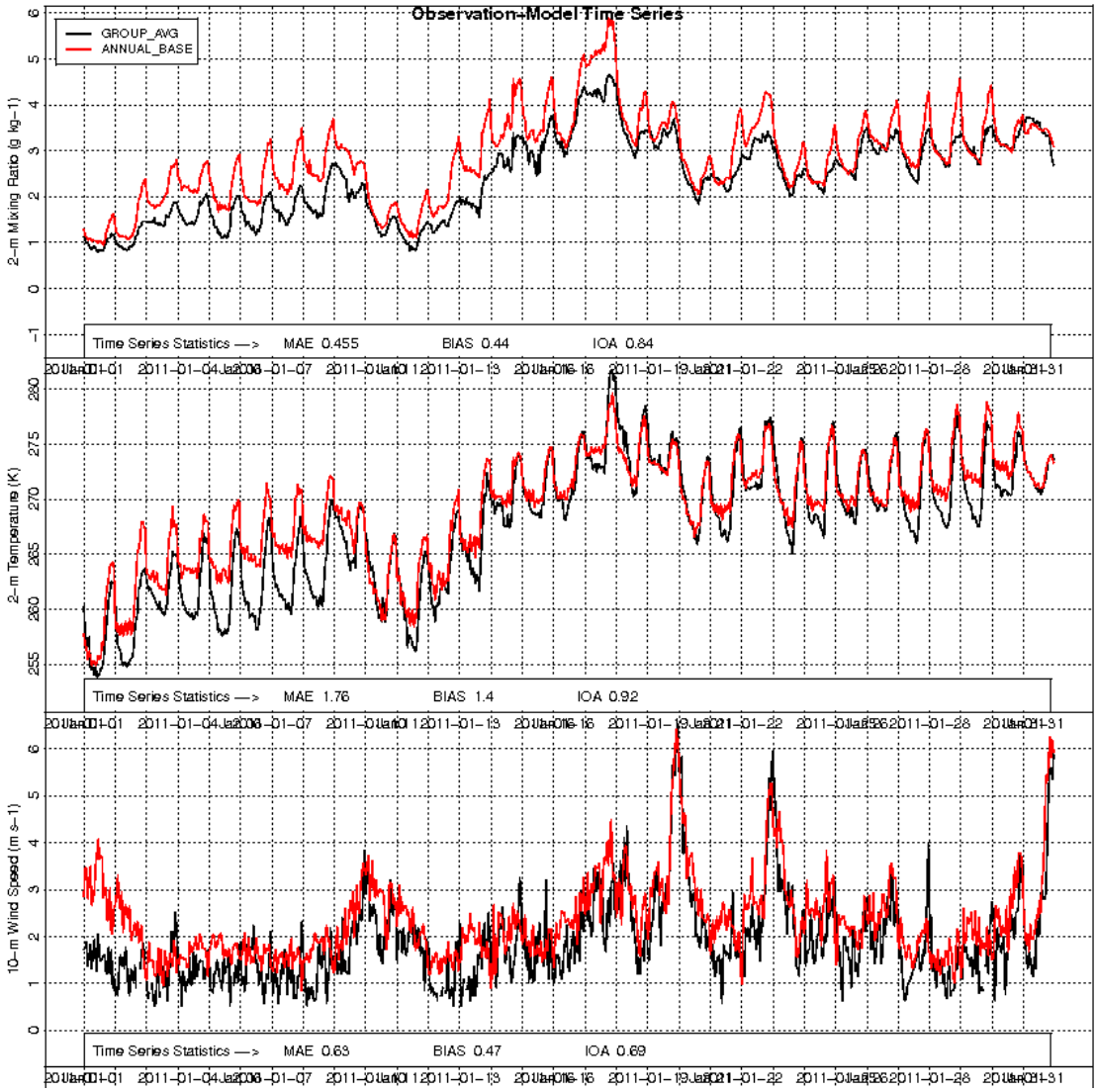

Figure 3-2. January 2011 Utah observation-model time series of mixing ratio (top, kg/kg), temperature (middle, K), and wind speed (bottom, m/s).

Wintertime wind speed bias and error statistics for the entire 4 km modeling domain and the states of Colorado, Wyoming, and Utah are presented in Table 3-3. Winds are roughly 0.5 m/s too slow in WRF averaged across all stations in the 4 km domain. The bias benchmark (≤±0.5 m/s) is slightly exceeded during the months of January and February for the 4 km domain. Colorado and Wyoming show the greatest under-prediction of wind speed in the three-state region. No remarkable temporal patterns could be attributed to the wind speed bias across the domain (Figure 3-2, bottom).

Table 3-3. Wind speed monthly bias and root mean squared error (m/s) over the 4 km domain, Colorado, Wyoming, and Utah for the winter months of December, January, and February 2011. Values in red are beyond defined threshold values.

Bias / RMSE (m/s)	DEC.	JAN.	FEB.
4-km Domain	-0.5 / 1.8	**-0.6** / 1.8	**-0.6** / 2.0
CO	-0.7 / 1.7	-0.5 / 1.6	-0.7 / 2.0
WY	-0.4 / **2.1**	**-0.6** / **2.2**	**-0.6** / **2.2**
UT	-0.2 / 1.8	-0.2 / 1.6	0.0 / 1.9

Wintertime mixing ratio bias and error statistics for the 4 km modeling domain and three states are presented in Table 3-4. WRF consistently has a moist bias across the three states of 0.3 to 0.4 g/kg and the entire 4 km domain, but nowhere does the model over-prediction exceed the bias complex benchmark threshold of ≤±1.0 g/kg. As shown in Figure 3-2, it is worth noting that the mixing ratio bias is much higher during daytime hours across Utah in January 2011. The higher WRF mixing ratio than observed could be due to overstated precipitation, although as shown in Chapter 4 the WRF January 2011 monthly total precipitation appeared to match the PRISM data fairly well during the winter.

Table 3-4. Mixing ratio monthly bias and mean absolute error (kg/kg) over the 4 km domain, Colorado, Wyoming, and Utah for the winter months of December, January, and February 2011.

Bias / MAE (g/kg)	DEC.	JAN.	FEB.
4-km Domain	0.4 / 0.5	0.4 / 0.5	0.4 / 0.6
CO	0.4 / 0.5	0.4 / 0.5	0.4 / 0.6
WY	0.3 / 0.4	0.3 / 0.4	0.4 / 0.5
UT	0.3 / 0.4	0.4 / 0.6	0.3 / 0.5

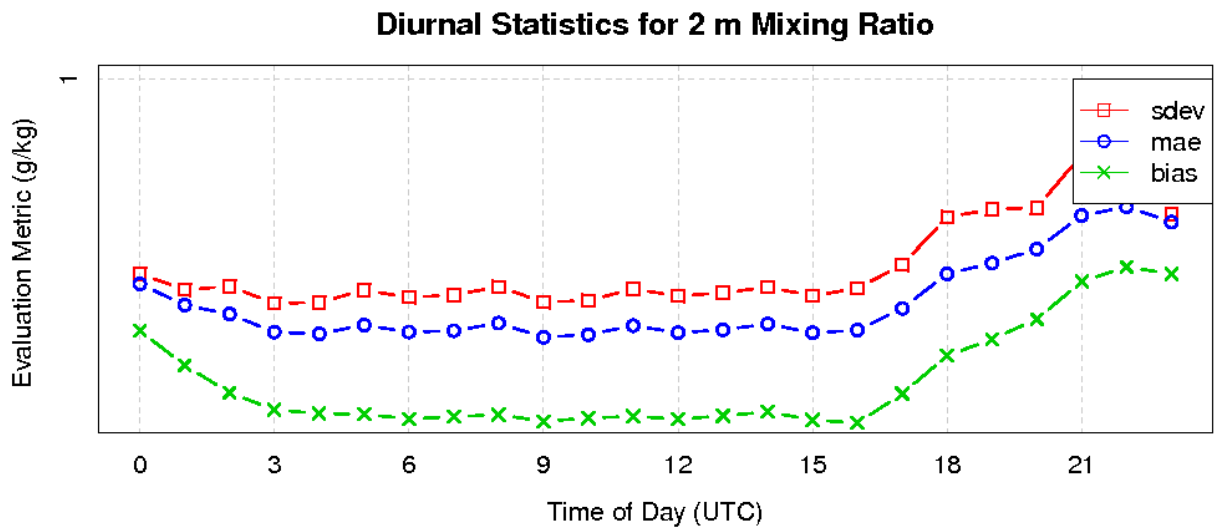

Figure 3-3. Diurnal average mixing ratio time series of standard deviation, mean absolute error, and bias (kg/kg) for January 2011 over all stations in the 4 km domain.

3.1.2 Spring 2011

Springtime (March, April, May) temperature bias and error statistics for the entire 4 km modeling domain and the states of Colorado, Wyoming, and Utah are presented in Table 3-5. WRF has an overall slight cool bias (approximately 0.3 K) across the 4 km domain. Temperature under-prediction is greatest in Wyoming during March, with WRF running approximately 1 K too cool in that state, but the complex bias benchmark (≤±1.0 K) is not exceeded.

A closer look at the diurnal time series of temperature bias across the 4 km domain in April (Figure 3-4) shows that temperatures are under-predicted during nighttime hours, but then show a shift towards over-prediction immediately after sunrise (approximately 1200-1500 UTC). This contributes to the earlier thinking that WRF maybe mixing the nighttime temperature inversion too quickly leading to warmer than observed temperatures immediately following sunrise when the PBL starts the mixing process.

Table 3-5. 2-m temperature monthly bias and mean absolute error (K) over the 4 km domain, Colorado, Wyoming, and Utah for the spring months of March, April, and May 2011.

Bias / MAE (K)	MAR.	APR.	MAY
4-km Domain	-0.3 / 1.7	-0.3 / 1.4	-0.2 / 1.4
CO	-0.1 / 1.8	-0.3 /1.6	-0.4 / 1.5
WY	-1.0 / 1.8	-0.3 / 1.3	0.3 / 1.2
UT	0.0 / 1.4	-0.1 / 1.3	0.1 / 1.4

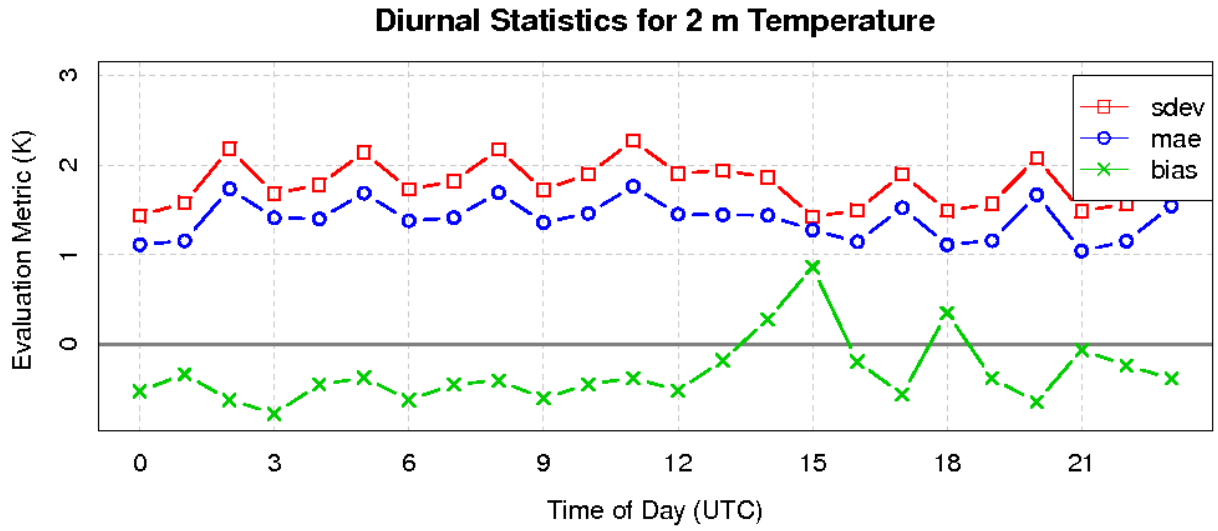

Figure 3-4. Diurnal average temperature time series of standard deviation, mean absolute error, and bias (K) for April 2011 over all stations in the 4 km domain.

Springtime wind speed bias and error statistics for the entire 4 km modeling domain and the states of Colorado, Wyoming, and Utah are presented in Table 3-6. The negative wind speed bias present in WRF during the winter months continued into the spring months and increased in magnitude slightly over the 4 km domain with bias values in the -0.6 to -0.8 m/s occurring in CO and WY that exceeds the bias benchmark (≤±0.5 m/s), although the benchmark is achieved in UT (-0.1 to -0.2 m/s). Wind speeds are under-predicted in WRF by ~0.6 m/s during each month in the March-May period in the 4 km domain, slightly exceeding the benchmark of ≤±0.5 m/s. Similar to the winter months, the wind speed under-prediction is driven by locations in Colorado, Wyoming, and other states outside the three-state focus area.

Table 3-6. Wind speed monthly bias and root mean squared error (m/s) over the 4 km domain, Colorado, Wyoming, and Utah for the spring months of March, April, and May 2011. Values in red are beyond defined threshold values.

Bias / RMSE (m/s)	MAR.	APR.	MAY
4-km Domain	-0.6 / 2.0	-0.6 / 2.1	-0.6 / 2.0
CO	-0.8 / 2.0	-0.8 / 2.2	-0.8 / 2.1
WY	-0.6 / 2.3	-0.7 / 2.2	-0.7 / 2.0
UT	-0.1 / 1.8	-0.2 / 2.0	-0.2 / 1.9

Springtime mixing ratio bias and error statistics for the 4 km modeling domain and three states are presented in Table 3-7. Mixing ratio is again slightly over-predicted in WRF across the 4 km domain. The over-prediction is greatest in the early spring (March) and then tapers off towards late spring (May). The benchmark numbers for mixing ratio bias and error are achieved during this period.

Table 3-7. Mixing ratio monthly bias and mean absolute error (kg/kg) over the 4 km domain, Colorado, Wyoming, and Utah for the spring months of March, April, and May 2011.

Bias / MAE (g/kg)	MAR.	APR.	MAY
4-km Domain	0.3 / 0.6	0.2 / 0.6	0.0 / 0.7
CO	0.4 / 0.7	0.3 / 0.7	0.2 / 0.47
WY	0.5 / 0.6	0.4 / 0.6	0.1 / 0.47
UT	0.2 / 0.6	-0.1 / 0.6	-0.2 / 0.7

3.1.3 Summer 2011

Table 3-8 shows that there is near zero temperature bias during each of the three summer months (June, July, August) when all stations in the 4 km domain are aggregated. However, a closer look at the spatial patterns of temperature bias across the 4 km domain in Figure 3-5 reveals a regional dichotomy in the bias signal across the domain resulting in the "cancelling" effect. WRF slightly under-predicts temperatures (1 K or less) across much of the western and southern areas of the 4 km domain, including the states of Idaho, Utah, New Mexico, Arizona, and southwestern Colorado. On the other hand, WRF slightly over-predicts temperatures (1 K or less) across the northern and eastern portions of the domain, including Wyoming, eastern South Dakota and Nebraska and northeastern Colorado. Similar to the spring months, temperatures are slightly too cool during the overnight hours and then become too warm immediately after sunrise compared to the observations, suggesting an inversion mixing problem in the model. Regardless, WRF does well simulating the large diurnal temperature swings typical to this area of the country.

Table 3-8. 2-m temperature monthly bias and mean absolute error (K) over the 4 km domain, Colorado, Wyoming, and Utah for the summer months of June, July, and August 2011.

Bias / MAE (K)	JUN.	JUL.	AUG.
4-km Domain	-0.1 / 1.5	0.0 / 1.5	0.0 / 1.5
CO	-0.2 / 1.6	0.0 / 1.5	-0.2 / 1.5
WY	0.5 / 1.3	0.4 / 1.3	0.2 / 1.4
UT	-0.1 / 1.4	0.2 / 01.4	0.2 / 1.5

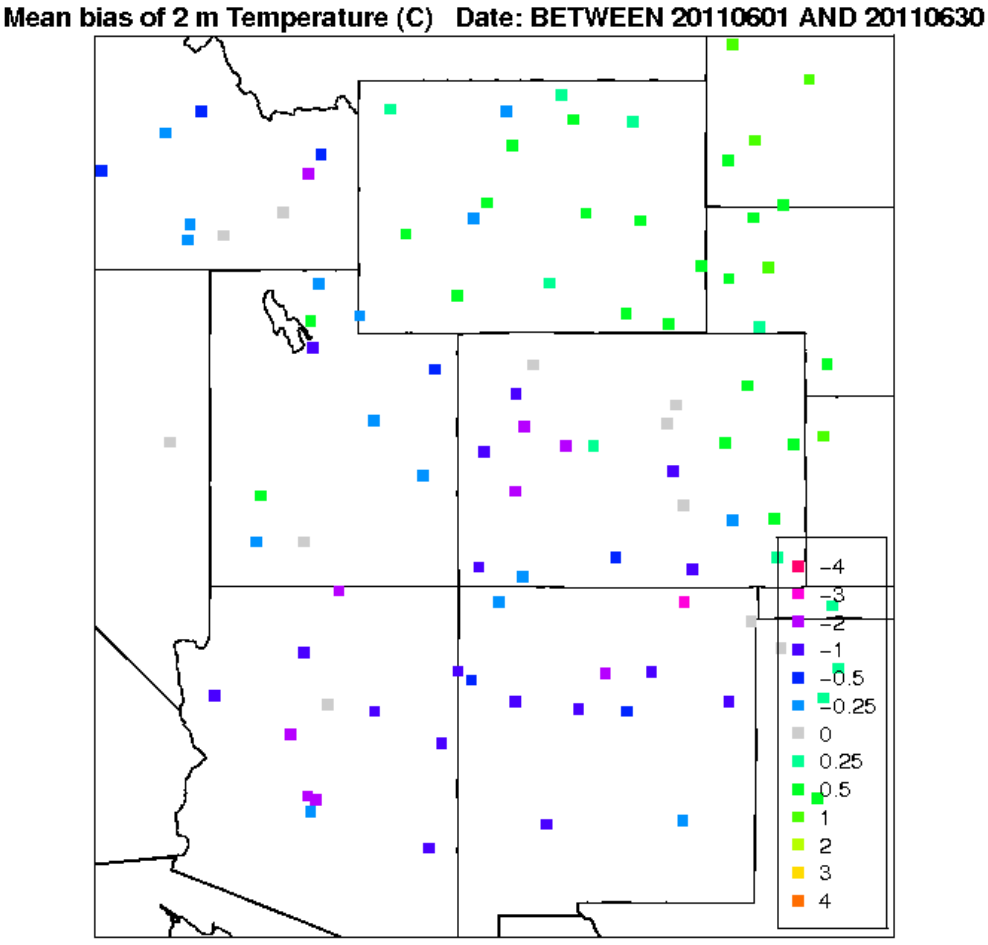

Figure 3-5. Mean bias of 2-m temperature (K) for June 2011 across the 4 km modeling domain.

WRF slightly under-predicts wind speeds across a majority of the 4 km domain, resulting in a -0.4 to -0.5 m/s negative bias over the domain as a whole in the summertime months (Table 3-9). Spatial patterns of wind speed bias across the 4 km domain are similar to other seasons, with a handful of stations in Utah having a small positive bias. The wind speed bias and error benchmark criteria are usually met and WRF's performance in simulating wind speed is generally good.

Table 3-9. Wind speed monthly bias and root mean squared error (m/s) over the 4 km domain, Colorado, Wyoming, and Utah for the summer months of June, July, and August 2011.

Bias / RMSE (m/s)	JUN.	JUL.	AUG.
4-km Domain	-0.5 / 2.0	-0.4 / 1.9	-0.4 / 1.9
CO	**-0.7** / 2.0	**-0.6** / 1.9	-0.5 / 1.9
WY	**-0.7** / **2.1**	-0.4 / 1.9	-0.4 / 1.9
UT	-0.1 / 1.8	-0.1 / 1.8	-0.1 / 1.7

Finally, the mixing ratio bias and error statistics for the summer months are shown in Table 3-10. The under-prediction of mixing ratio across the 4 km domain seen in the late spring months continues into the summer months, with WRF having a negative bias of -0.3 to -0.6 g/kg domain-wide. The under-prediction of mixing ratio in the summer months could be tied to the difficulty in simulating summertime convective precipitation; although misrepresentation of individual synoptic-scale rain events could also be contributing to the overall negative bias (precipitation performance is discussed in Chapter 4). Even with these issues, the mixing ratio performance benchmarks are achieved during the summer months.

Table 3-10. Mixing ratio monthly bias and mean absolute error (kg/kg) over the 4 km domain, Colorado, Wyoming, and Utah for the summer months of June, July, and August 2011.

Bias / MAE (g/kg)	JUN.	JUL.	AUG.
4-km Domain	-0.3 / 1.0	-0.6 / 1.5	-0.5 / 1.4
CO	-0.2 / 1.2	-0.4 / 1.4	-0.2 / 1.3
WY	-0.3 / 1.0	-0.4 / 1.3	-0.1 / 1.1
UT	-0.4 / 0.9	-0.8 / 1.4	-0.8 / 1.4

3.1.4 Fall 2011

The fall months (September, October, November) feature a domain-average 0.2 K warm bias in September transitioning to a domain-average -0.5 K cool bias in the month of November (Table 3-11). The transition from under- to over-prediction in the 4 km domain is driven largely in part by a handful of

stations in Colorado and Wyoming. Utah exhibits a small warm bias throughout the fall months (+0.2 to +0.5 K), mainly due to over-prediction of nighttime temperatures during the cooler months.

Table 3-11. 2-m temperature monthly bias and mean absolute error (K) over the 4 km domain, Colorado, Wyoming, and Utah for the fall months of September, October, and November 2011.

Bias / MAE (K)	SEP.	OCT.	NOV.
4-km Domain	0.2 / 1.4	-0.1 / 1.3	-0.5 / 1.7
CO	0.0 / 1.4	-0.1 / 1.3	-0.6 / 1.9
WY	0.4 / 1.3	-0.1 / 1.3	-1.0 / 2.1
UT	0.4 / 1.5	0.5 / 1.4	0.2 / 1.6

WRF's under-prediction of wind speed across the 4 km domain persists into the fall months, as depicted in Table 3-12. There is a 0.5 m/s negative bias during the months of September and October, and a 0.6 m/s negative bias during November, which slightly exceeds the performance benchmark for wind speed bias. Utah, on the other hand, continues with a slight underestimation of wind speed (-0.2 to -0.3 m/s) that achieves the benchmark.

Table 3-12. Wind speed monthly bias and mean absolute error (m/s) over the 4 km domain, Colorado, Wyoming, and Utah for the fall months of September, October, and November 2011. Values in red are beyond defined threshold values.

Bias / RMSE (m/s)	SEP.	OCT.	NOV.
4-km Domain	-0.5 / 1.6	-0.5 / 1.7	**-0.6** / 1.9
CO	-0.5 / 1.6	-0.5 / 1.6	**-0.7** / 1.9
WY	-0.4 / 1.7	-0.5 / 1.8	**-0.7** / **2.3**
UT	-0.2 / 1.6	-0.2 / 1.5	-0.3 / 1.6

Lastly, mixing ratio and error statistics are presented in Table 3-13. Mixing ratio is under-predicted by approximately -0.3 to -0.4 g/kg across much of the 4 km domain during September and October, but trends towards slight over-prediction in November, especially in the states of Colorado and Wyoming. Mixing ratio remains under-predicted in Utah through all three fall months. Worth noting are the exaggerated spikes in mixing ratio in WRF seen in the Wyoming time series during November 2011 (Figure 3-6).

Table 3-13. Mixing ratio monthly bias and mean absolute error (kg/kg) over the 4 km domain, Colorado, Wyoming, and Utah for the fall months of September, October, and November 2011.

Bias / MAE (g/kg)	SEP.	OCT.	NOV.
4-km Domain	-0.4 / 1.0	-0.3 / 0.7	0.0 / 0.5
CO	-0.3 / 0.9	-0.2 / 0.6	0.1 / 0.5
WY	0.0 / 0.8	-0.1 / 0.5	0.5 / 0.3
UT	-0.5 / 1.0	-0.6 / 0.8	-0.2 / 0.5

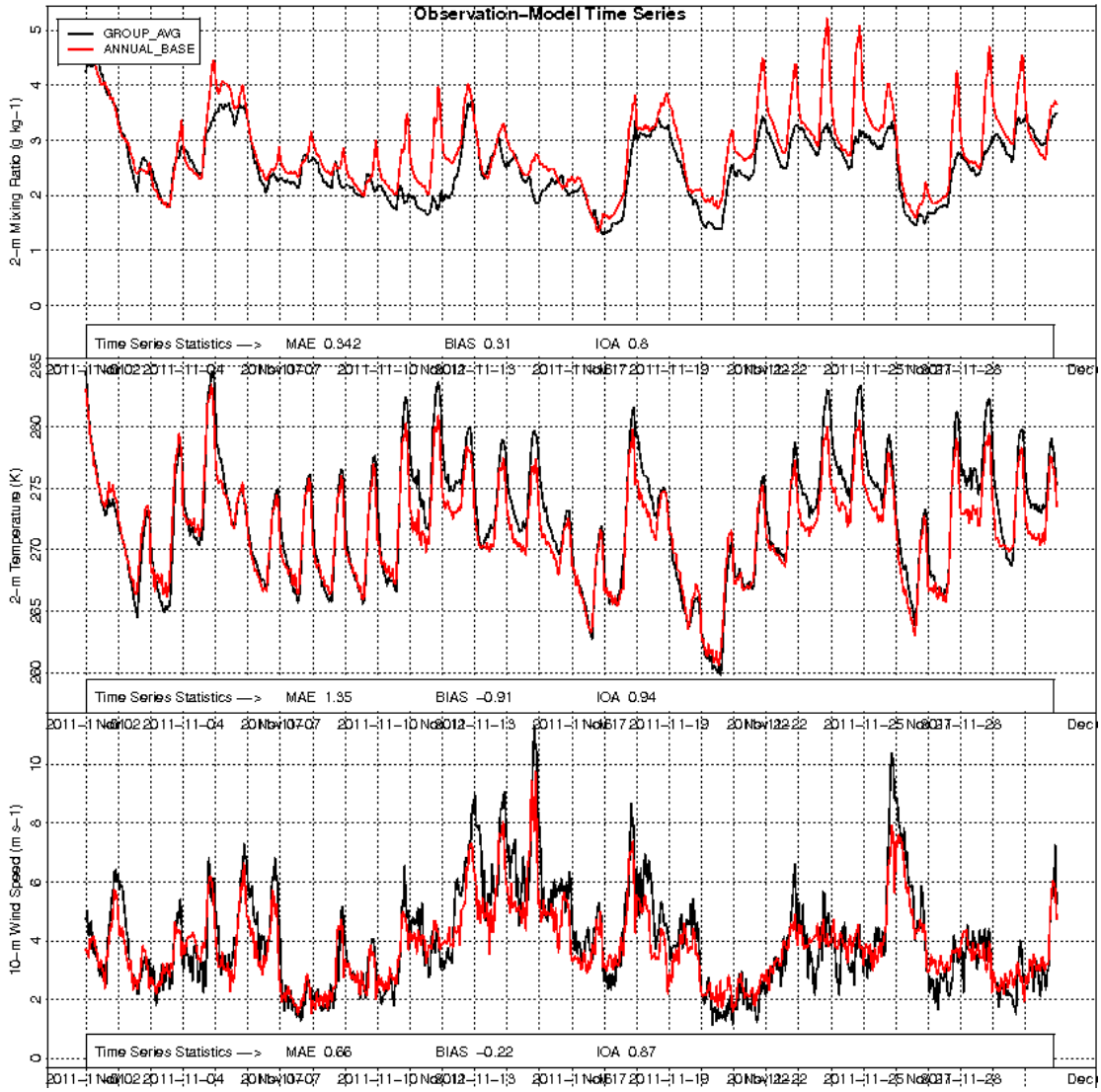

Figure 3-6. November 2011 Wyoming observation-model time series of mixing ratio (top, kg/kg), temperature (middle, K), and wind speed (bottom, m/s).

3.2 Monthly Quantitative Model Performance

The monthly model performance of the 2011 WRF 4 km simulation for surface meteorological variables within the states of Colorado, Utah and Wyoming are analyzed using SoccerPlots. SoccerPlots display monthly bias on the x-axis and error on the y-axis along with the simple and complex benchmarks, when the monthly symbols fall within the box, they achieve the benchmark (score a goal).

3.2.1 Monthly Temperature Performance

Figure 3-7 displays the WRF 4 km monthly temperature soccerplots for the states of Colorado, Utah and Wyoming. In Colorado, all months achieve the complex temperature benchmark and the simple temperature benchmark is achieved for 10 of the 12 months, albeit with a slight cool bias. November and February just barely fail to achieve the simple temperature benchmark in Colorado due to being too cool and too high of an error, respectively.

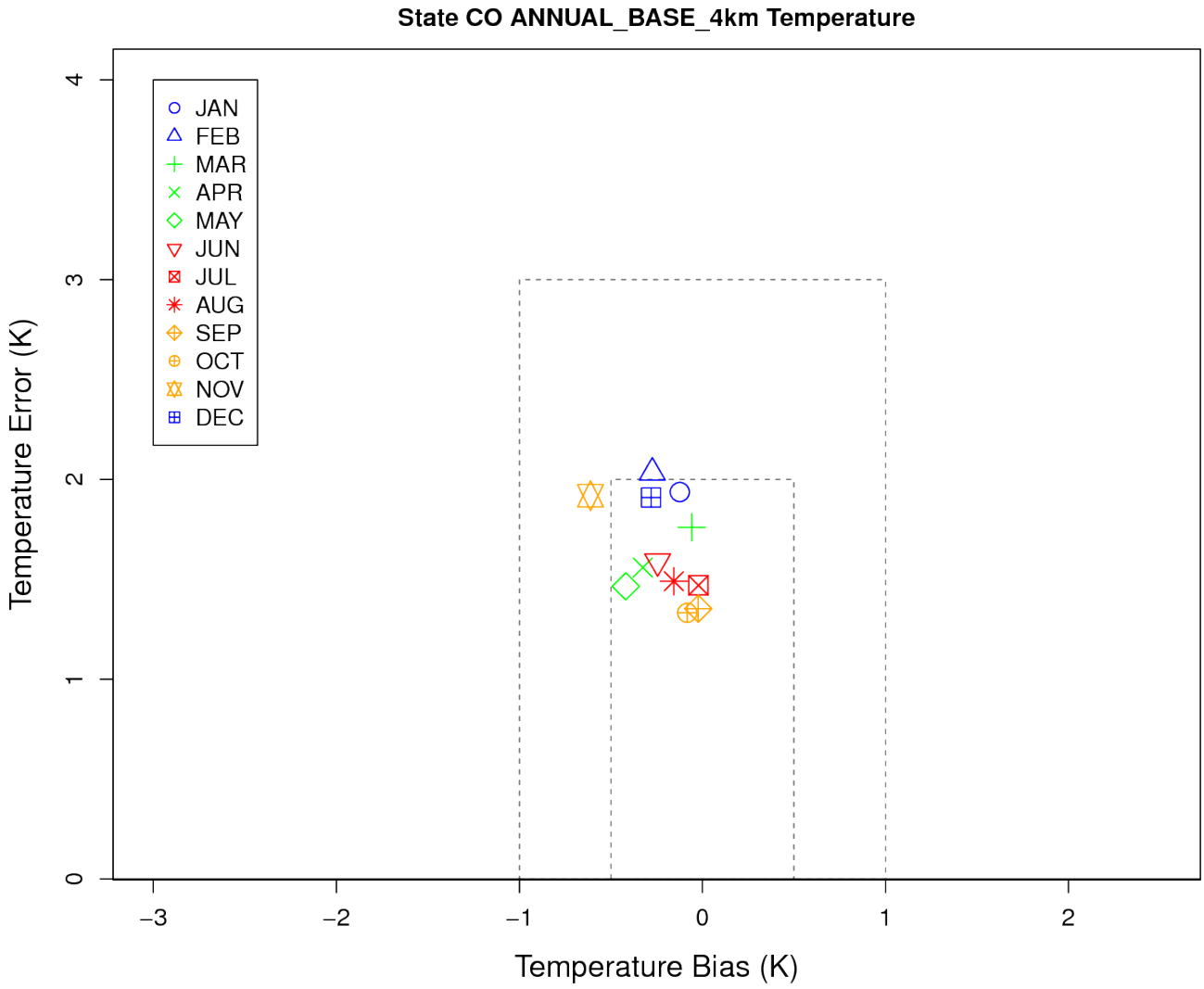

Figure 3-7a. Soccerplot of monthly temperature error and bias (K) for 4km domain over Colorado.

WRF achieves the simple temperature benchmark in Utah for 10 of 12 months with a warm bias. The warm bias is greater for the winter months with December falling just outside the simple but within the complex temperature benchmark and the January temperature bias being so warm (~1.4 K) that it fails to achieve the complex benchmark (≤±2.0 K).

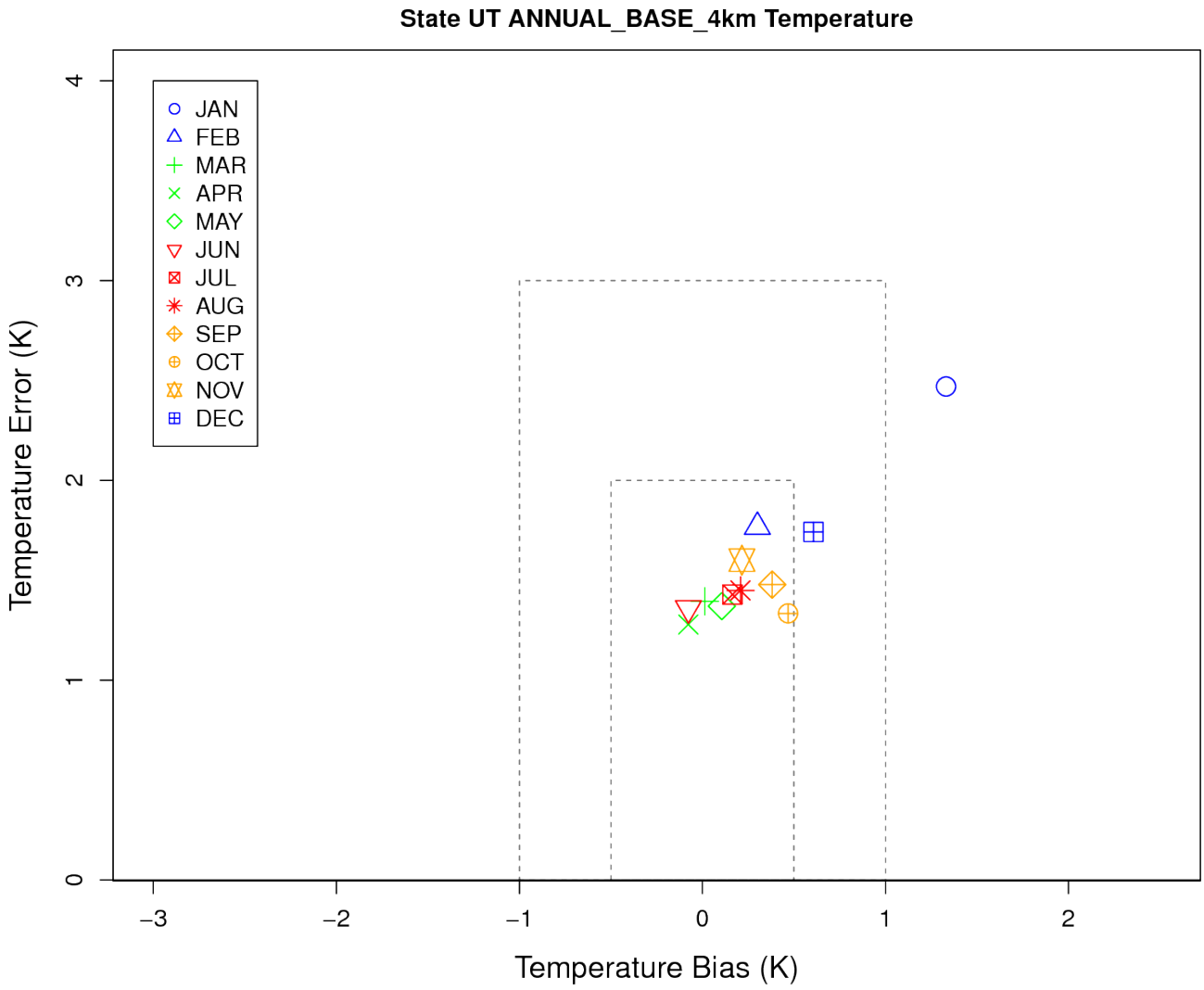

Figure 3-7b. Soccerplot of monthly temperature error and bias (K) for 4 km domain over Utah.

The WRF temperature performance in Wyoming has a warm bias in the warm months (May-Aug) and a cold bias in the cool months (Nov-Mar), although the complex temperature benchmark is always achieved. WRF achieves the simple temperature benchmark during the warm months with the monthly temperature bias and error falling between the simple and complex benchmarks during the cooler months.

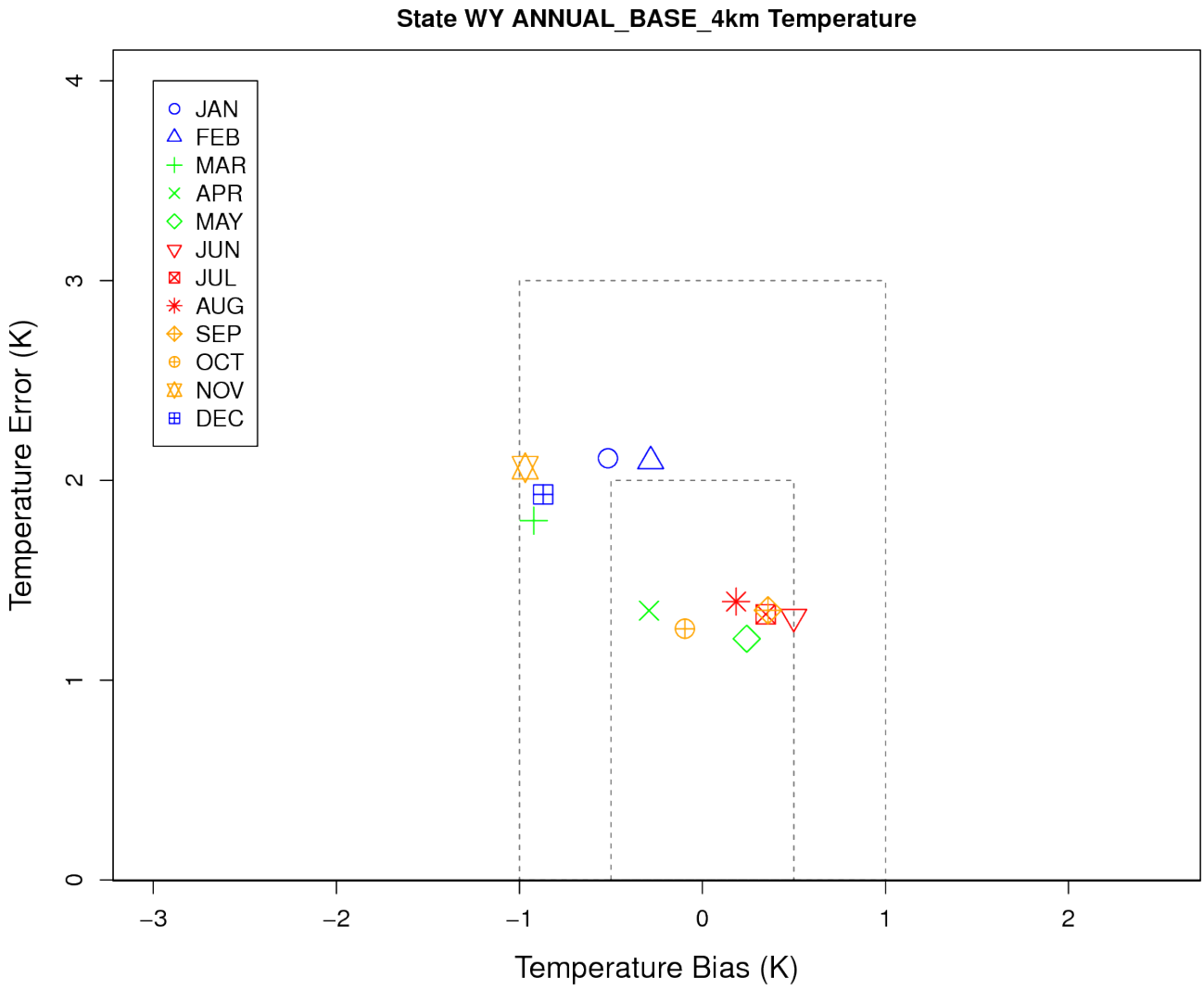

Figure 3-7c. Soccerplot of monthly temperature error and bias (K) for 4 km domain over Wyoming.

3.2.2 Monthly Mixing Ratio Performance

WRF achieves the mixing ratio bias simple benchmark in Colorado for all months as well as the simple benchmark for error for all months except the three summer months whose error lies between the simple and complex error benchmarks (Figure 3-8a).

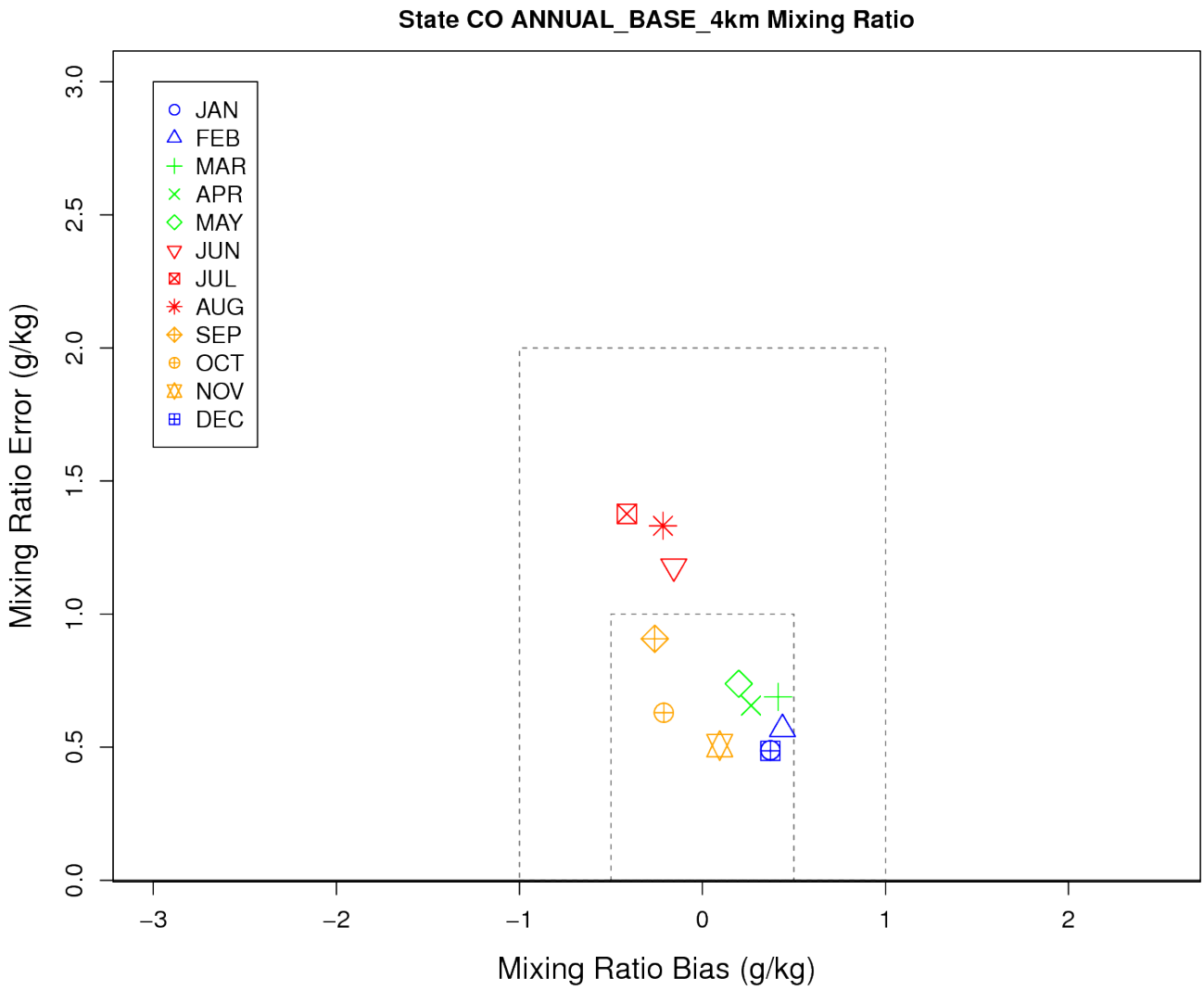

Figure 3-8a. Soccerplot of monthly mixing ratio error and bias (g/kg) for 4km domain over Colorado.

The monthly mixing ratio performance in Utah achieves or nearly achieves the simple benchmark in Utah for all months but July and August (Figure 3-8b). The winter months have a too wet bias and the warmer months are too dry with July and August so dry in Utah that the mixing ratio falls between the simple and complex benchmarks.

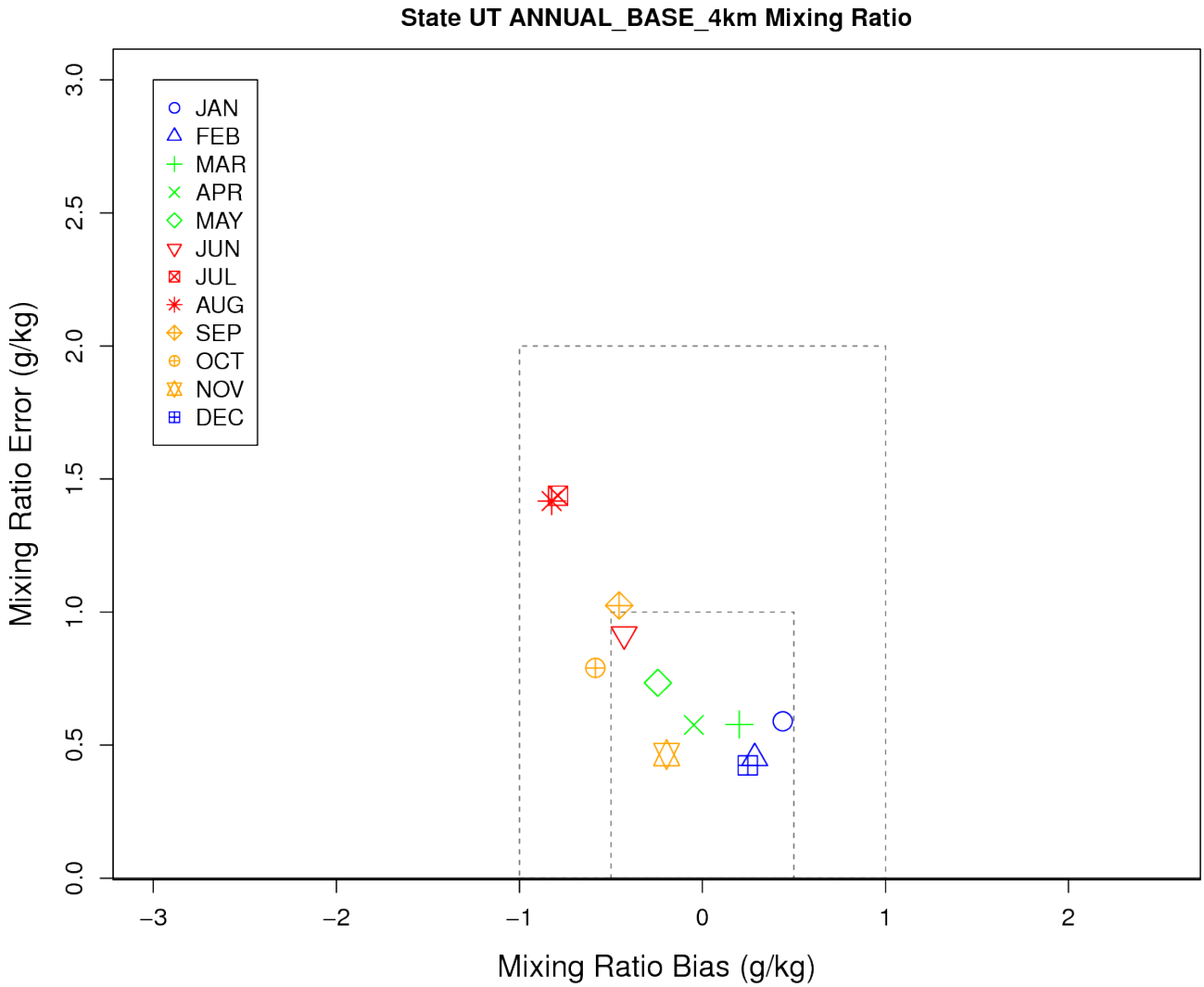

Figure 3-8b. Soccerplot of monthly mixing ratio error and bias (g/kg) for 4km domain over Utah.

The Wyoming monthly mixing ratio performance is similar to Colorado and Utah with a slight wet bias in the cooler months and dry bias in the warmer months. The simple mixing ratio bias benchmark is achieved for all months and error complex benchmark achieved for all months with the summer months the worst performing failing to achieve the simple benchmark for July and August.

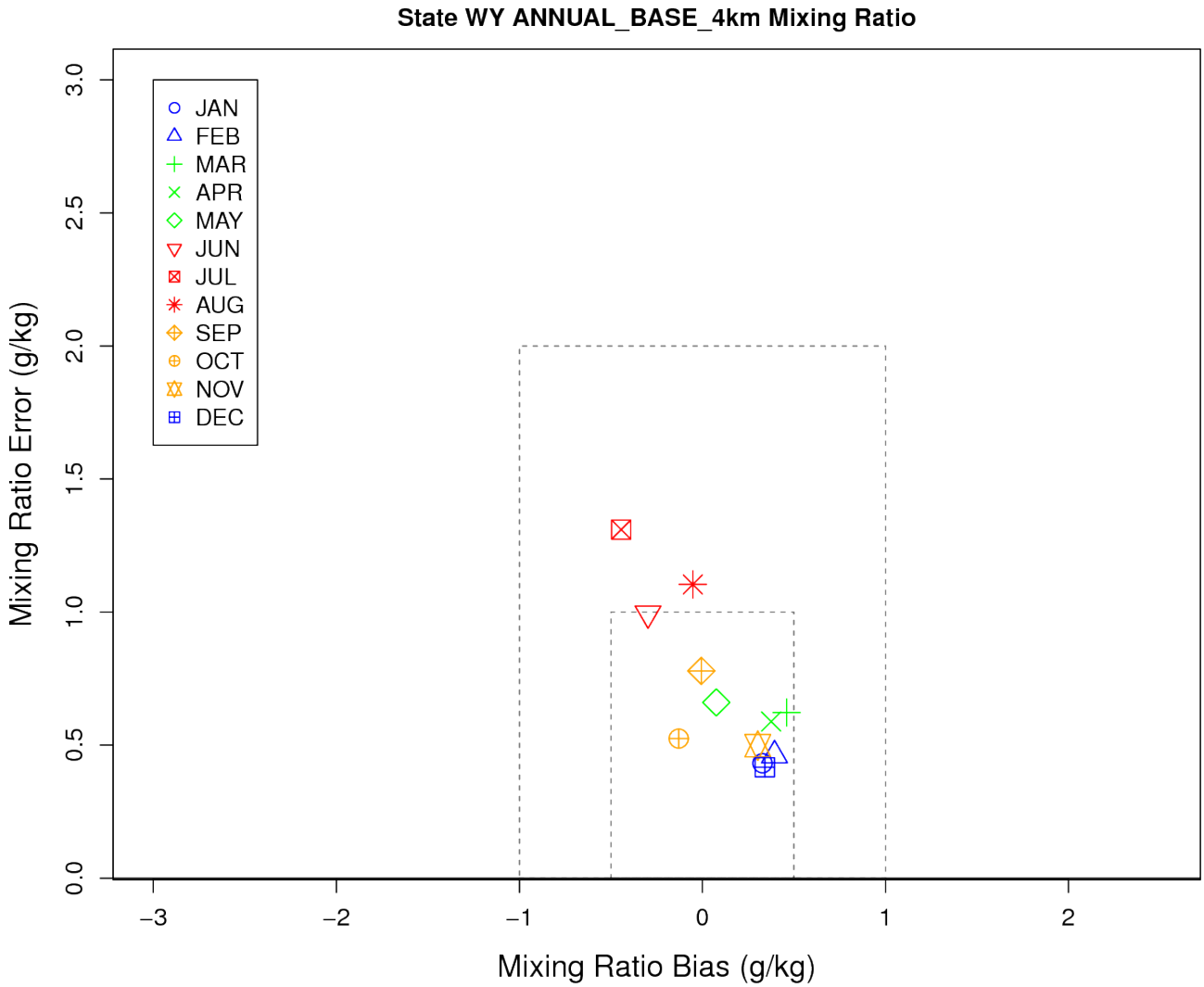

Figure 3-8c. Soccerplot of monthly mixing ratio error and bias (g/kg) for 4 km domain over Wyoming.

3.2.3 Monthly Wind Speed Performance

Monthly wind speed model performance in Colorado is characterized by too slow winds with monthly bias falling between the simple (-0.5 m/s) and complex (-1.0 m/s) benchmarks for all months (Figure 3-9a). Monthly wind speed error is clustered around the simple benchmark (2.0 m/s). All months achieve the complex wind speed benchmark but not the simple benchmark.

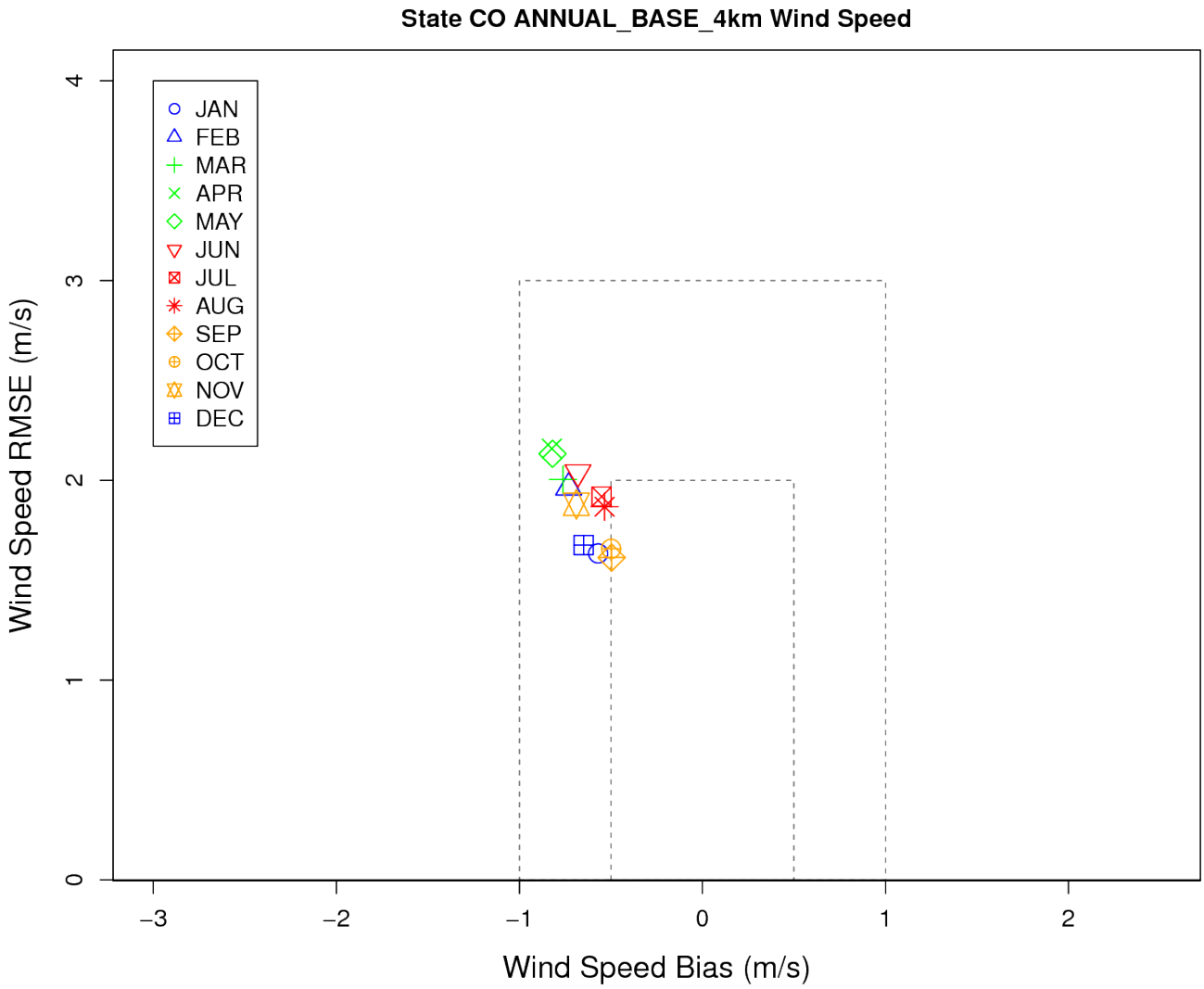

Figure 3-9a. Soccerplot of monthly wind speed error and bias (m/s) for 4km domain over Colorado.

Monthly wind speed performance in Utah is fairly good with near zero bias and achieving the simple wind speed benchmark for all months (Figure 3-9b). The wind speed bias ranges from approximately 0.0 to -0.3 m/s and error ranges from approximately 1.5 to 2.0 m/s.

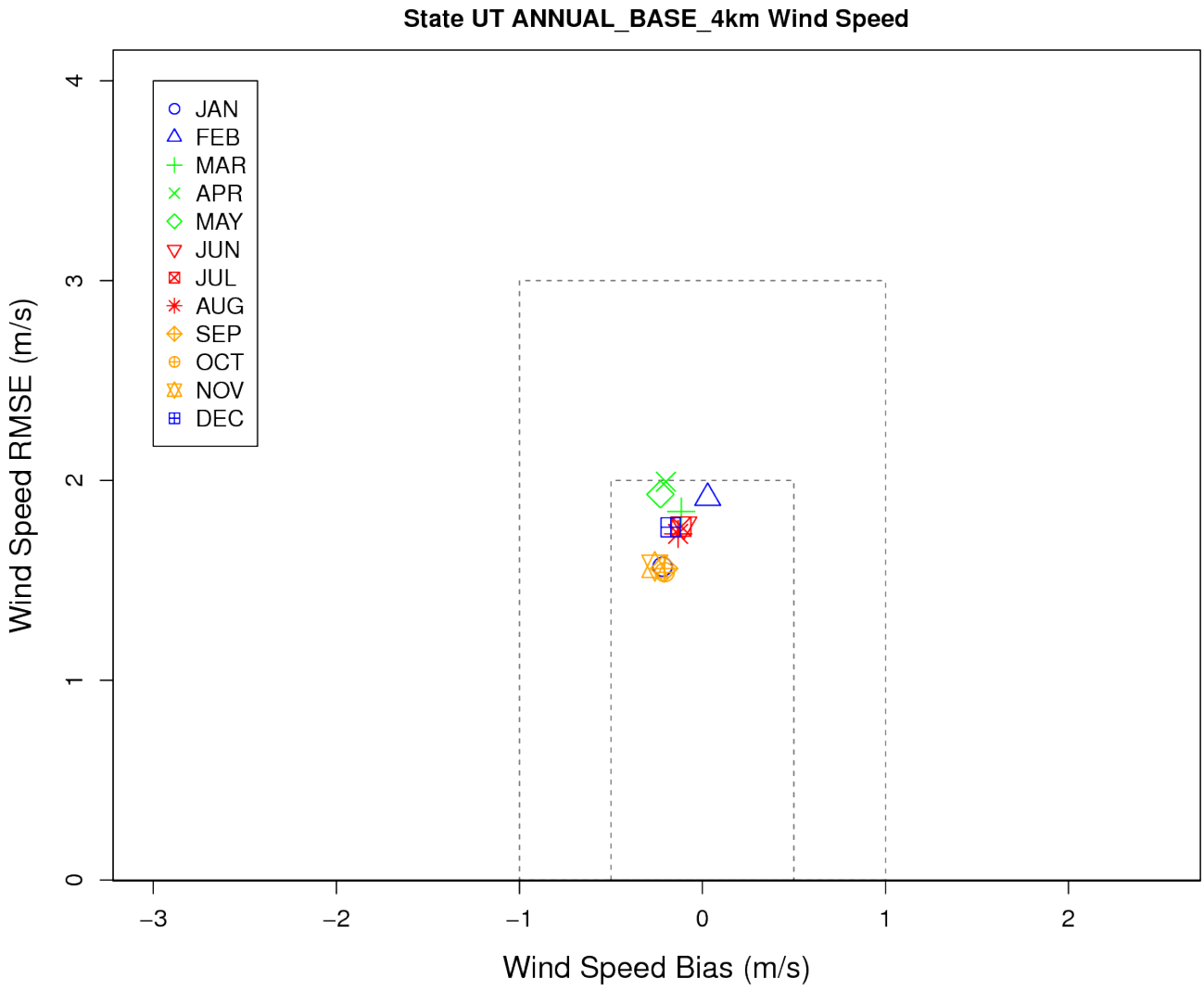

Figure 3-9b. Soccerplot of monthly wind speed error and bias (m/s) for 4km domain over Utah.

Like Colorado, monthly wind speed performance in Utah has a slow bias of approximately -0.4 to -0.8 m/s with error clustered around the 2.0 m/s simple benchmark. All months achieve the complex wind speed benchmark.

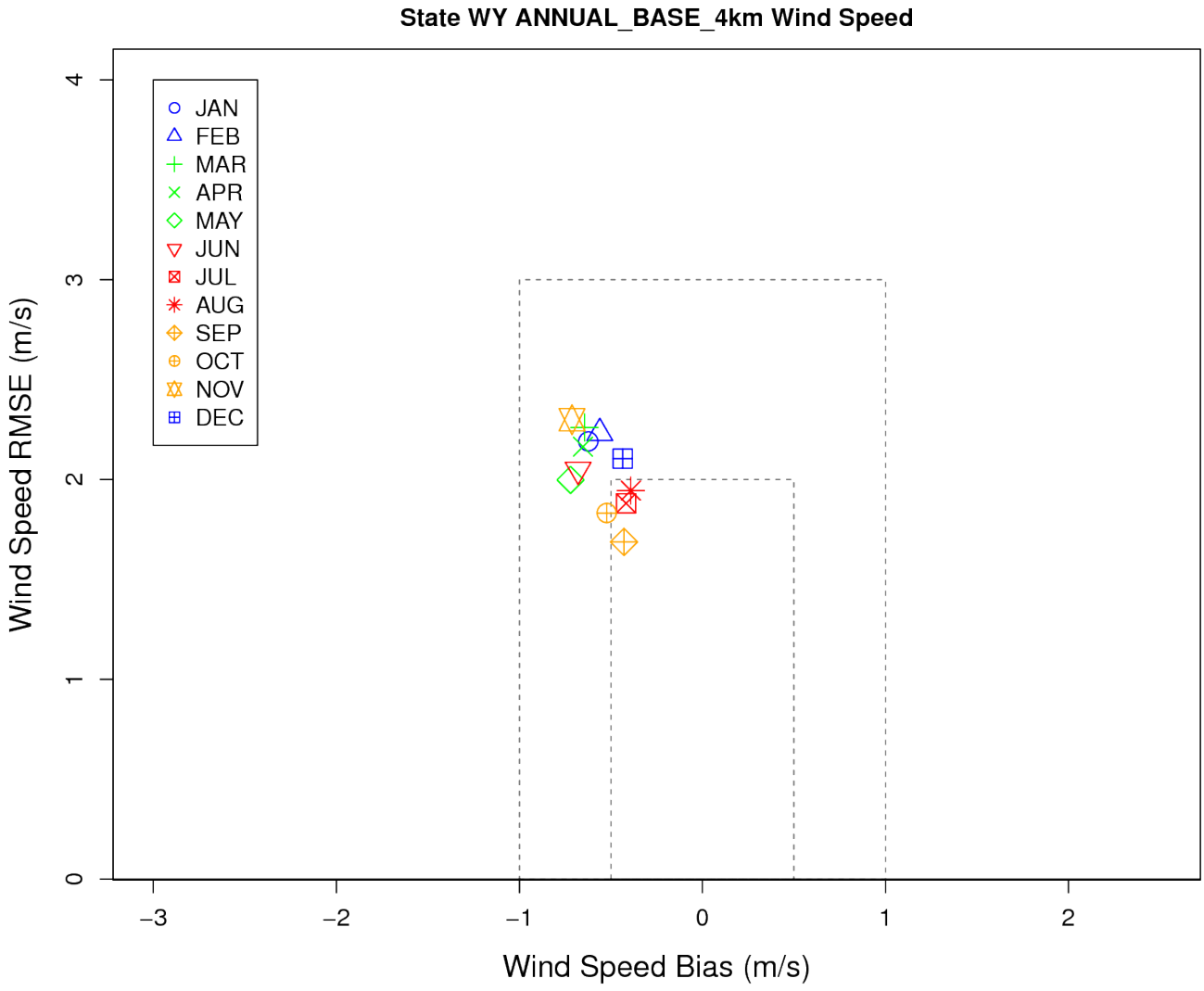

Figure 3-9c. Soccerplot of monthly wind speed error and bias (m/s) for 4 km domain over Wyoming.

3.2.4 Monthly Wind Direction Performance

Monthly wind direction performance in Colorado achieves the simple bias metric (≤±10 degrees) with wind direction falling between the simple and complex benchmark (Figure 3-10a).

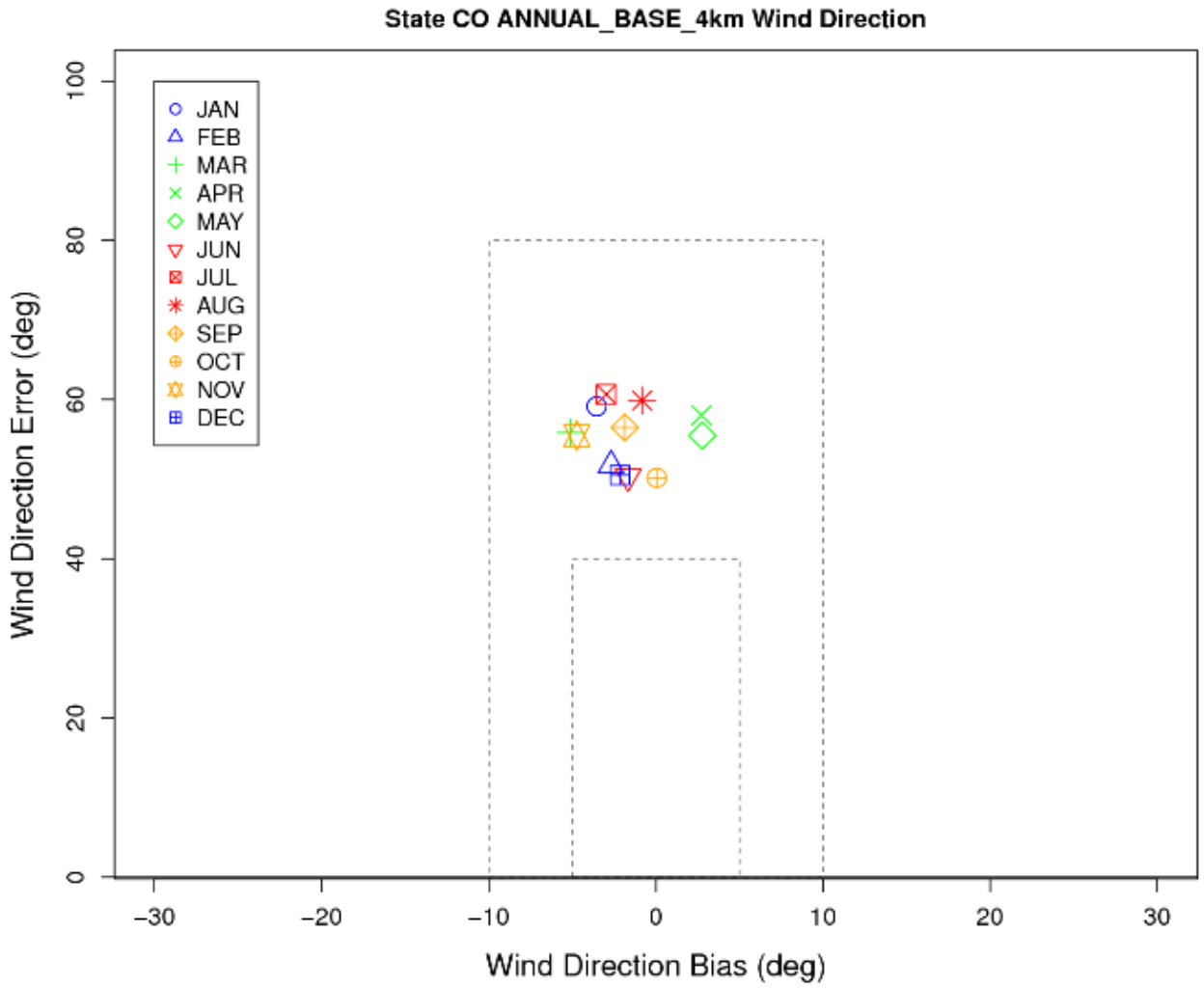

Figure 3-10a. Soccerplot of monthly wind direction error and bias for 4km domain over Colorado.

Wind direction performance in Utah has high error in the 50 to 80 degree range and mostly a negative bias that exceeds the complex benchmark for February (Figure 3-10b). The winter months perform worse than the warmer months.

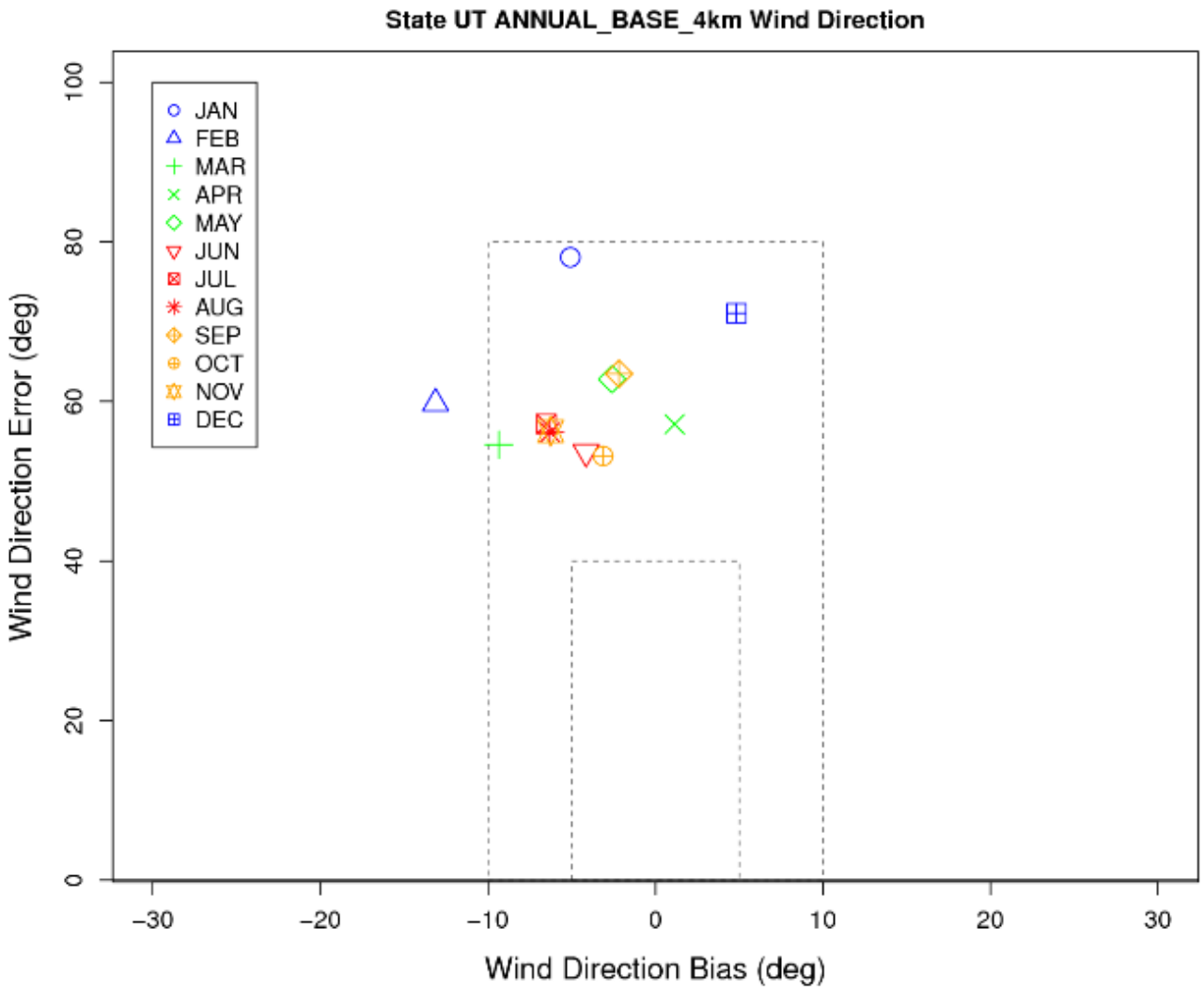

Figure 3-10b. Soccerplot of monthly direction error and bias for 4km domain over Utah.

As seen in Utah, monthly wind direction performance in Wyoming mostly has a negative bias with the cooler months (Dec, Jan, Feb and Mar) being more negative than the warmer months (Figure 3-10c). The complex wind direction bias and error benchmark is achieved or nearly achieved for all months and the simple wind direction bias is achieved for the warmer months.

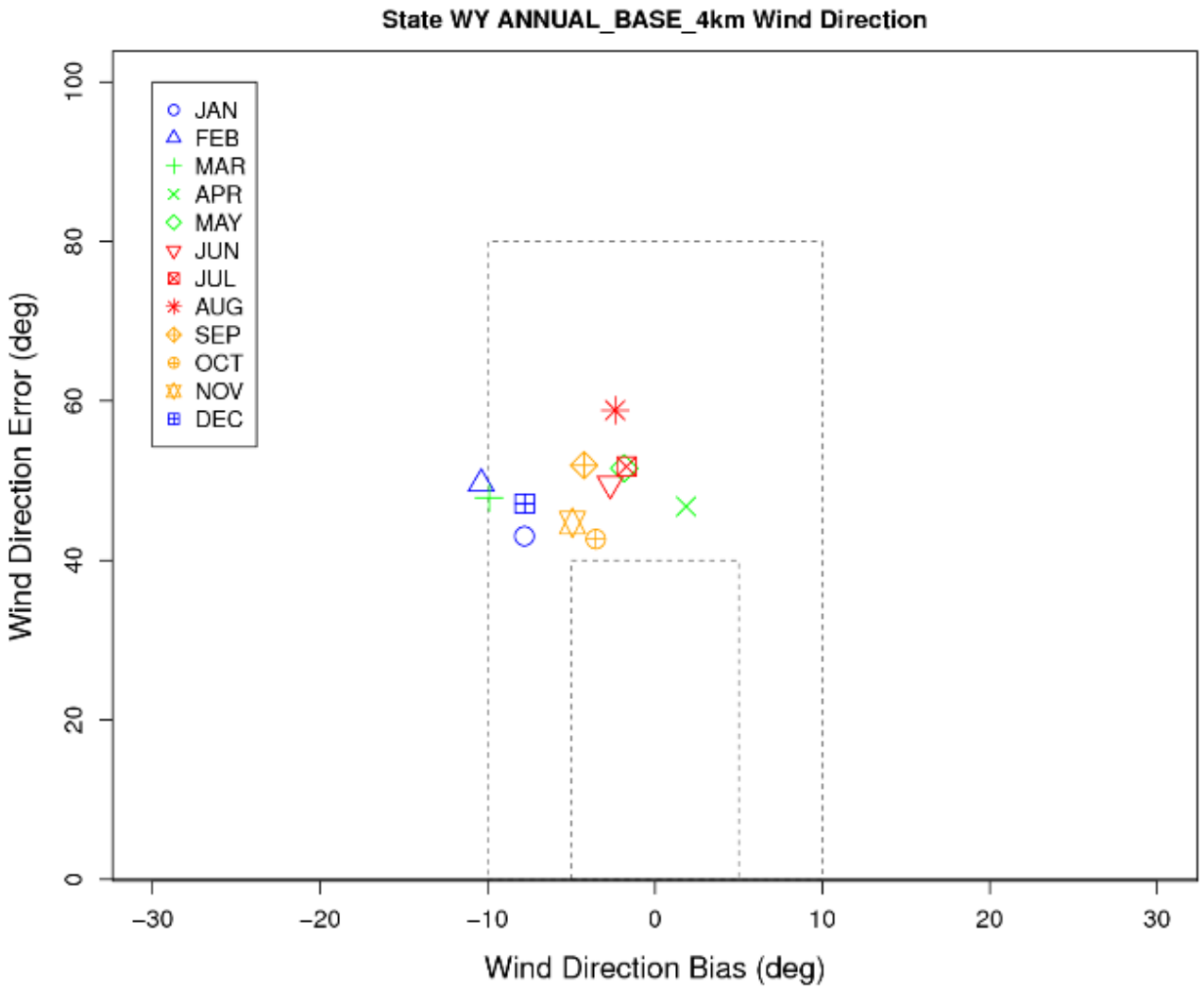

Figure 3-10c. Soccerplot of monthly wind direction error and bias for 4 km domain over Wyoming.

3.3 Additional Results

Appendix A displays mixing ratio, temperature and wind speed bias and error performance statistics for each state in the 12 km WESTUS modeling domain annually and by season.

An electronic docket is also included with this report that contains several other plots illustrating the WRF 2011 4 and 12 km model performance. The Three-State Data Warehouse (3SDW) hosts these additional plots at the following address:

ftp://viking.cira.colostate.edu/3SDW/3SAQS/2011/Base11a/plots/MET/

Quantatative performance plots for the 3SAQS 2011 WRF modeling on the 12 and 4 km modeling domains are included in the docket. The four types of plots available in this electronic docket include soccer, spatial surface, summary, and time series plots. Examples of the soccer, spatial surface, and time series plots are included in this report. Example summary plot is shown in Figure 3-11 for WRF 4 km domain temperature performance in January and July 2011. The summary plot contain an extensive list of monthly model performance metrics and display for the WRF 4 and 12 km simulation for all sites across the 4 km three-state and 12 km WESTUS domain, respectively. Performance metrics include number of data points used, correlation coefficient, standard deviation and three types of bias and error. Graphical displays include scatter plot, comparison of the bias and mean absolute error (MAE) as a function of the observed quantity and box plots of the distribution of the observed and predicted meteorological variables. For example, the WRF 4 km temperature performance in January across the 4 km domain has a high correlation (0.95), a tendency to overestimate the observed low and underestimation the observed high temperatures with the observed and predictions distributions of temperatures matching each other very well (Figure 3-11a). Similar WRF 4 km performance results are seen in July only the modeled temperatures do not go as low as what was observed (Figure 3-11b).

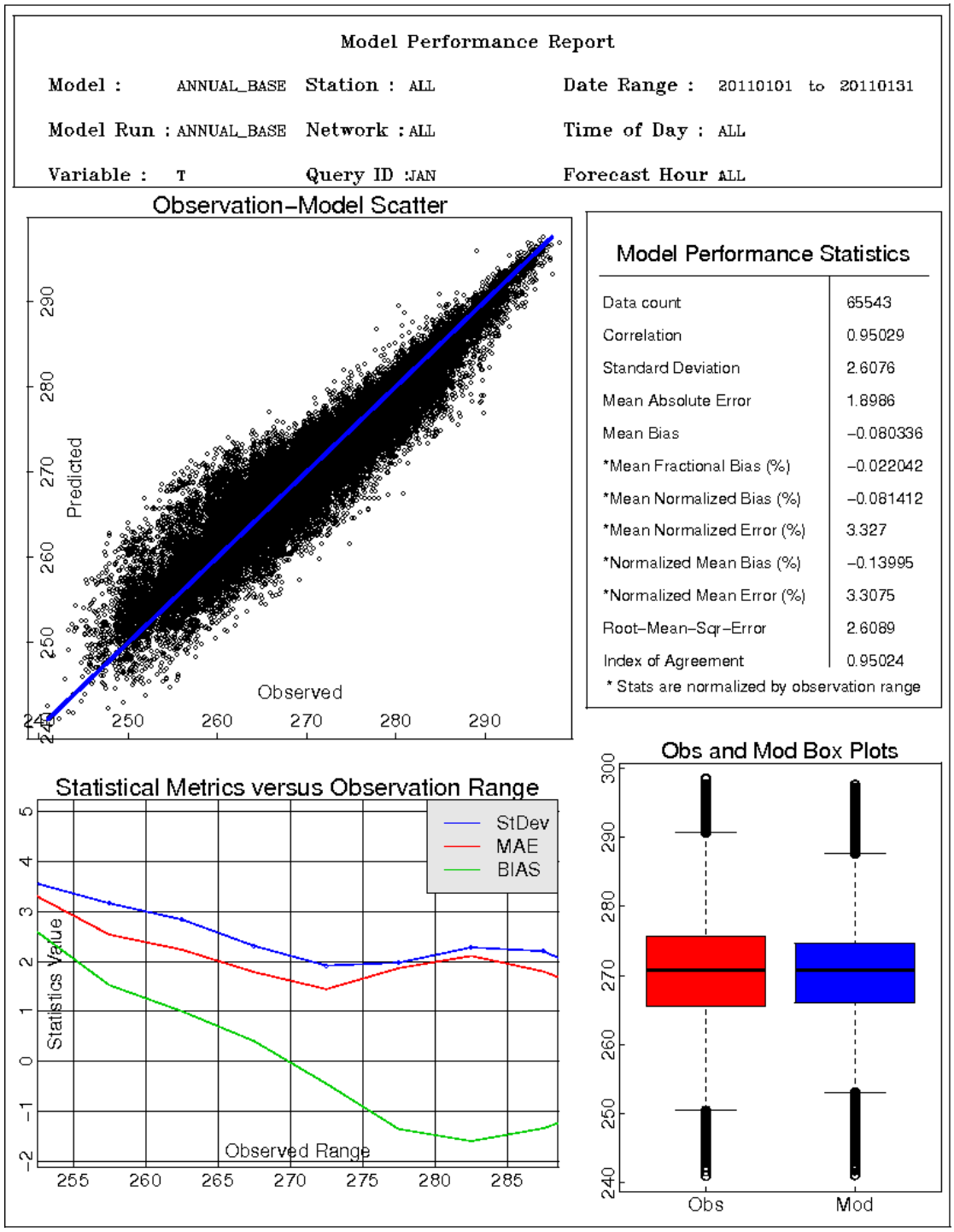

Figure 3-11a. AMET WRF 4 km summary temperature model performance plot for all sites in the 4 km domain and the month of January 2011.

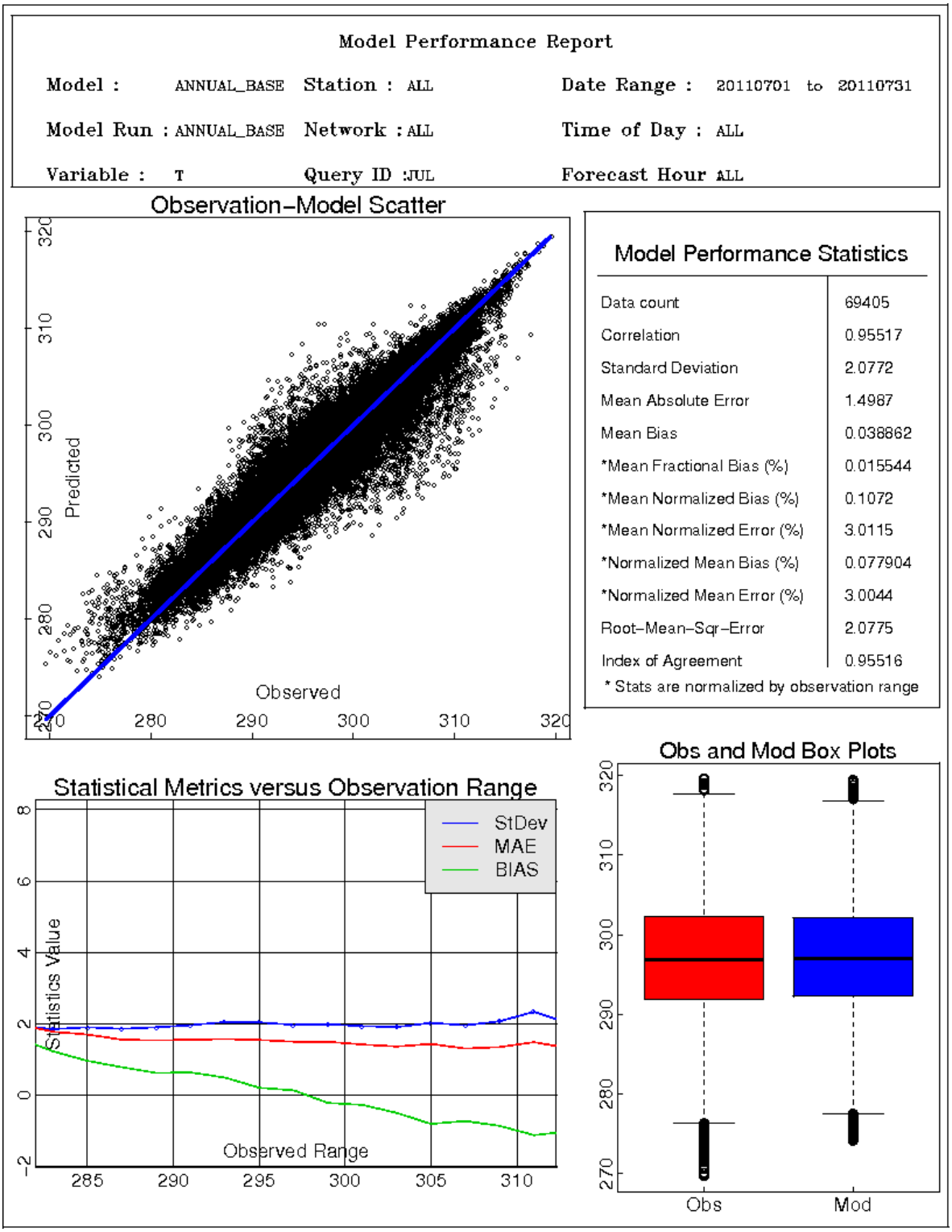

Figure 3-11b. AMET WRF 4 km summary temperature model performance plot for all sites in the 4 km domain and the month of July 2011.

4.0 PRECIPITATION EVALUATION

The WRF precipitation was evaluated by comparing spatial fields of monthly total precipitation estimates against monthly spatial fields of precipitation using the PRISM interpolation procedure. The Parameter-elevation Relationships on Independent Slopes Model (PRISM) uses approximately 13,000 precipitation measurement sites across the 48 contiguous United States and interpolates them to a < 1 km grid using regression weights based primarily on the physiographic similarity of station to the grid cell (Daly et al., 2008[19]). Factors considered are location, elevation, coastal proximity, topographic facet orientation, vertical atmospheric layer, topographic position and orographic effectiveness of the terrain. The PRISM interpolation approach represents a significant improvement over other techniques used to spatially interpolate observed precipitation that failed to account for factors that influence precipitation away from the observations such as orographic effects. However, it is still an interpolation technique that may not always capture all effects on precipitation and is just limited to precipitation within the 48 conterminous United States. The PRISM interpolation procedure will be particularly challenged during summer convective precipitation events (thunderstorms) that can be very spotty and isolated. Such events can occur between the rainfall monitoring sites so would not be present in the observations and hence the PRISM analysis fields.

4.1 Comparison of Monthly Precipitation Fields

The PRISM precipitation analysis fields were aggregated to the WRF 36, 12 and 4 km domains and the monthly total PRISM and WRF precipitation amounts were compared for each month of 2011. Figure 5-1 through 5-12 compares the monthly PRISM (top) and WRF (bottom) precipitation fields for the 4 km three-state (a) and 12 km WESTUS (b) WRF domains and, respectively, January through December 2011. Note that PRISM data does not include regions outside of the U.S., which is not an issue for the 4 km three-state domain that is completely contained within the U.S., but is an issue for the 12 km WESTUS domain that includes portions of Canada, Mexico and the Pacific Ocean that are not covered by the PRISM data. Thus, care must be taken in the interpretation of the WRF and PRISM monthly precipitation amounts in the 12 km WESTUS domain and the viewer needs to visually mask the WRF results in areas not covered by PRISM when comparing them to the PRISM data. In the 12 km WESTUS domain WRF 12 km monthly precipitation spatial maps, the areas outside the U.S. where PRISM analysis fields are not available are shed to aid in the comparisons.

Table 4-1 displays compares summary statistics about the monthly total PRISM and WRF precipitation across the grid cells in the 4 km three-state and 12 km WESTUS domains. Shown are the average, 10th percentile and 90th percentile monthly precipitation amounts. For the 12 km WESTUS domain, only those grid cells in the U.S. covered by the PRISM analysis fields are used in the calculations for both the PRISM and WRF 12 km statistics. It is difficult to see any

[19] Physiographically sensitive mapping of the climatological temperature and precipitation across the conterminous United States. C. Daley, M. Halbleib, J. Smith, W. Gipson, M. Doggett, G. Taylor, J. Curtis and P. Pasteris. *Int. J. Climatol.* (2008). http://prism.oregonstate.edu/documents/Daly2008_PhysiographicMapping_IntJnlClim.pdf

trends in the domain wide 4 km precipitation statistics, although the WRF 12 km average precipitation is higher than PRISM for all the months except January.

Table 4-1. PRISM and WRF domain-wide monthly precipitation statistics across the 4 km three-state and 12 km WESTUS domains.

Month	Average			10th Percentile			90th Percentile		
4 km	PRISM	WRF	Diff	PRISM	WRF	Diff	PRISM	WRF	Diff
Jan	0.73	0.64	-12.3%	0.00	0.01	NA	1.83	1.62	-11.5%
Feb	1.10	1.09	-0.9%	0.29	0.32	10.3%	2.27	2.06	-9.3%
Mar	1.34	1.14	-14.9%	0.21	0.01	-95.2%	3.13	2.79	-10.9%
Apr	2.09	1.99	-4.8%	0.49	0.04	-91.8%	4.20	4.17	-0.7%
May	3.23	2.43	-24.8%	0.39	0.02	-94.9%	6.28	5.90	-6.1%
Jun	1.27	0.95	-25.2%	0.00	0.00	NA	2.86	2.48	-13.3%
Jul	1.66	1.86	12.0%	0.45	0.36	-20.0%	3.16	3.66	15.8%
Aug	1.27	1.54	21.3%	0.41	0.29	-29.3%	2.35	3.27	39.1%
Sep	0.96	1.30	35.4%	0.28	0.23	-17.9%	1.84	2.92	58.7%
Oct	1.66	1.44	-13.3%	0.71	0.50	-29.6%	2.83	2.49	-12.0%
Nov	0.98	0.86	-12.2%	0.31	0.16	-48.4%	1.99	1.68	-15.6%
Dec	0.87	1.06	21.8%	0.20	0.19	-5.0%	1.83	2.27	24.0%
12 km									
Jan	0.90	0.88	-2.2%	0.00	0.04	NA	3.56	3.01	-15.4%
Feb	0.99	1.56	57.6%	0.24	0.25	4.2%	3.63	3.28	-9.6%
Mar	1.40	2.07	47.9%	0.05	0.03	-40.0%	4.92	4.32	-12.2%
Apr	1.58	2.61	65.2%	0.04	0.03	-25.0%	5.24	5.47	4.4%
May	2.01	3.00	49.3%	0.12	0.05	-58.3%	6.33	6.42	1.4%
Jun	1.28	1.96	53.1%	0.00	0.02	NA	4.62	4.84	4.8%
Jul	1.13	1.55	37.2%	0.10	0.16	60.0%	4.04	3.47	-14.1%
Aug	0.95	1.25	31.6%	0.04	0.03	-25.0%	3.56	2.89	-18.8%
Sep	0.73	1.07	46.6%	0.15	0.12	-20.0%	2.34	2.44	4.3%
Oct	1.11	1.46	31.5%	0.44	0.34	-22.7%	3.32	2.95	-11.1%
Nov	1.19	1.61	35.3%	0.13	0.13	0.0%	4.79	4.15	-13.4%
Dec	1.12	1.51	34.8%	0.16	0.12	-25.0%	4.08	3.71	-9.1%

4.1.1 January 2011

Figure 5-1a compares the PRISM (top) and WRF (bottom) January 2011 monthly precipitation amounts within the 3SAQS 4 km domain. There is enhanced precipitation in the PRISM January data over higher terrain features across the Rocky Mountains; these include the Sawtooth range in Idaho, the Teton, Absaroka, Wyoming and Wind River ranges in Wyoming, and the Front, Medicine Bow and other ranges in Colorado that stretch into southern Wyoming. The WRF spatial pattern of monthly precipitation in January 2011 and the 4 km domain matches the PRISM patterns very well, although the WRF monthly precipitation intensity is not as great as PRISM over the Idaho and western Wyoming terrain features. The WRF January precipitation

matches the PRISM analysis fields almost exactly over the Colorado Rock Mountains. However, WRF also has elevated January precipitation over the Black Hills in northeastern Wyoming that is not reflected in the PRISM data.

In the 12 km WESTUS domain January precipitation comparisons, both PRISM and WRF have intense areas of precipitation in the Pacific Northwest (PNW) coastal areas, the northern Rocky Mountains, including the Bitterroot Range along the border of Idaho and Montana, and in southeastern Texas into southern Louisiana (Figure 5-1b). Note that WRF seemingly has more widespread and intense precipitation in the northern PNW region, but this is an artifact of PRISM not included any precipitation in Canada.

4.1.2 February 2011

In February 2011, both WRF and PRISM estimate enhanced precipitation over the high terrain features in Idaho, Wyoming and Colorado portions of the 4 km domain as seen for January discussed above; however in February elevated precipitation is also seen over the high terrain features in Utah including the Wasatch Range (Figure 5-2a). The spatial patterns of the February PRISM and WRF precipitation in the 4 km domain are very similar. In the 12 km domain, both PRISM and WRF estimate enhanced precipitation along the west coast stretching from the PNW down to San Diego as well as over the Sierra Nevada mountains (Figure 5-2b). There is also good agreement in the PRISM and WRF enhanced precipitation in the Rocky Mountain region. PRISM estimates intense February monthly precipitation in Missouri and Arkansas that is reproduced by WRF, only not quite as intensely.

4.1.3 March 2011

There is good agreement in the spatial patterns of precipitation between the PRISM and WRF March monthly precipitation in the 4 km domain (Figure 5-3a). WRF tends to estimate more precipitation over the Big Horn Mountains in north-central Wyoming and up into the northeastern corner of the 4 km domain. PRISM and WRF also both estimate enhanced precipitation across the New Mexico-Colorado state line.

The National Climatic Data Center (NCDC) found that March 2011 was one of the wettest March months on record for WA, OR and CA with precipitation much above normal[20]. This is reflected in the PRISM and WRF 12 km results (Figure 5-3b) with large amounts of precipitation occurring in these three states that exceed 8 inches per month in both the PRISM and WRF estimates. Higher precipitation also occurs in the Rocky Mountain with PRISM estimated enhanced precipitation in the eastern border of the 12 km domain over Louisiana, Arkansas and Missouri that is not as intense in the WRF fields.

4.1.4 April 2011

In April 2011, the WRF estimates enhanced precipitation over the Rocky Mountains and other high terrain features in the 4 km domain that agrees well with the PRISM data (Figure 4-4a).

[20] http://www.ncdc.noaa.gov/temp-and-precip/maps.php?imgs%5B%5D=statewidepcpnrank&year=2011&month=3&ts=1&submitted=Submit

However, WRF also estimates high precipitation in eastern Wyoming into South Dakota and Nebraska that is not reflected in the PRISM data. There is reasonably good agreement between the spatial patterns of April precipitation from PRISM and WRF, although WRF estimates higher precipitation in the Dakotas and vicinity (Figure 4-4b).

4.1.5 May 2011

May 2011 was the second wettest May in a 117 year period of record in Wyoming and Utah with Montana, Nebraska and the Dakotas also have precipitation that was much above normal[21]. This is reflected in the PRISM and WRF May 2011 precipitation plots for the 4 and 12 km domain (Figure 4-5). A blob of elevated precipitation occurs centered on the MT/WY state-line that extends north and southward in both PRISM and WRF. WRF may understate the precipitation in Utah in May and estimates too much precipitation in eastern Oregon-Washington and Idaho.

4.1.6 June 2011

The extent of precipitation in June 2011 is much less than previous months with some occurrence in the general vicinity of the Teton Range as well as in the eastern portion of the domain (Figure 4-6a). The WRF results are spottier than PRISM and include a blob in eastern Colorado that is in Nebraska in the PRISM data. Within the 12 km domain WRF is overestimating precipitation along the northern Rocky Mountains from western Montana, to Idaho and into Wyoming. WRF captures the higher PRISM precipitation in the Dakotas and Nebraska and further east fairly well. June 2011 was the wettest June on record in California where the PRISM and WRF agree fairly well but don't look remarkably wet, which is due to California always being very dry in June.

4.1.7 July 2011

The spatial distribution of the WRF July monthly precipitation in the 4 km domain does not match the PRISM data very well (Figure 4-7a). The WRF July precipitation estimates are very spotty with large amounts in central and southern Colorado and in spots across the 4 km domain. PRISM, on the other hand, estimates less precipitation in central-southern Colorado as well as in South Dakotas and Nebraska. July precipitation in the 4 km domain will be due to convective cells that can be very isolated and are semi-random. Precipitation from these isolated thunderstorms may not be well captured in the observed rainfall that is used by PRISM to generate the precipitation analysis fields.

The July 2011 monthly precipitation comparison for the 12 km WESTUS domain is shown in Figure 4-7b. Again the agreement between WRF and PRISM is not as good as the previous months. The WRF estimate intense precipitation In Mexico as well as high values in Canada, which since missing in PRISM makes the precipitation comparison look worse than it is.

[21] http://www.ncdc.noaa.gov/temp-and-precip/maps.php?imgs%5B%5D=statewidepcpnrank&year=2011&month=5&ts=1&submitted=Submit

4.1.8 August 2011

Like July, WRF estimates higher and more widespread precipitation in August 2011 than PRISM (Figure 4-8). In the PRISM plots individual sites with elevated precipitation are seen as yellow dots that were affected by convective showers, but the elevated precipitation does propagate out from the individual sites due to the PRISM interpolation procedure incorporating the neighboring precipitation monitoring sites with lower precipitation. However, in WRF, as well as in the real atmosphere, a thundershower cell will move around and sometimes the convective cell will be over a rainfall gauge and then move on to where there are no gauges where the precipitation is not captured by the PRISM analysis algorithms. The PRISM interpolation procedure appears to be designed more to pick up orographic, terrain and coastal effects on precipitation, which aren't as important factors for summer convective precipitation compared to synoptic storms.

4.1.9 September 2011

In September 2011, both PRISM and WRF estimate that precipitation occurs across New Mexico into Arizona with some also occurring in southern Colorado, only WRF estimates higher monthly precipitation totals than PRISM (Figure 4-9a). WRF matches the PRISM precipitation patterns for September across the 4 km domain well, just with more intensity. WRF also matches the spatial patterns of the PRISM September precipitation across the 12 km WESTUS domain with elevated amounts occurring in the PNW, Louisiana and AZ-NM-CO (Figure 4-9b).

4.1.10 October 2011

By October 2011 precipitation starts to become more synoptic and less driven by convection resulting in good agreement between the WRF and PRISM monthly precipitation patterns (Figure 4-10a). The PRISM and WRF October precipitation fields exhibit elevated amounts over the high terrain features in the 4 km domain. Across the 12 km WESTUS domain, both PRISM and WRF estimated high precipitation amounts along the west coast from the PNW down to northern California, over the Rocky Mountain region and over central Texas (Figure 4-10b).

4.1.11 November 2011

There is good agreement between the PRISM and WRF November precipitation across the 4 km domain (Figure 4-11a). Both PRISM and WRF estimate high monthly rainfall in Arkansas that exceeds 8 inches/month as well as in the PNW in November 2011 (Figure 4-11b).

4.1.12 December 2011

In December 2011, PRISM and WRF estimate elevated precipitation in southeast Idaho, over the Teton Range and in east-central Arizona and into west-central New Mexico (Figure 4-12a). Utah and western Colorado is relatively dry in December in both the PRISM and WRF fields. In December across the 12 km WESTUS domain, both PRISM and WRF estimate high precipitation in the PNW, northern Idaho into western Montana, in Arizona-New Mexico and in the Texas-Louisiana-Arkansas region (Figure 4-12b). PRISM exhibits December monthly precipitation in northern Louisiana/southern Arkansas that exceeds 9 inches per month, whereas in the same location WRF estimates values in the 6-8 inches per month range.

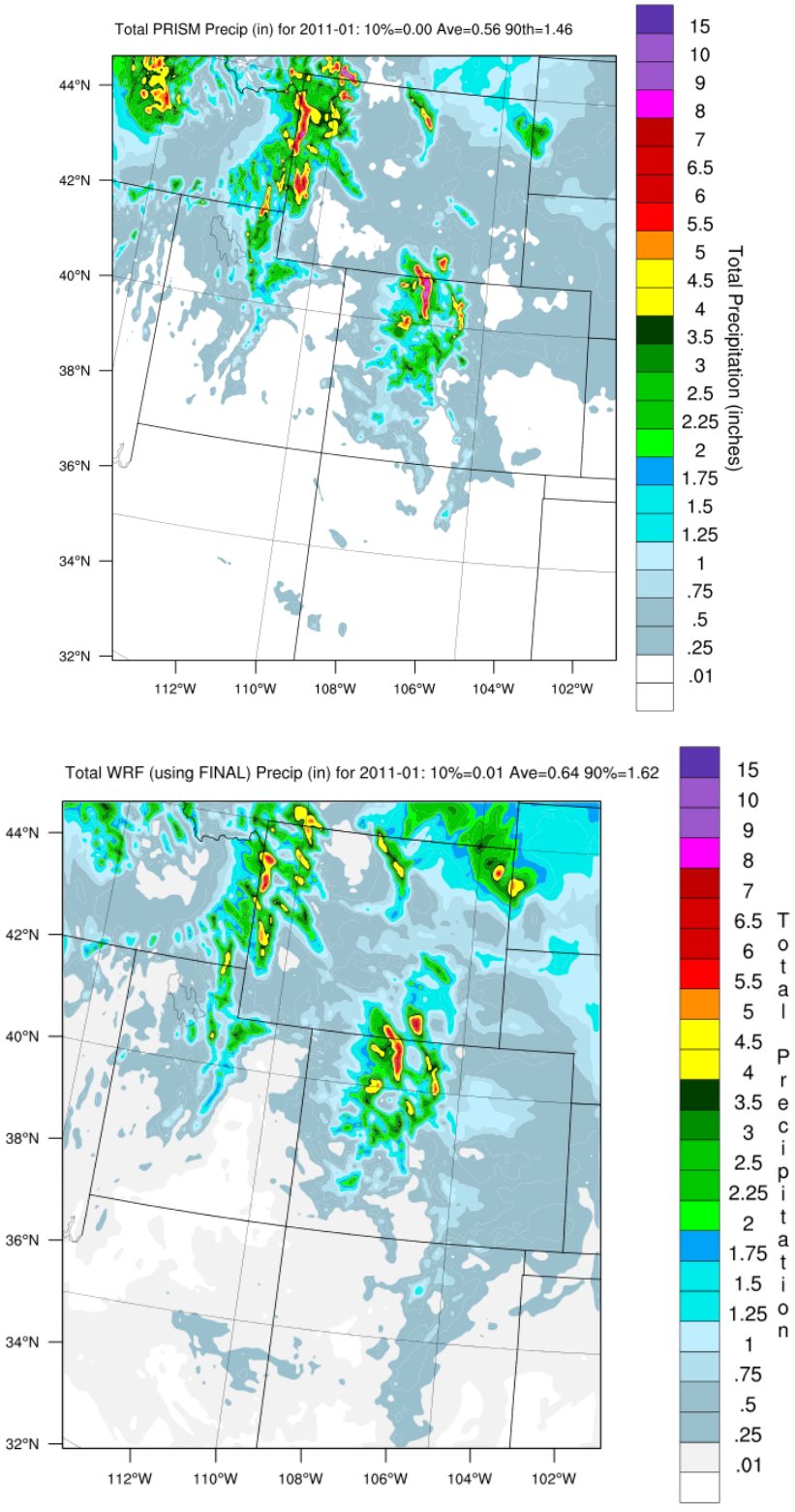

Figure 4-1a. Comparison of monthly total precipitation (inches) from PRISM (top) and WRF (bottom) for the 4 km three-state (d03) domain and the month of January 2011.

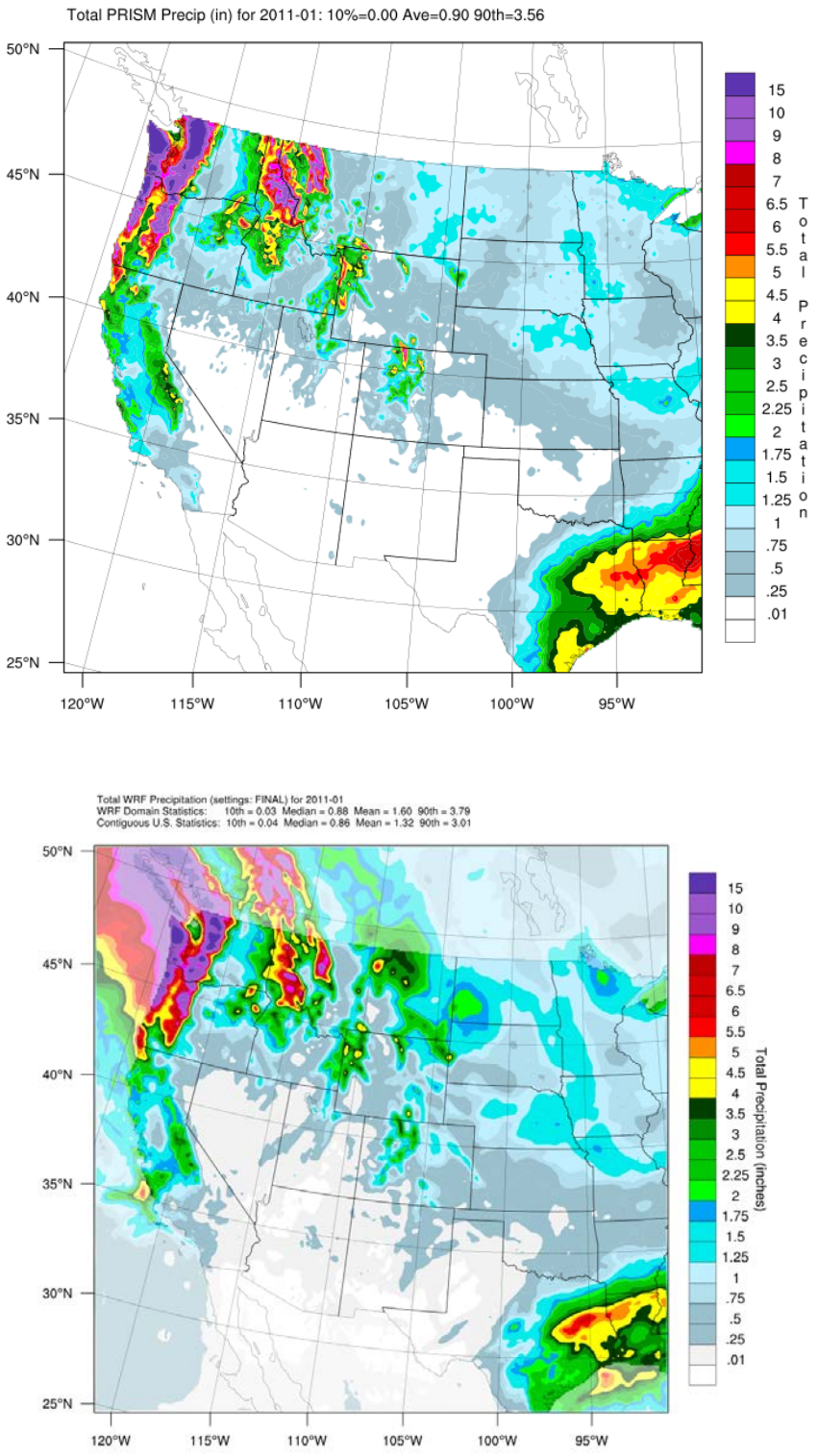

Figure 4-1b. Comparison of monthly total precipitation (inches) from PRISM (top) and WRF (bottom) for the 12 km WESTUS (d02) domain and the month of January 2011.

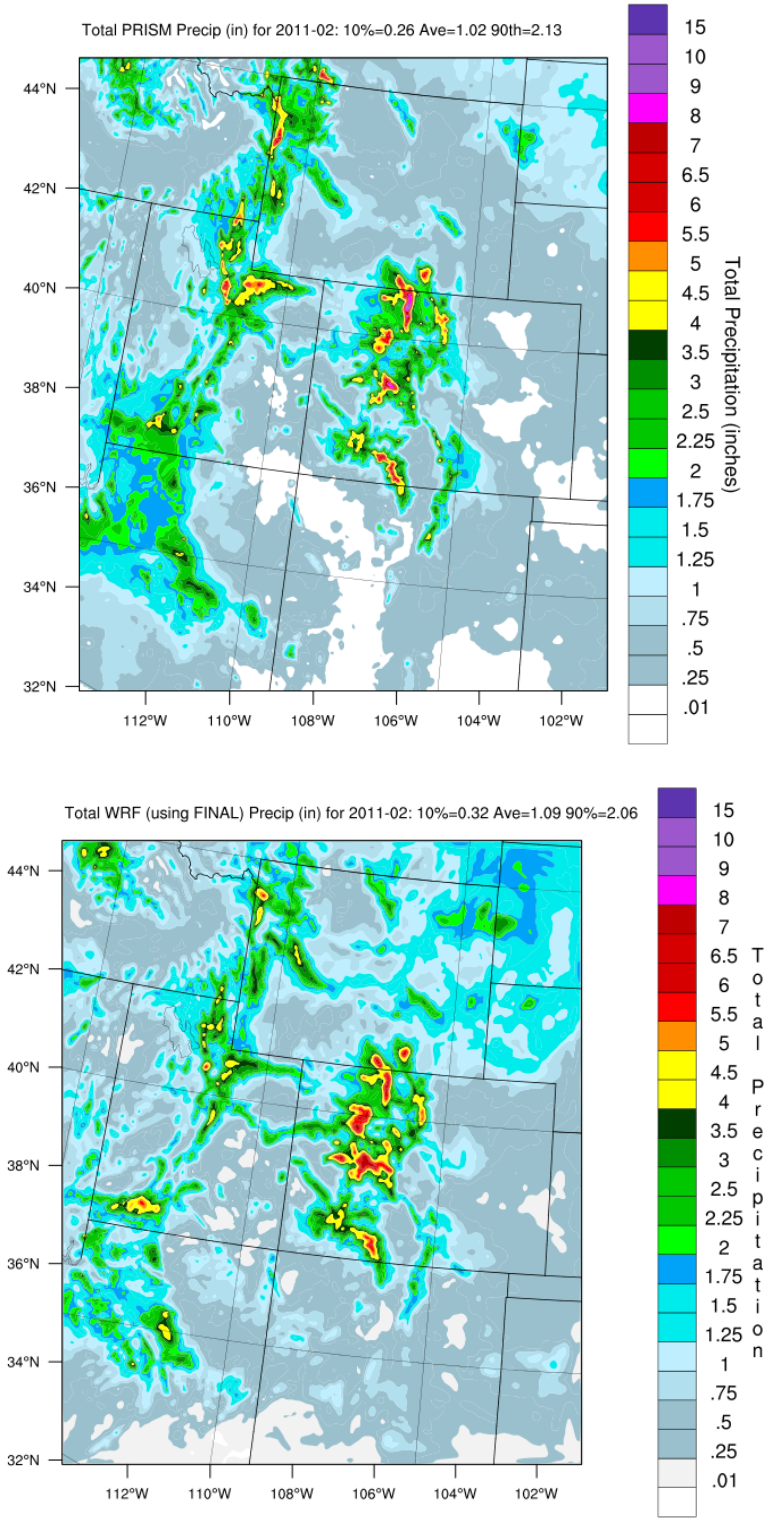

Figure 4-2a. Comparison of monthly total precipitation (inches) from PRISM (top) and WRF (bottom) for the 4 km three-state (d03) domain and the month of February 2011.

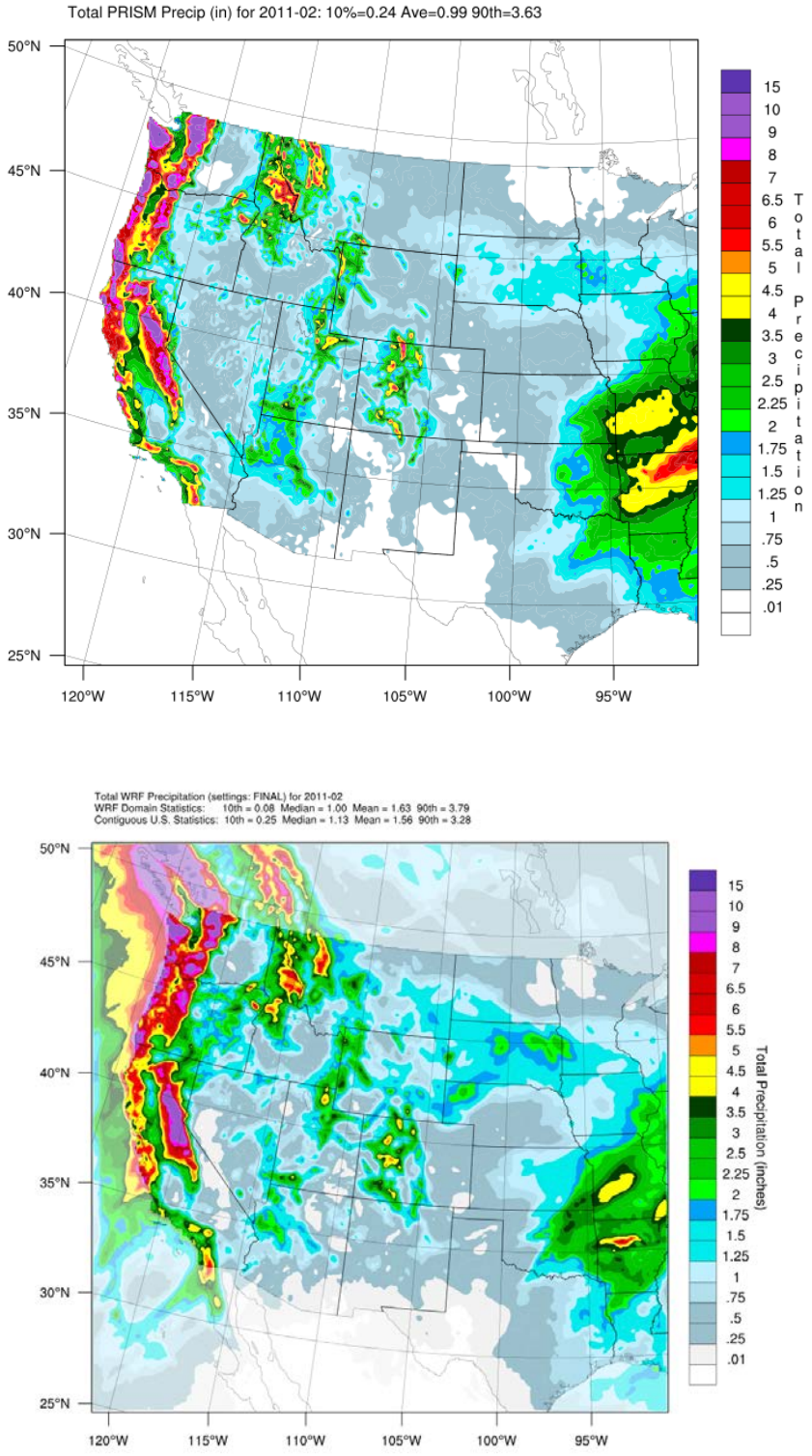

Figure 4-2b. Comparison of monthly total precipitation (inches) from PRISM (top) and WRF (bottom) for the 12 km WESTUS (d02) domain and the month of February 2011.

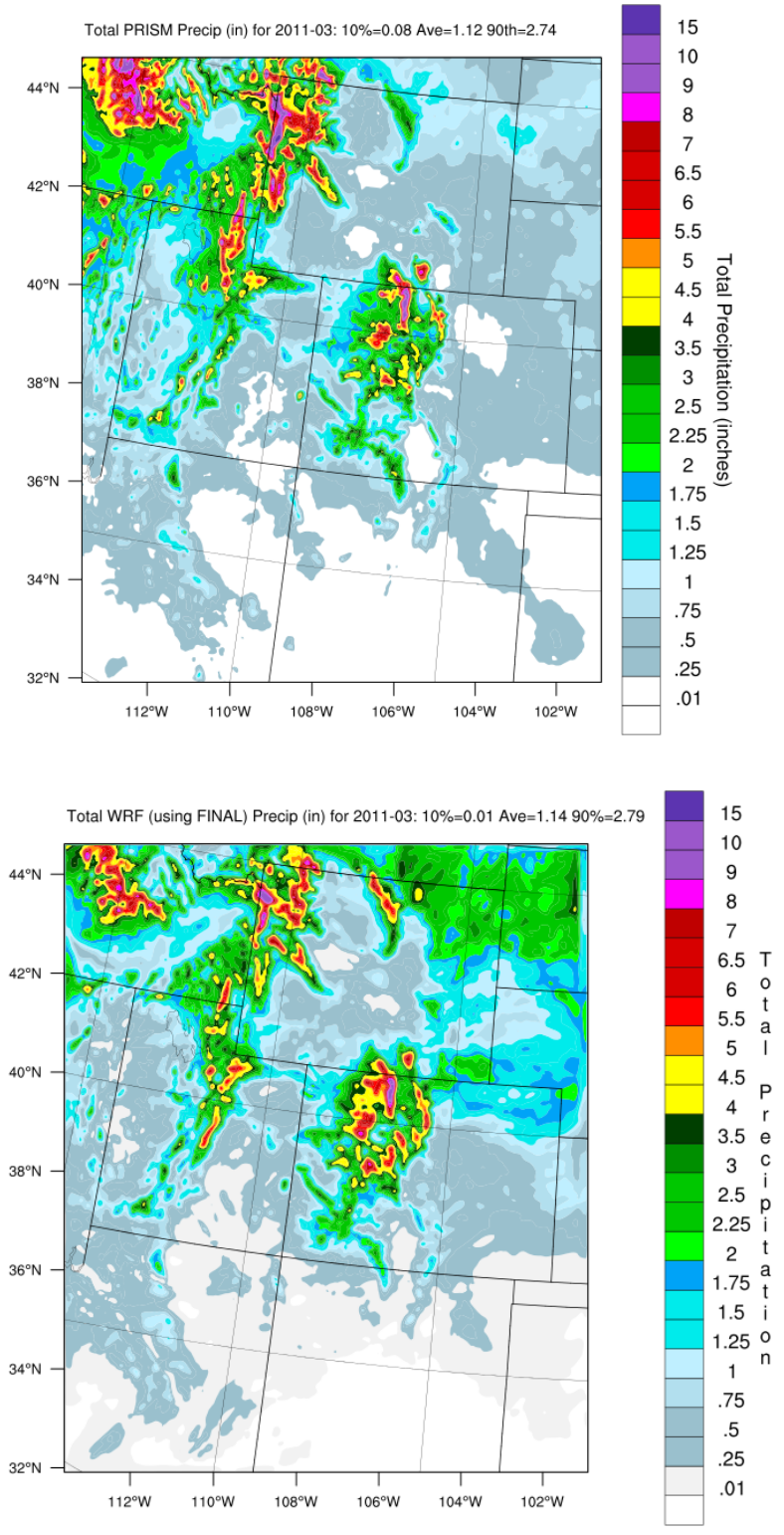

Figure 4-3a. Comparison of monthly total precipitation (inches) from PRISM (top) and WRF (bottom) for the 4 km three-state (d03) domain and the month of March 2011.

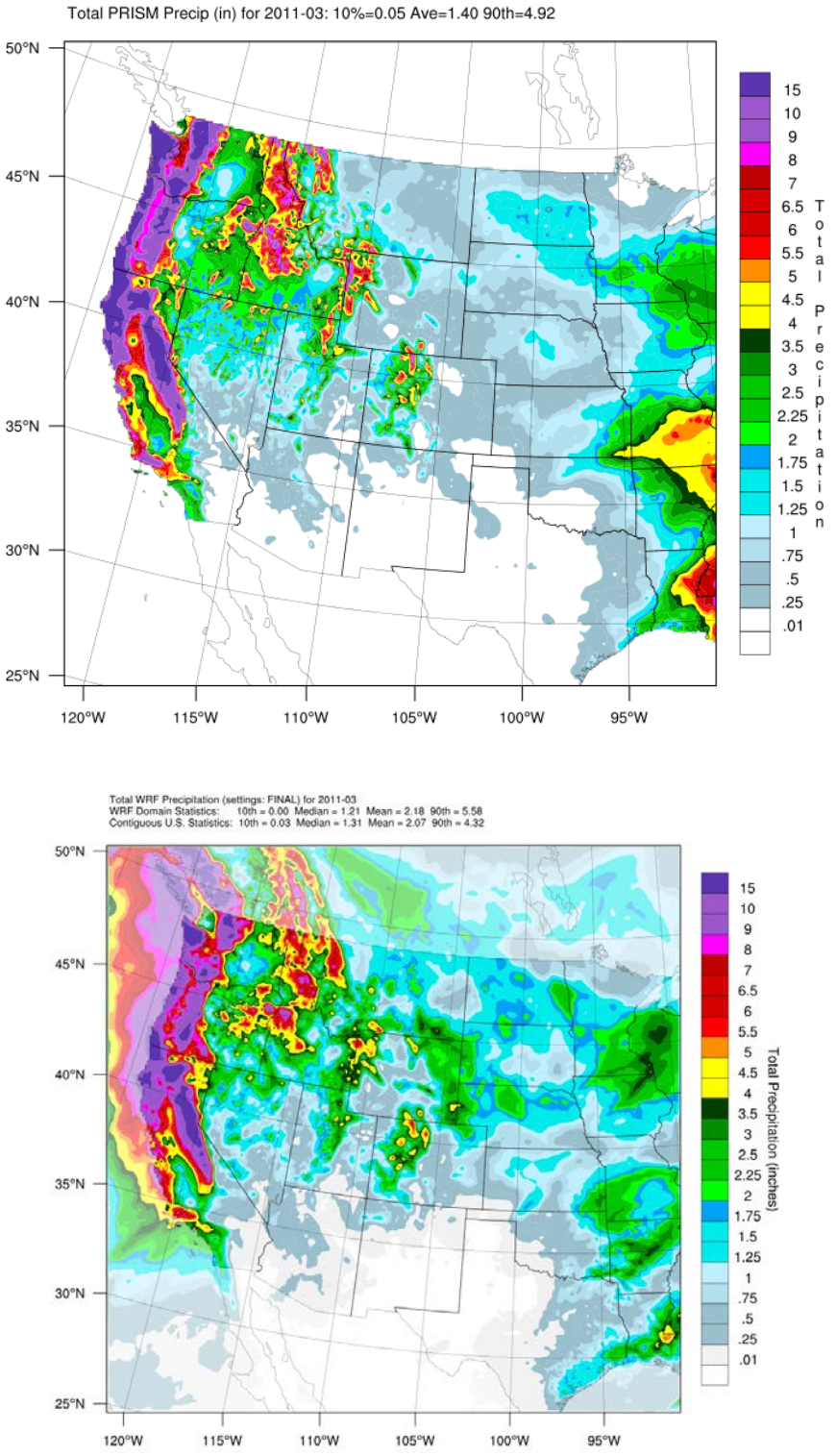

Figure 4-3b. Comparison of monthly total precipitation (inches) from PRISM (top) and WRF (bottom) for the 12 km WESTUS (d02) domain and the month of March 2011.

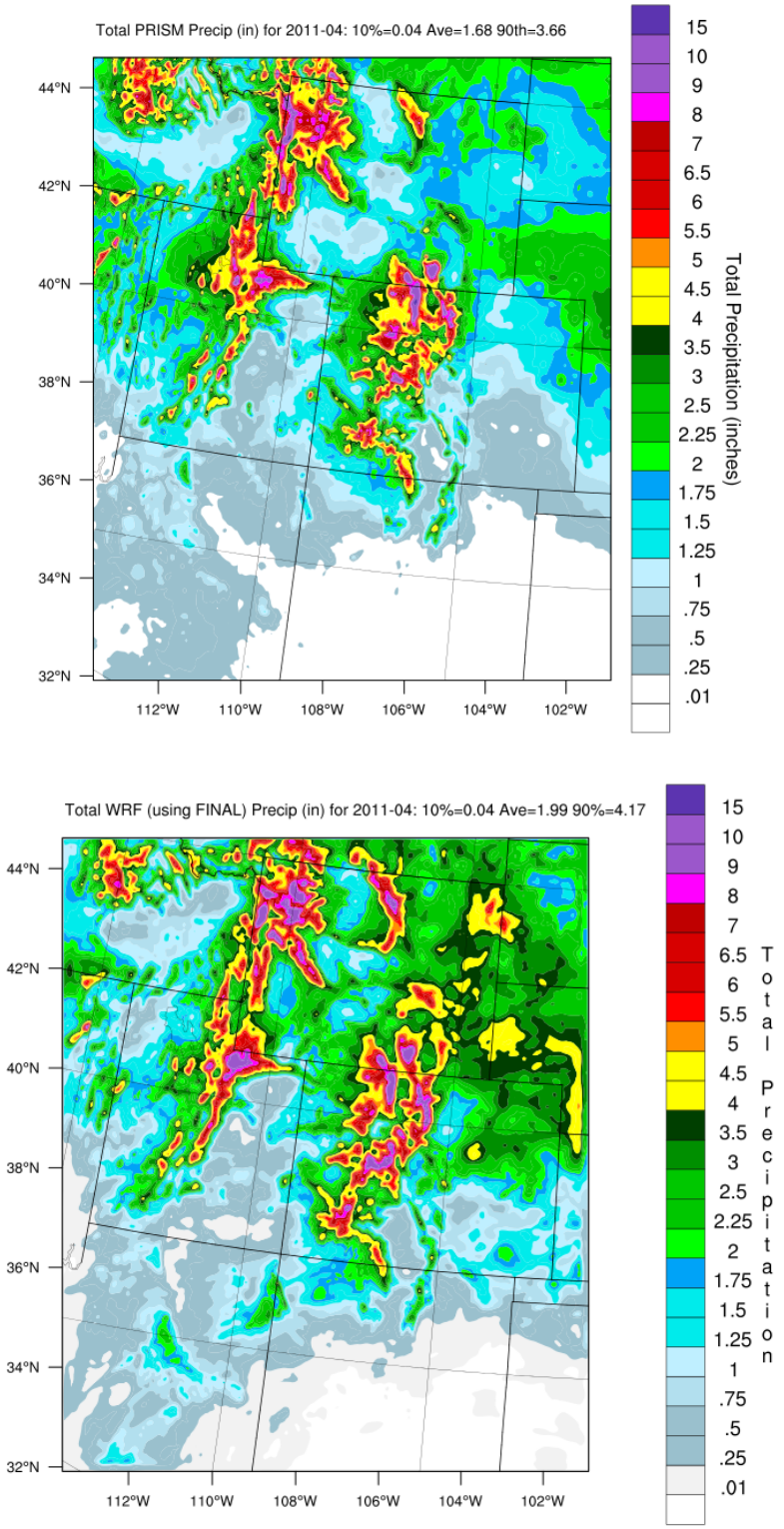

Figure 4-4a. Comparison of monthly total precipitation (inches) from PRISM (top) and WRF (bottom) for the 4 km three-state (d03) domain and the month of April 2011.

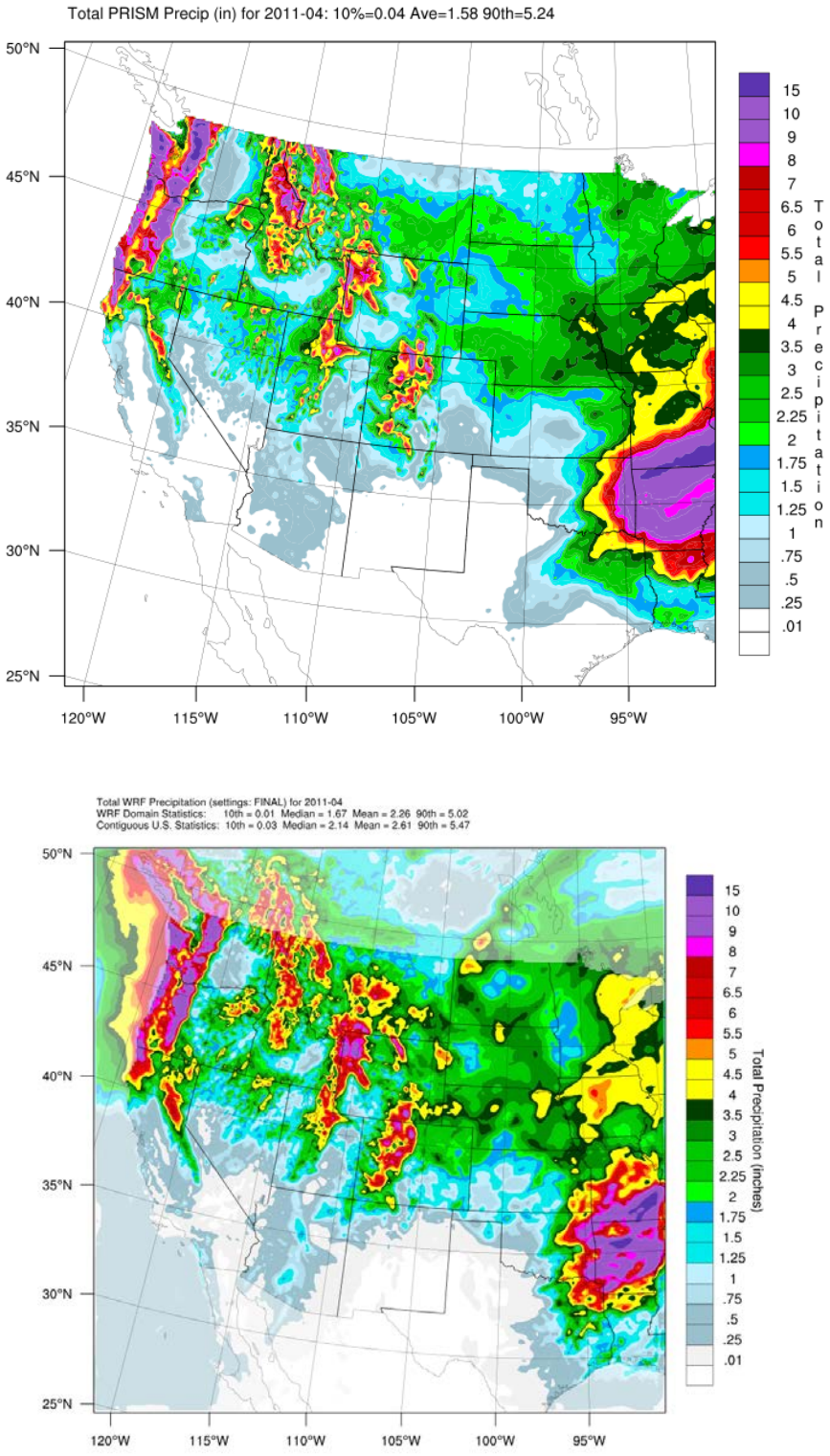

Figure 4-4b. Comparison of monthly total precipitation (inches) from PRISM (top) and WRF (bottom) for the 12 km WESTUS (d02) domain and the month of April 2011.

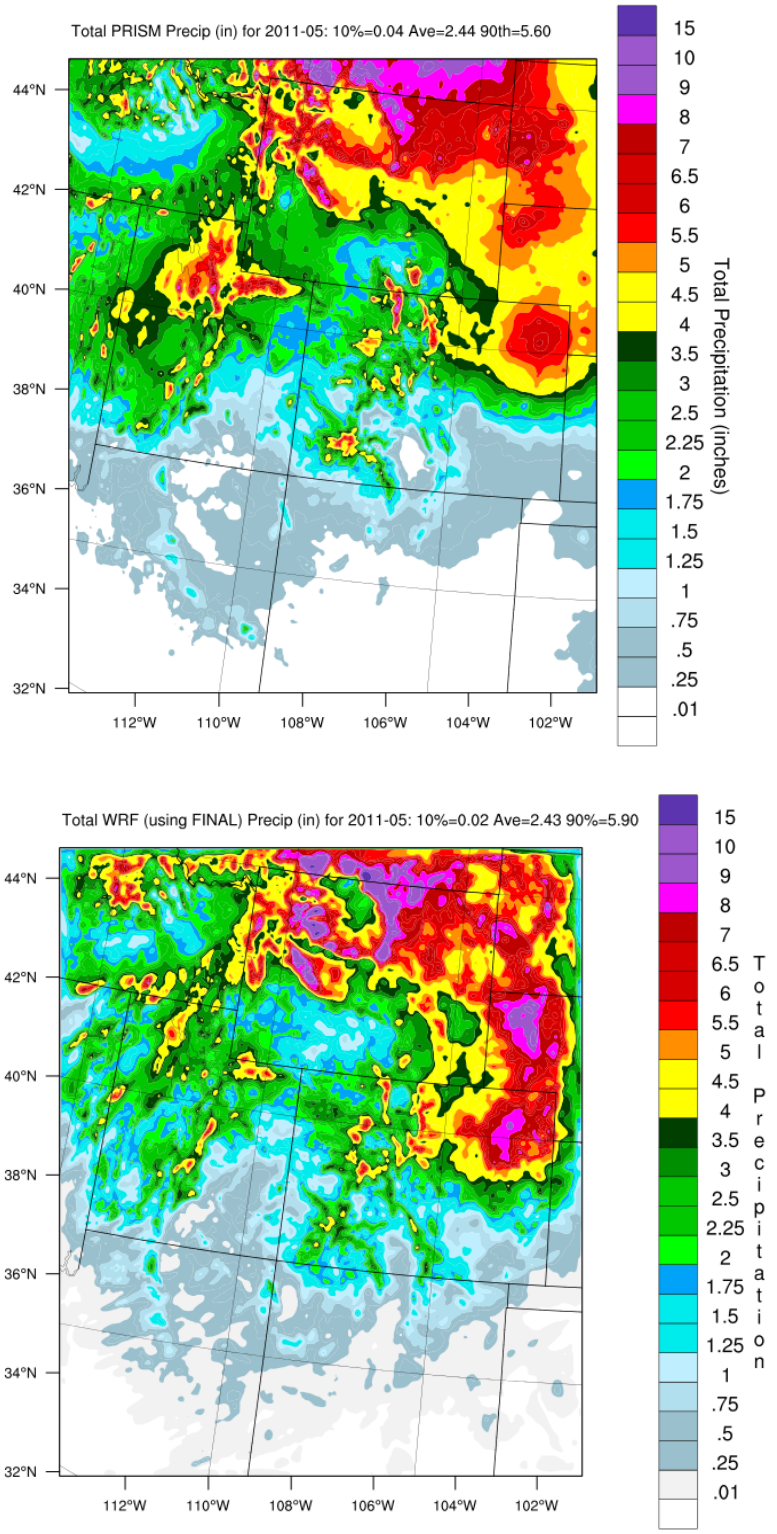

Figure 4-5a. Comparison of monthly total precipitation (inches) from PRISM (top) and WRF (bottom) for the 4 km three-state (d03) domain and the month of May 2011.

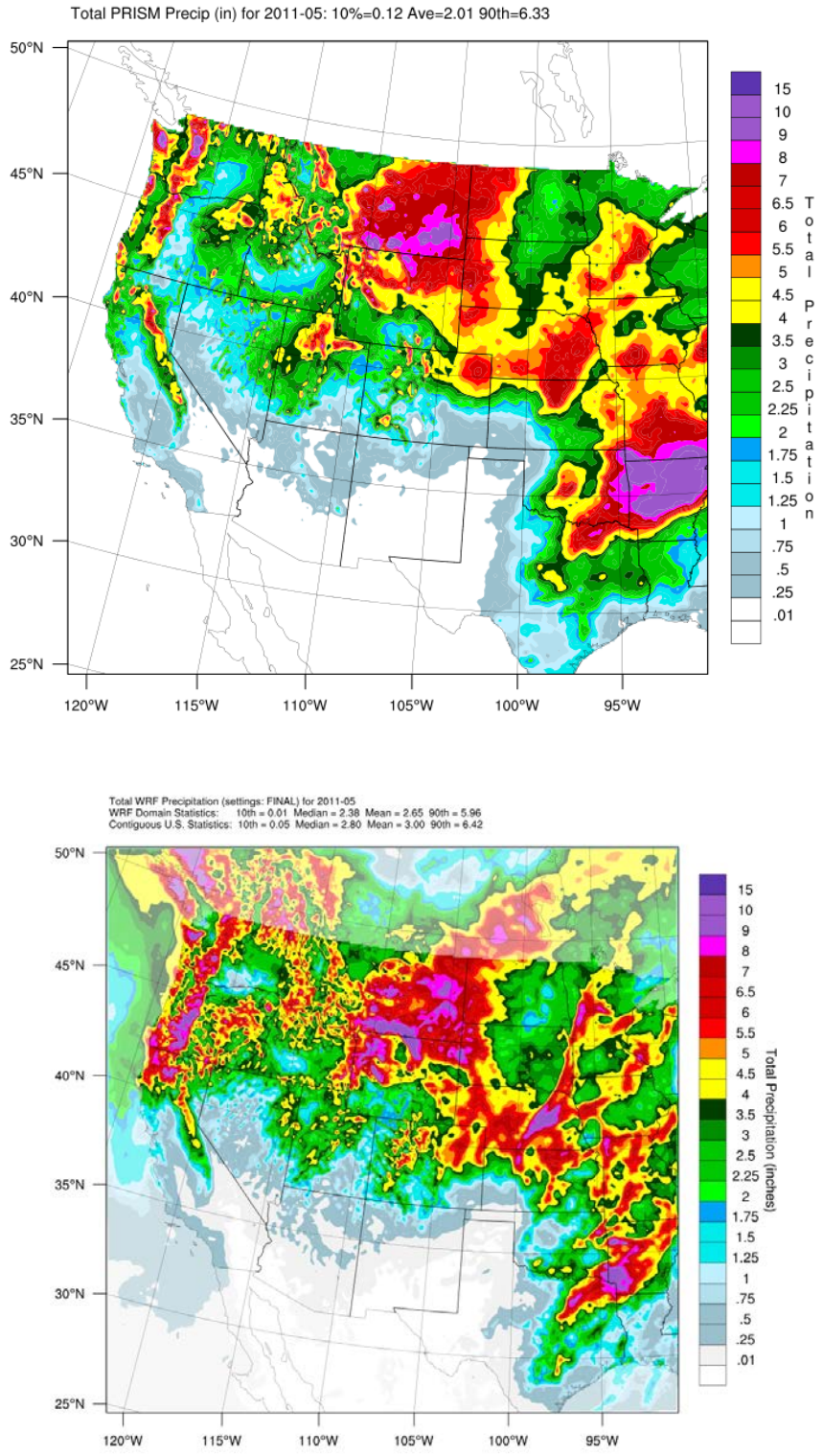

Figure 4-5b. Comparison of monthly total precipitation (inches) from PRISM (top) and WRF (bottom) for the 12 km WESTUS (d02) domain and the month of May 2011.

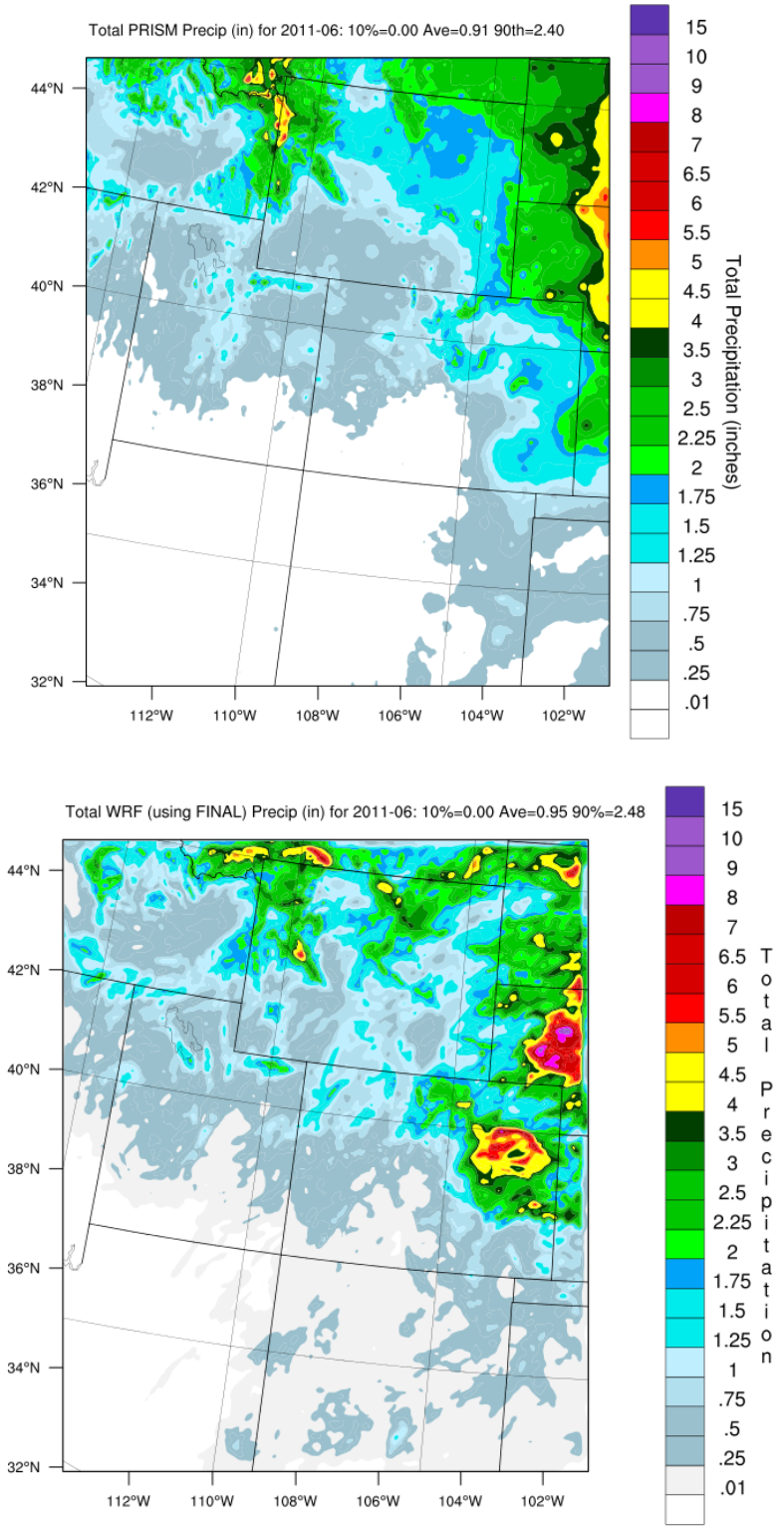

Figure 4-6a. Comparison of monthly total precipitation (inches) from PRISM (top) and WRF (bottom) for the 4 km three-state (d03) domain and the month of June 2011.

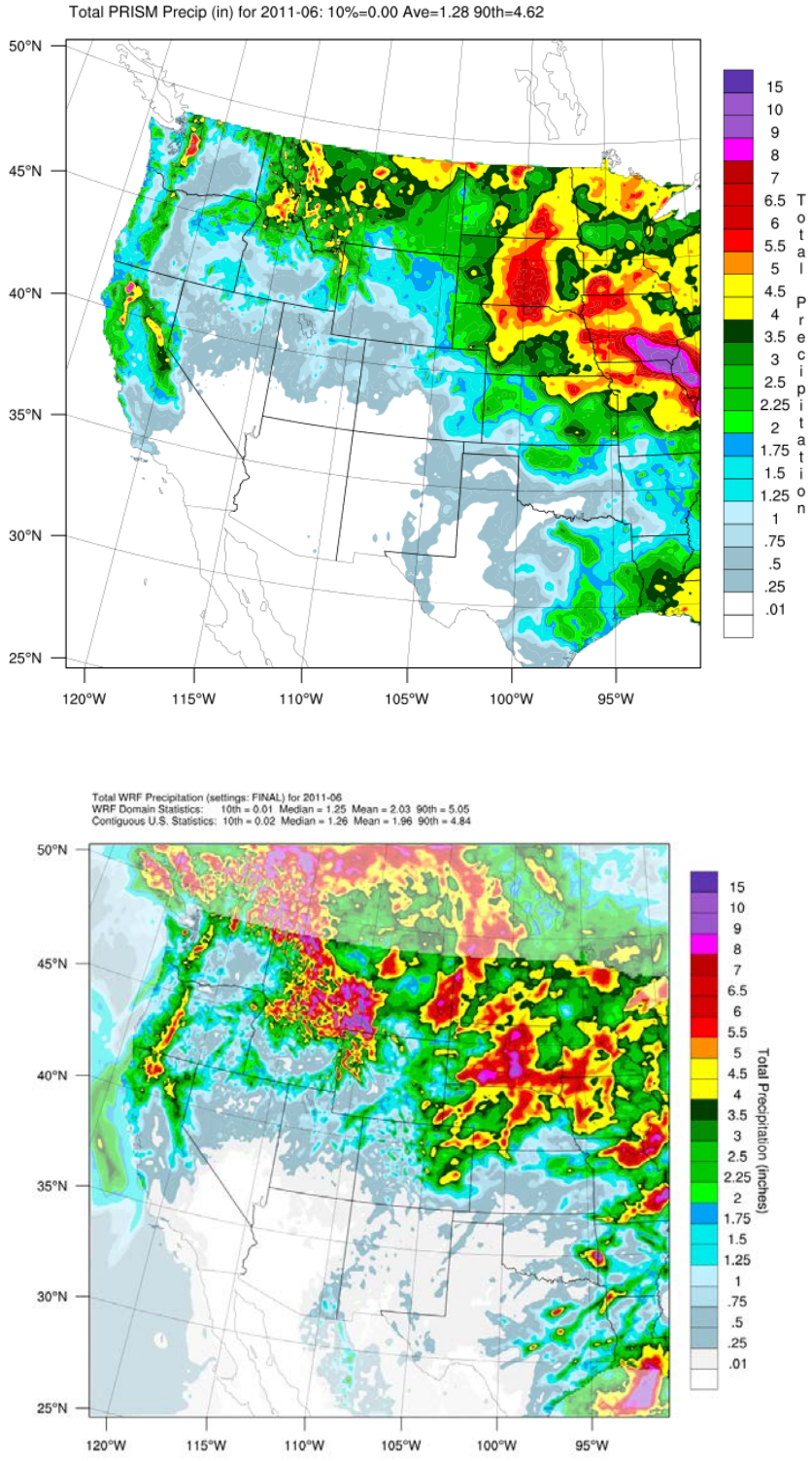

Figure 4-6b. Comparison of monthly total precipitation (inches) from PRISM (top) and WRF (bottom) for the 12 km WESTUS (d02) domain and the month of June 2011.

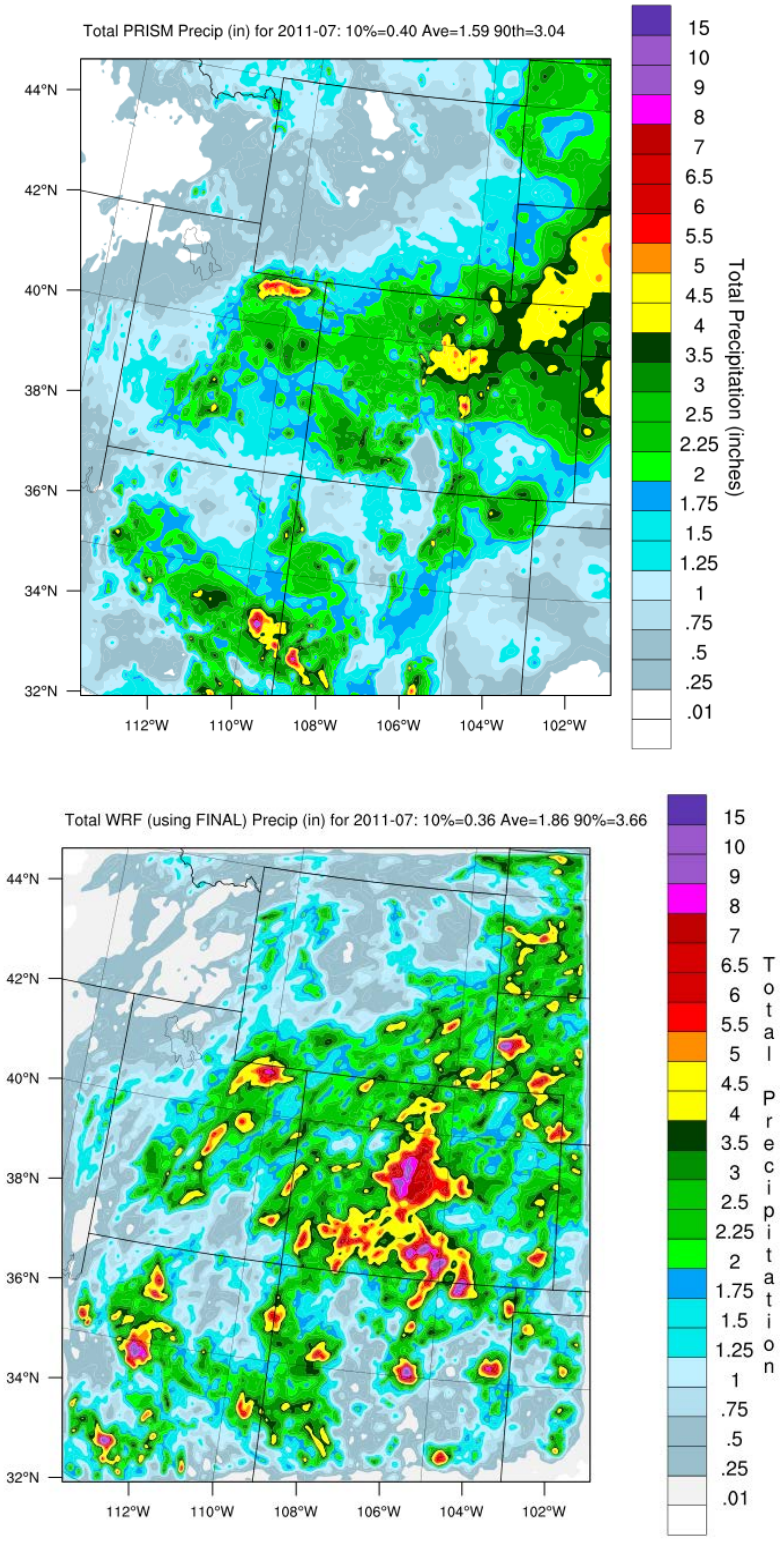

Figure4-7a. Comparison of monthly total precipitation (inches) from PRISM (top) and WRF (bottom) for the 4 km three-state (d03) domain and the month of July 2011.

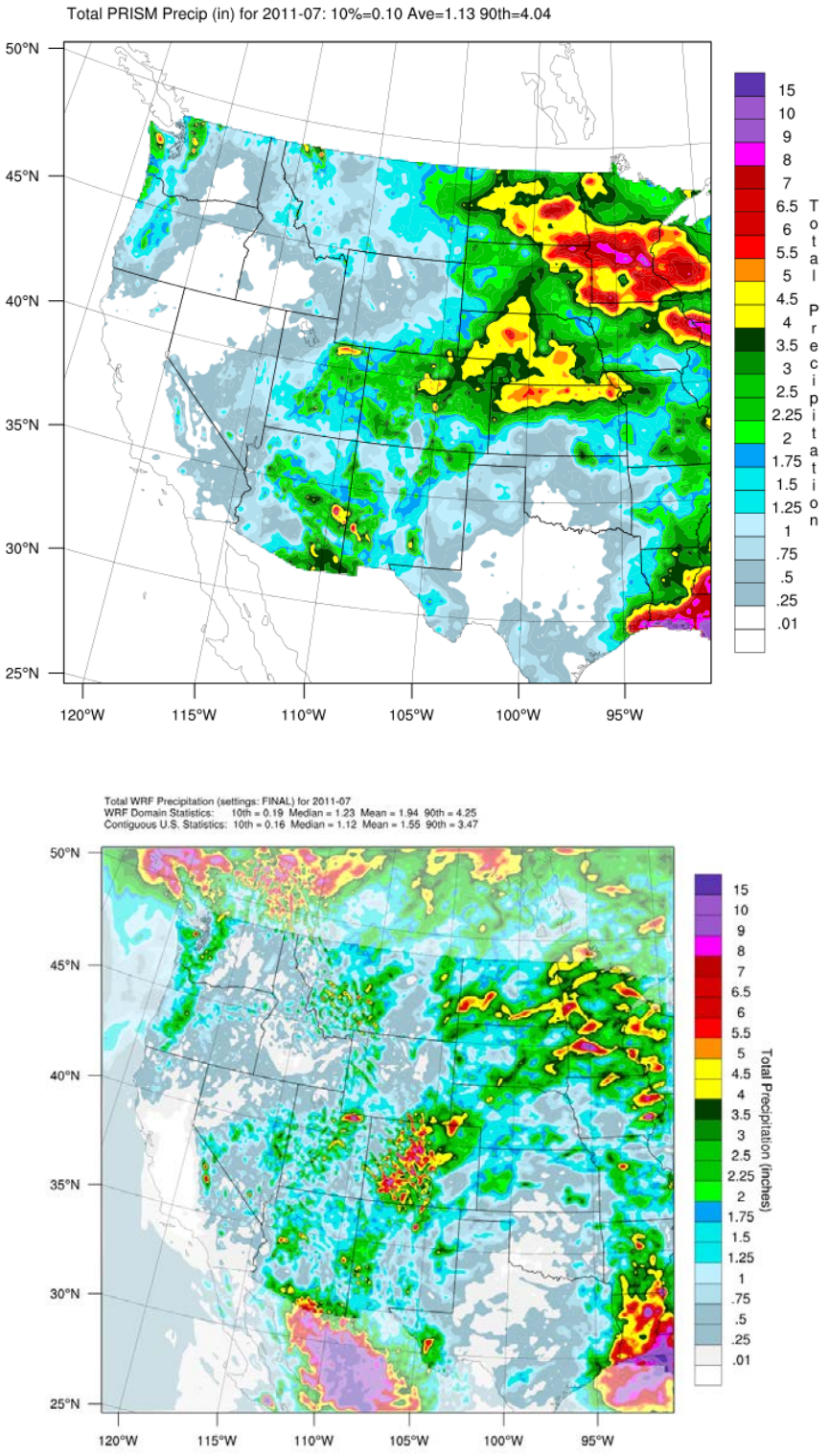

Figure 4-7b. Comparison of monthly total precipitation (inches) from PRISM (top) and WRF (bottom) for the 12 km WESTUS (d02) domain and the month of July 2011.

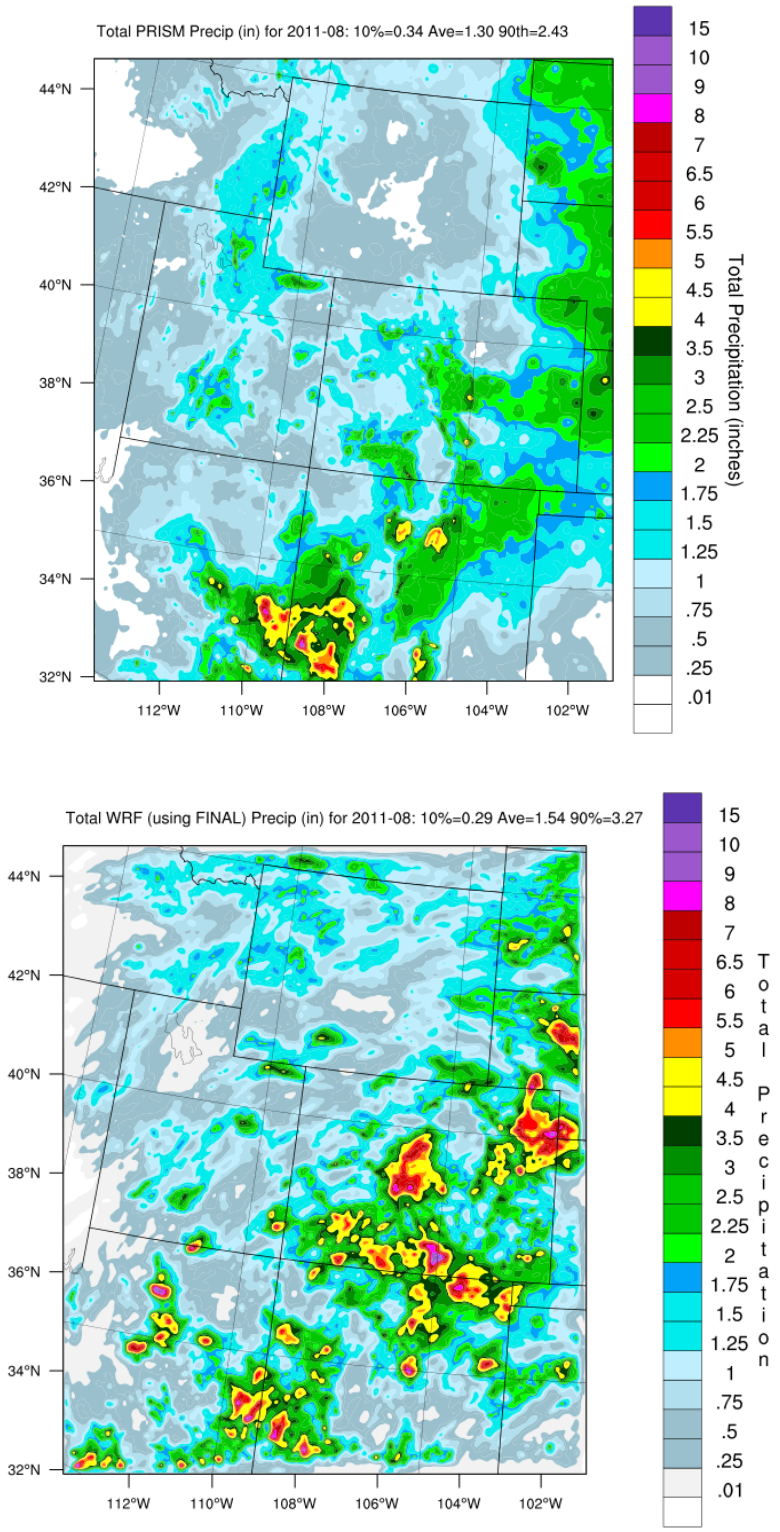

Figure 4-8a. Comparison of monthly total precipitation (inches) from PRISM (top) and WRF (bottom) for the 4 km three-state (d03) domain and the month of August 2011.

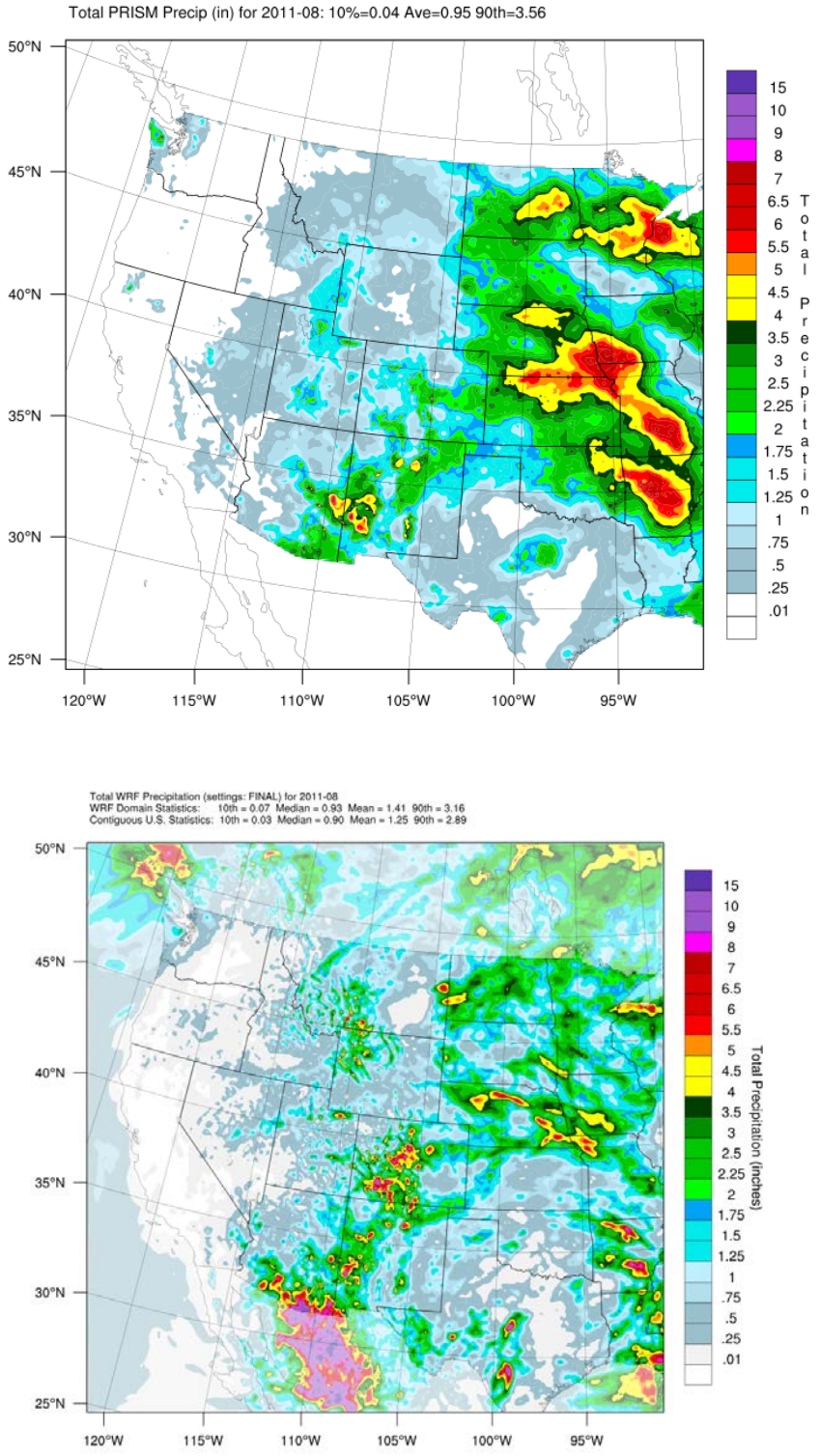

Figure 4-8b. Comparison of monthly total precipitation (inches) from PRISM (top) and WRF (bottom) for the 12 km WESTUS (d02) domain and the month of August 2011.

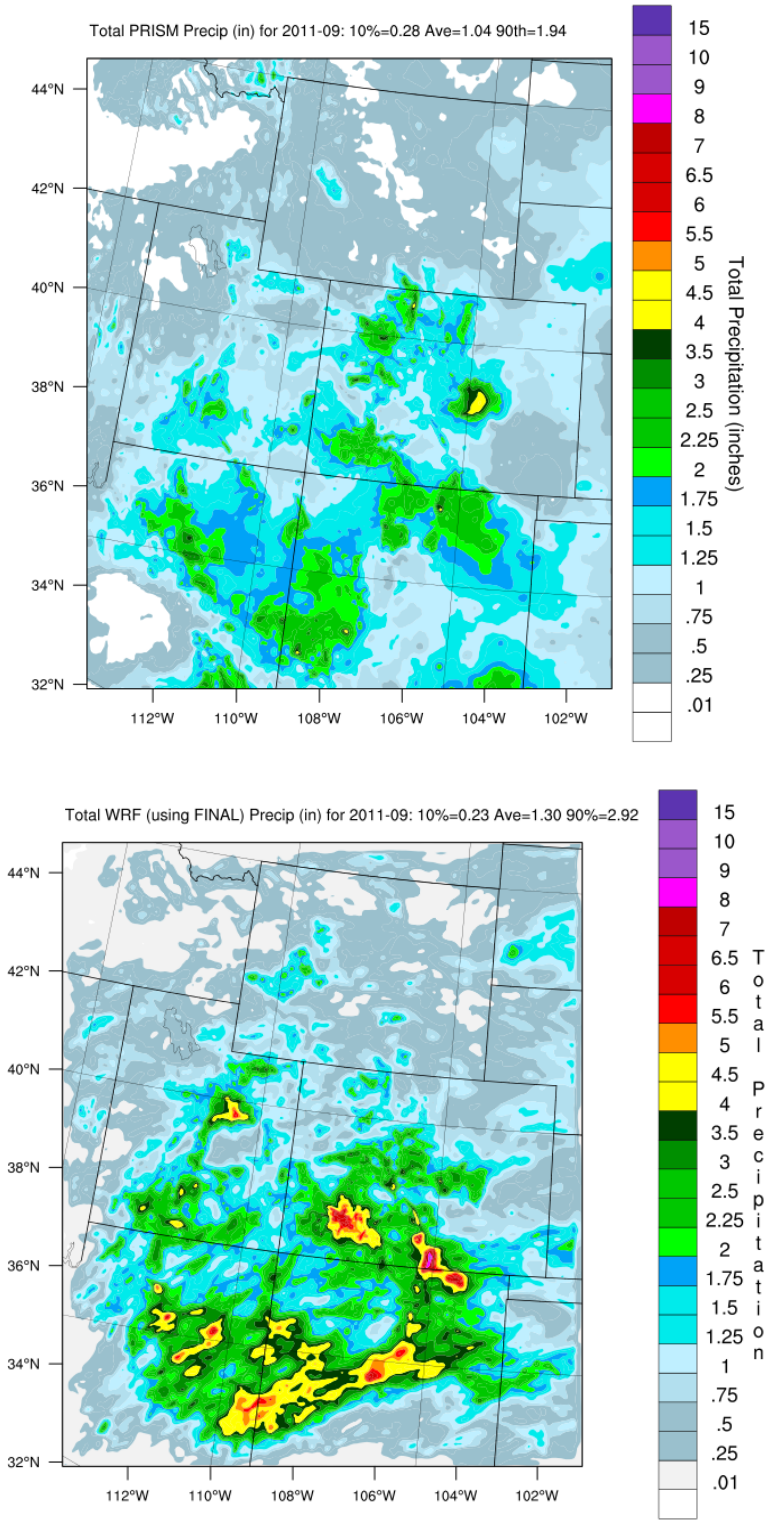

Figure 4-9a. Comparison of monthly total precipitation (inches) from PRISM (top) and WRF (bottom) for the 4 km three-state (d03) domain and the month of September 2011.

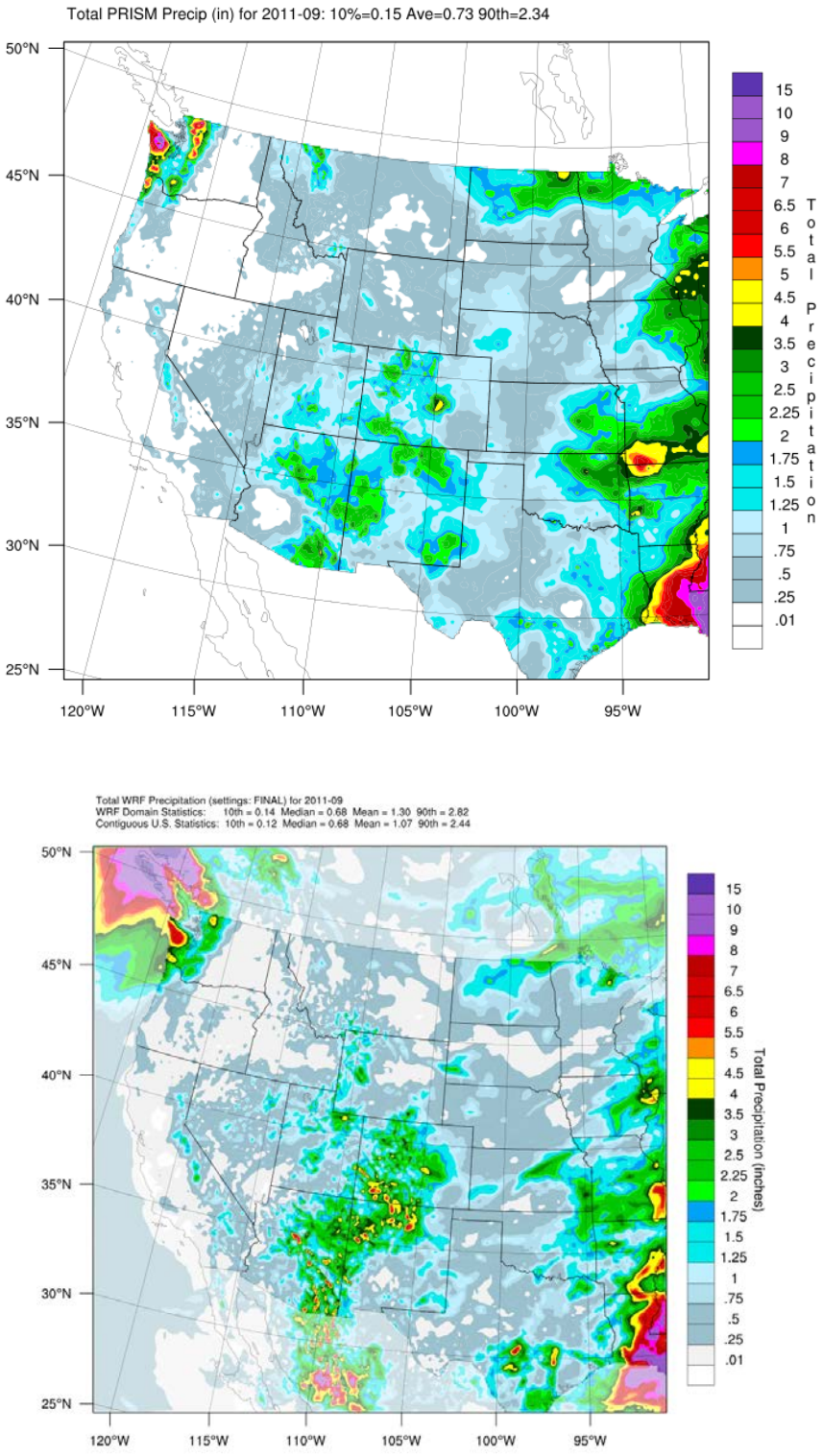

Figure 4-9b. Comparison of monthly total precipitation (inches) from PRISM (top) and WRF (bottom) for the 12 km WESTUS (d02) domain and the month of September 2011.

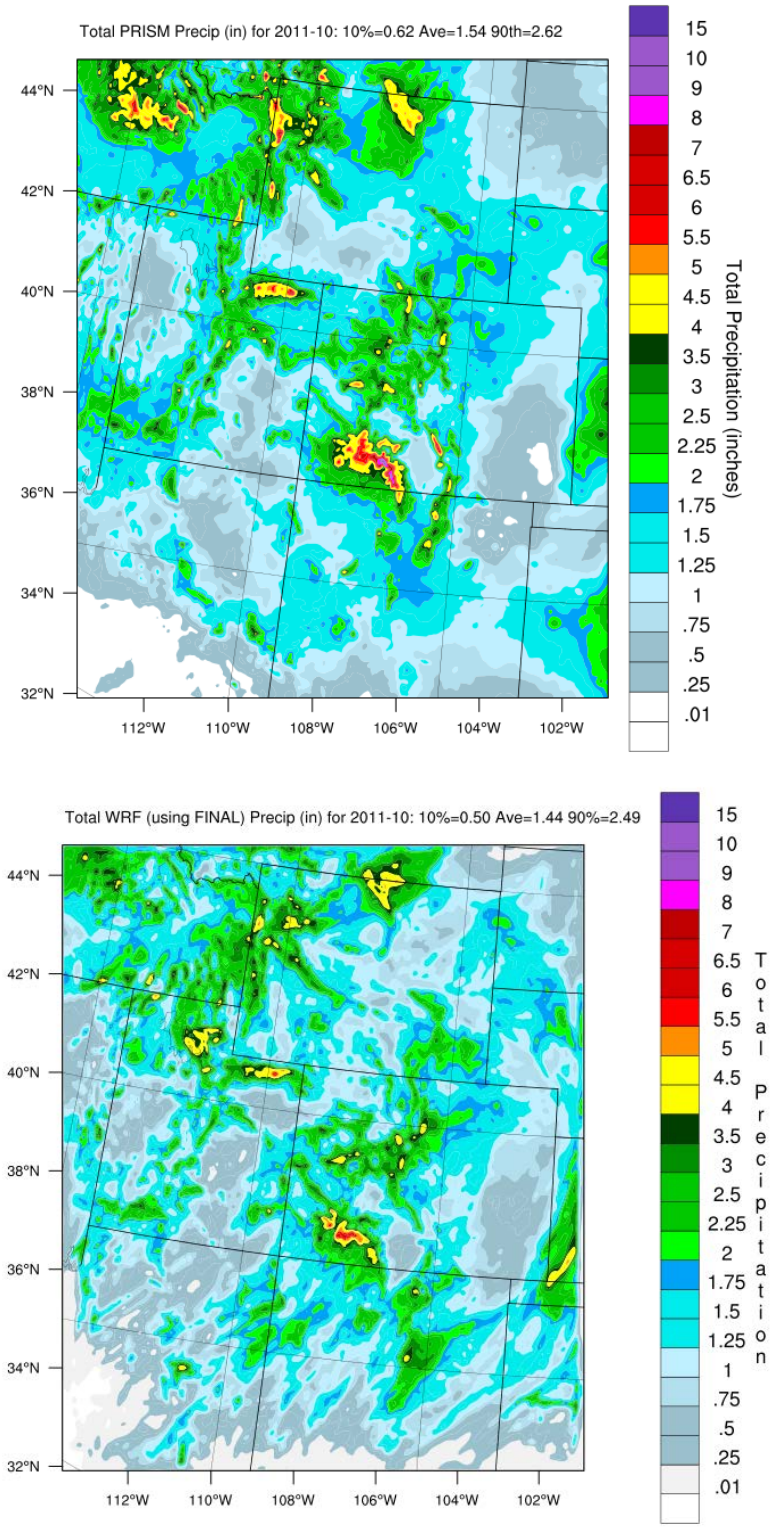

Figure 4-10a. Comparison of monthly total precipitation (inches) from PRISM (top) and WRF (bottom) for the 4 km three-state (d03) domain and the month of October 2011.

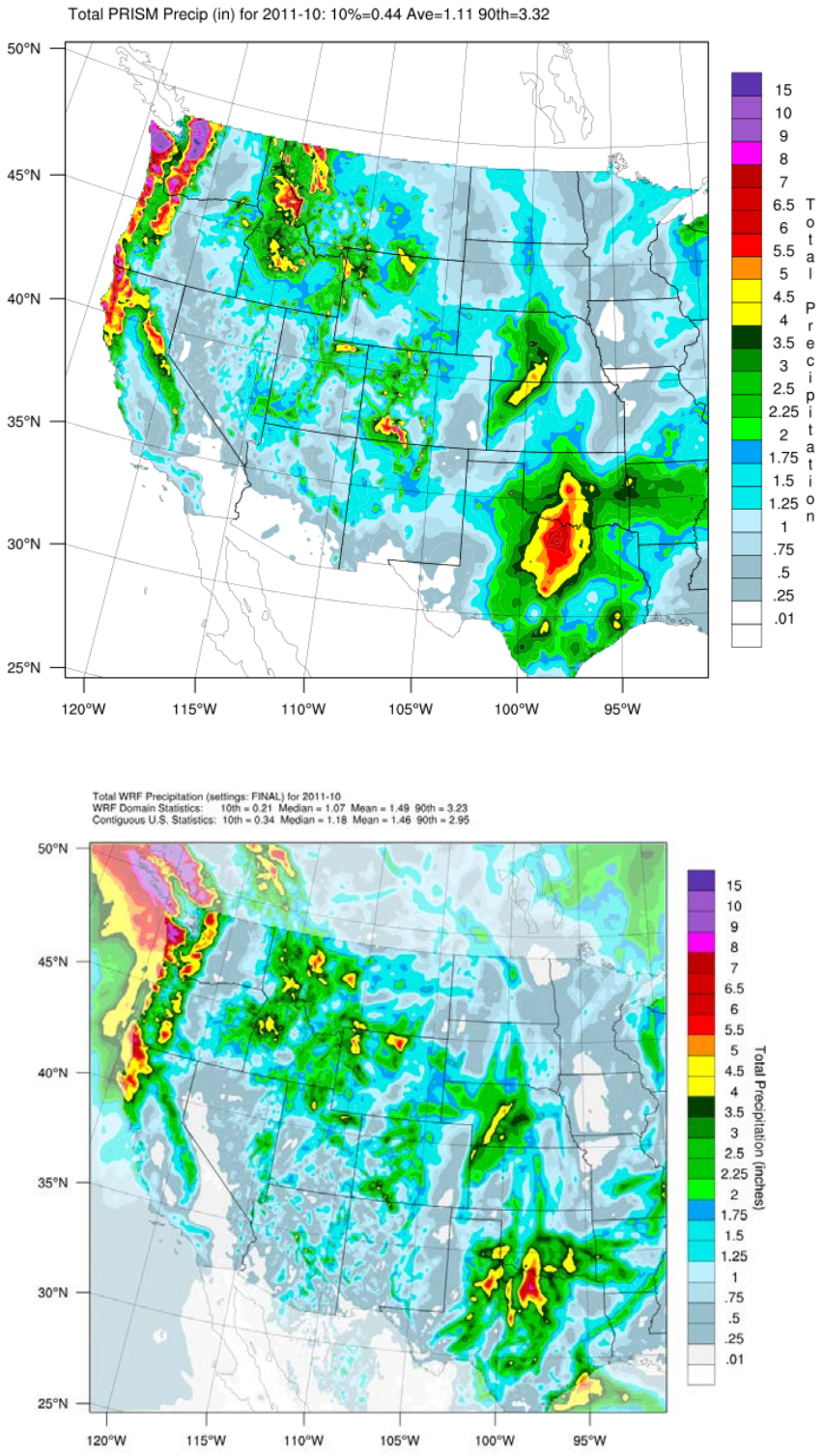

Figure 4-10b. Comparison of monthly total precipitation (inches) from PRISM (top) and WRF (bottom) for the 12 km WESTUS (d02) domain and the month of October 2011.

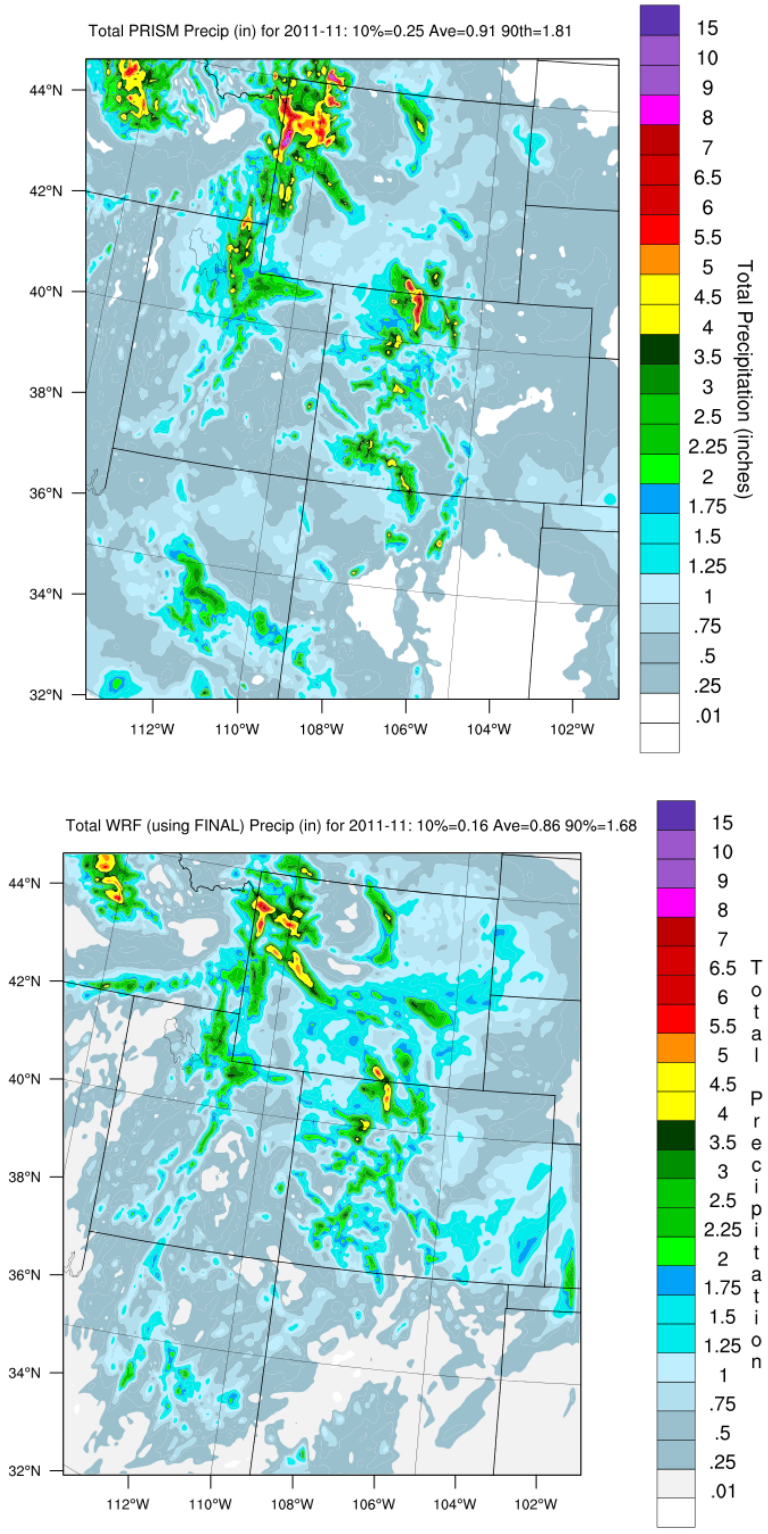

Figure 4-11a. Comparison of monthly total precipitation (inches) from PRISM (top) and WRF (bottom) for the 4 km three-state (d03) domain and the month of November 2011.

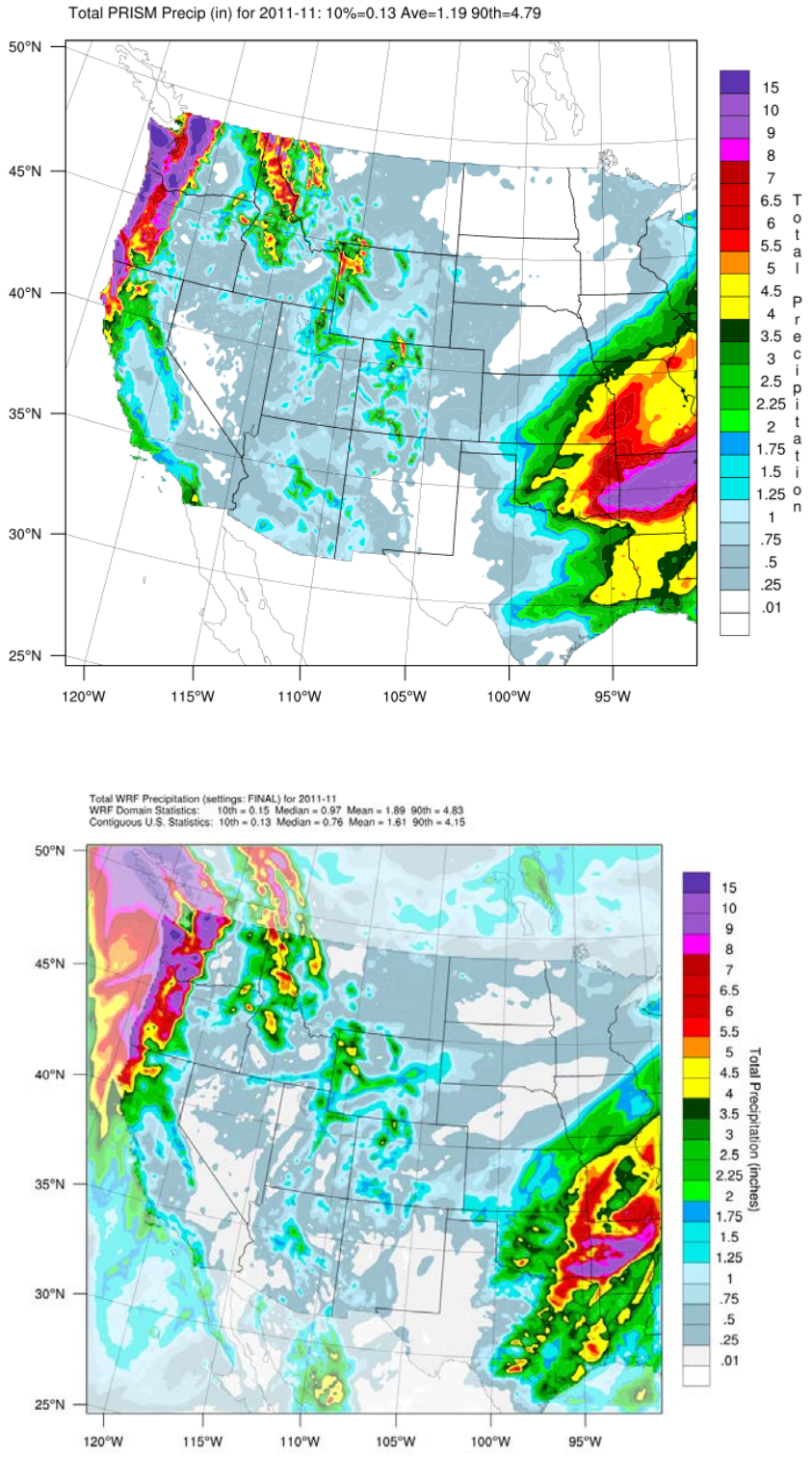

Figure 4-11b. Comparison of monthly total precipitation (inches) from PRISM (top) and WRF (bottom) for the 12 km WESTUS (d02) domain and the month of November 2011.

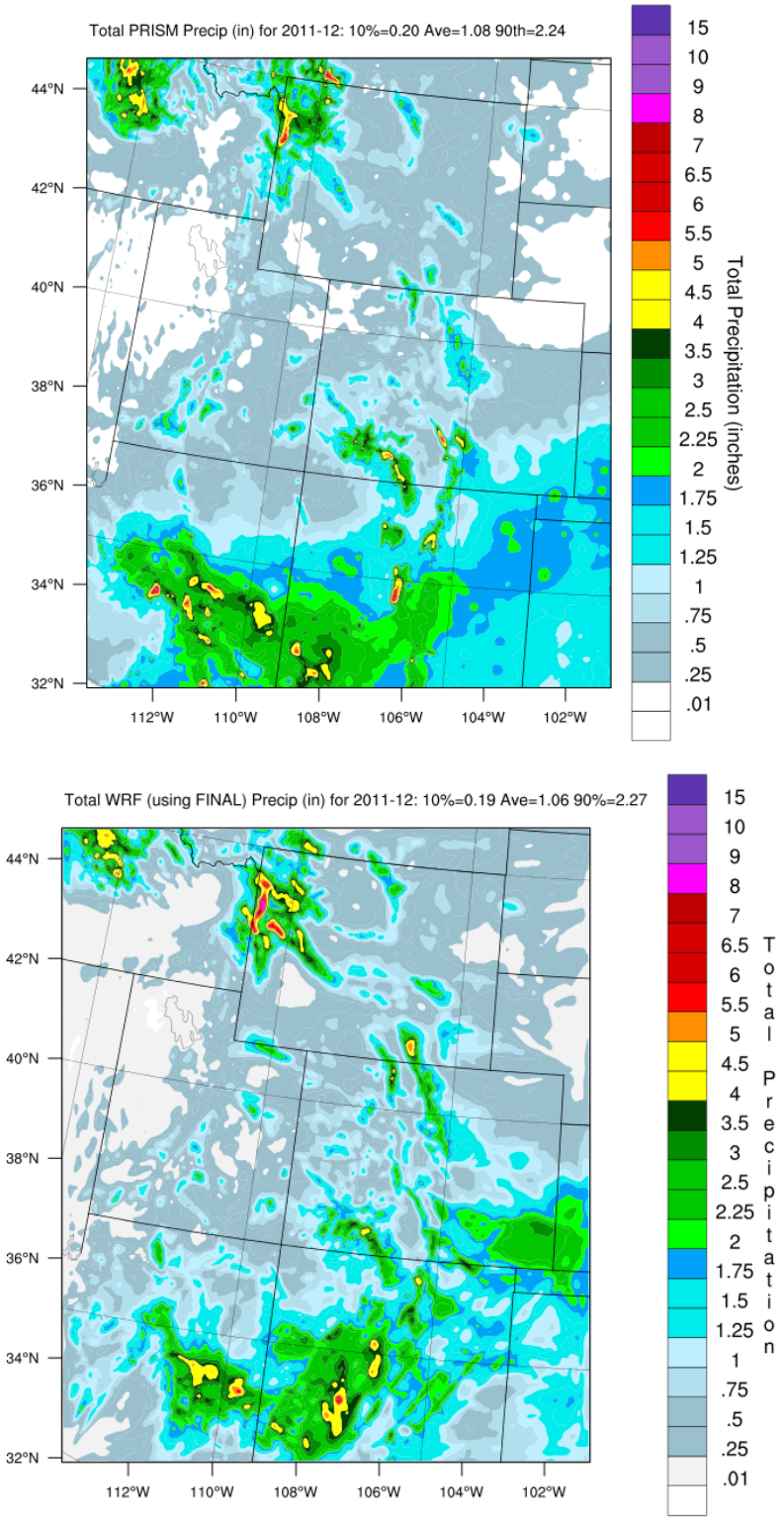

Figure 4-12a. Comparison of monthly total precipitation (inches) from PRISM (top) and WRF (bottom) for the 4 km three-state (d03) domain and the month of December 2011.

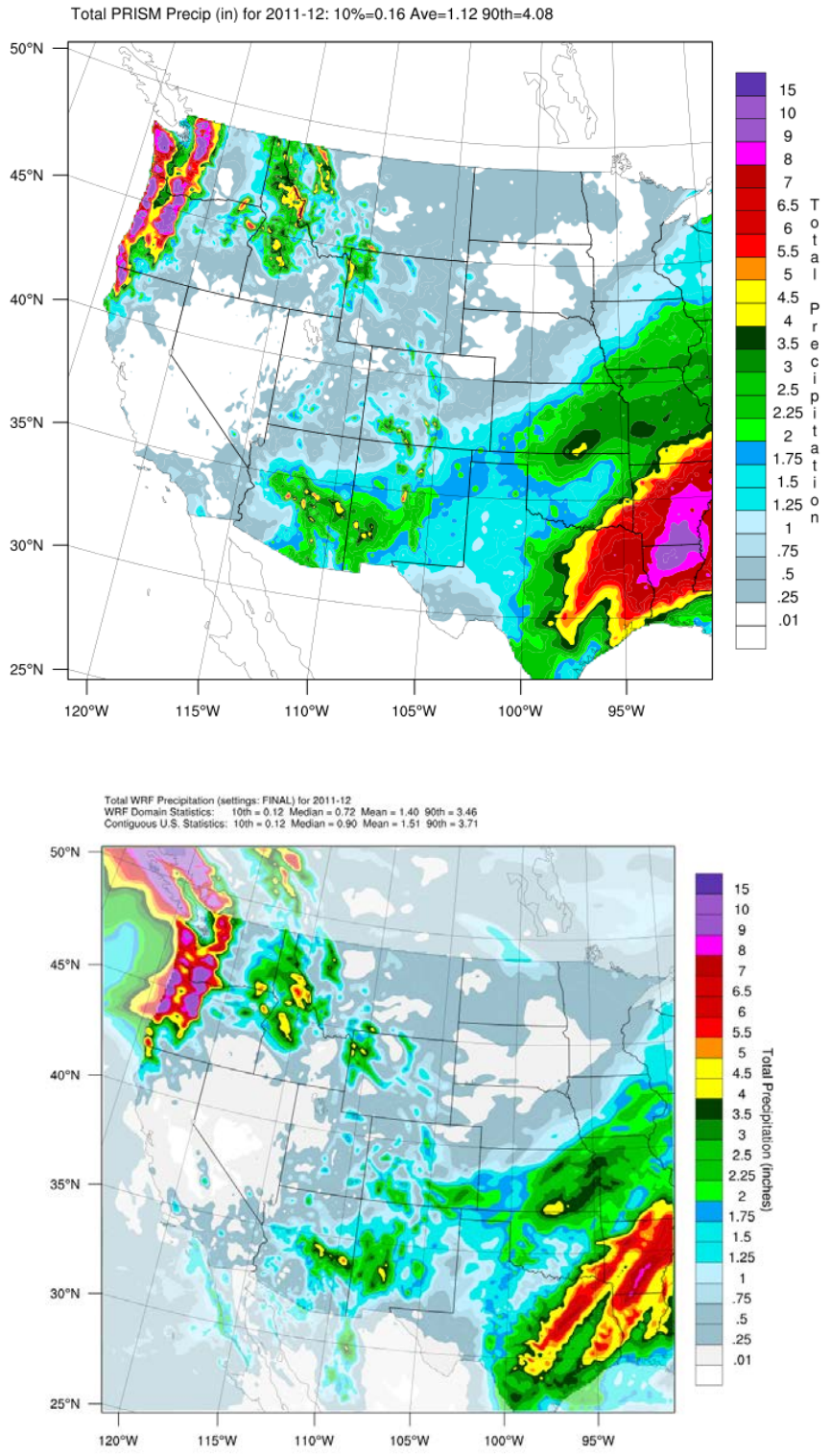

Figure 4-12b. Comparison of monthly total precipitation (inches) from PRISM (top) and WRF (bottom) for the 12 km WESTUS (d02) domain and the month of December 2011.

5.0 WRF MODEL PERFORMANCE EVALUATION FOR WINTER HIGH OZONE PERIOD

The WRF 2011 annual simulation included several periods with winter high observed ozone concentrations in the Jonah-Pinedale Anticline Development (JPAD) area in southwest Wyoming and within the Uinta Basin in Utah. There were 13 8-hour ozone exceedance (i.e., measured 8-hour ozone concentration greater or equal to 76.0 ppb) days in the JPAD area during February and March 2011 that occurred during the Upper Green River Winter Ozone Study (UGRWOS). A highest 8-hour ozone concentration of 123 ppb was measured on March 123 with a value of 121 ppb observed on March 3 and 12, 2011. The UGWOS collected special field study measurements that were used to evaluate the WRF 2011 performance during these wintertime conditions.

Although the current WRF 2011 36/12/4 km simulation was not configured for simulating the winter ozone event periods, a preliminary evaluation against meteorological observations during high winter ozone periods will help set the table for more focused WRF modeling of the high winter periods that are planned in next stage of the 3SAQS as part of the 3SAQS 2015 scope of work starting in October 2014.

The 3SAQS 2011 WRF 4 km modeling results were evaluated against two sets of meteorological measurements to evaluate model performance in the JPAD area during February and March 2011 when winter ozone events occurred. The first dataset was the NOAA routine Integrated Surface Hourly Observations database (ds3505 database) and the second dataset consisted of surface hourly measurements from nine sites used in the UGWOS. The locations of the nine UGRWOS surface monitoring sites are given in Table 5-1 and Figure 5-1. Also shown in Figure 5-1 is the location of the tall tower and tethered balloon where upper-air sound measurements were collected for temperature that is compared against the WRF vertical temperature profile estimates.

Table 5-1. Nine surface monitoring sites from the 2011 UGRWOS.

Site	Latitude	Longitude
Daniel South	42.79°N	110.06°W
Juel Springs	42.37°N	109.56°W
Mobile Trailer	42.68°N	109.81°W
Moxa	41.75°N	109.79°W
Pinedale	42.87°N	109.88°W
Boulder	42.72°N	109.75°W
South Pass	42.53°N	108.72°W
Big Piney	42.49°N	110.10°W
Wyoming Range	42.98°N	110.35°W

Figure 5-1.Locations of the nine UGRWOS surface monitoring sites.

The WRF model performance evaluation assessed the accuracy of the predicted surface, near surface and upper air meteorological parameters near the UGRB site and within the 4 km modeling domain. Meteorological modeling is often limited by the proximity of observational data to the location of interest, but the temporary meteorological station network created for the 2011 UGWOS study ensured that sufficient data is sampled near the basin.

Table 5-2 lists the meteorological model performance benchmarks for simple (Emery et al, 2001) and complex conditions, where we have adapted the complex benchmarks from Kemball-Cook et al., (2005). Note that the benchmarks differ slightly from those used in Chapter 3 since different software was used to generate the soccerplots.

Table 5-2. Meteorological model performance benchmarks for simple and complex conditions used to evaluate WRF winter model performance.

Table 5-2. Meteorological model performance benchmarks for simple and complex conditions used to evaluate WRF winter model performance.

Parameter	Simple	Complex
Temperature Bias	≤ ±0.5 K	≤ ±2.0 K
Temperature Error	≤ 2.0 K	≤ 3.5 K
Humidity Bias	≤ ±0.8 g/kg	≤ ±1.0 g/kg
Humidity Error	≤ 2.0 g/kg	≤ 2.0 g/kg
Wind Speed Bias	≤ ±0.5 m/s	≤ ±1.5 m/s
Wind Speed RMSE	≤ 2.0 m/s	≤ 2.5 m/s
Wind Direction Bias	≤ ±10 degrees	≤ ±10 degrees
Wind Direction Error	≤ 30 degrees	≤ 55 degrees

The elevated ozone concentrations occur in the JPAD area, the following conditions are necessary:

- White snow on ground.
- Clear skies or little cloud cover.
- Slow to stagnant wind speeds.
- Shallow surface inversion layer.

These cold pooling meteorological conditions with stagnant winds and shallow inversion allows VOC and NO_X emissions from oil and gas sources to pool and build up to produce high concentrations. The snow cover results in a high albedo that reflects ultraviolet radiation producing photochemical photolysis rates that are almost double their normal values and comparable to summer levels. These meteorological phenomena need to be kept in mind when evaluating WRF's ability to simulate winter conditions under high ozone episodes.

5.1 Winds

The WRF February and March 2011 model performance was fair against the UGRB on-site data (Figure 5-2) and reasonable against the routine ds3505 data (Figure 5-3). Wind direction bias was ≤±5 degrees using the UGRWOS data and even better for the ds3505 data but there was very high wind direction error that varied from 75-80 degrees for both months against on-site data, but met the complex benchmark (≤ 55 degrees) for the ds3505 data. Wind speeds were slightly negatively biased (0 to -0.5 m/s) against both on-site and ds3505 data. Wind speed index of agreement exceeded the benchmark against the ds3505 data, while the on-site data did not. Wind speed error were in the 2.5 to 3.0 m/s range using the UGRWOS data so failed to achieve the complex benchmark, whereas the complex benchmark was achieved using the ds3505 observations. Wind speed and direction errors for the two months suggest that WRF has some difficulty modeling wind speed and direction at small scales over complex terrain. As shown below, the February through March period corresponds to a significant number of strong surface inversions. The low wind speed and direction bias is encouraging and it is not surprising that WRF has high wind speed and direction errors under slow to stagnant wind conditions as occur during the winter ozone events.

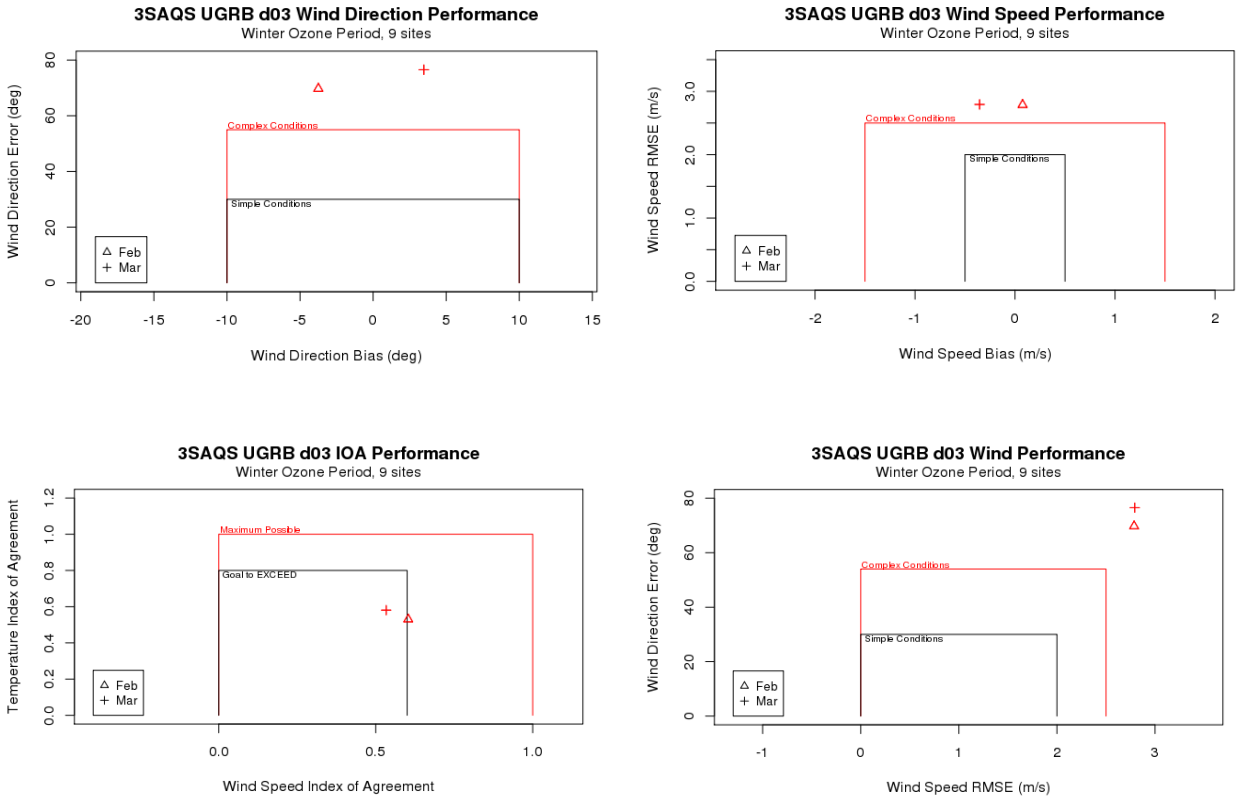

Figure 5-2. Soccer plots of averaged daily statistical performance for winds in the 4 km grid evaluated against nine local sites in the UGRB: (top left) wind direction error vs. wind direction bias; (top right) wind speed RMSE vs. wind speed bias; (bottom left) temperature IOA vs. wind speed IOA; (bottom right) wind direction error vs. wind speed RMSE.

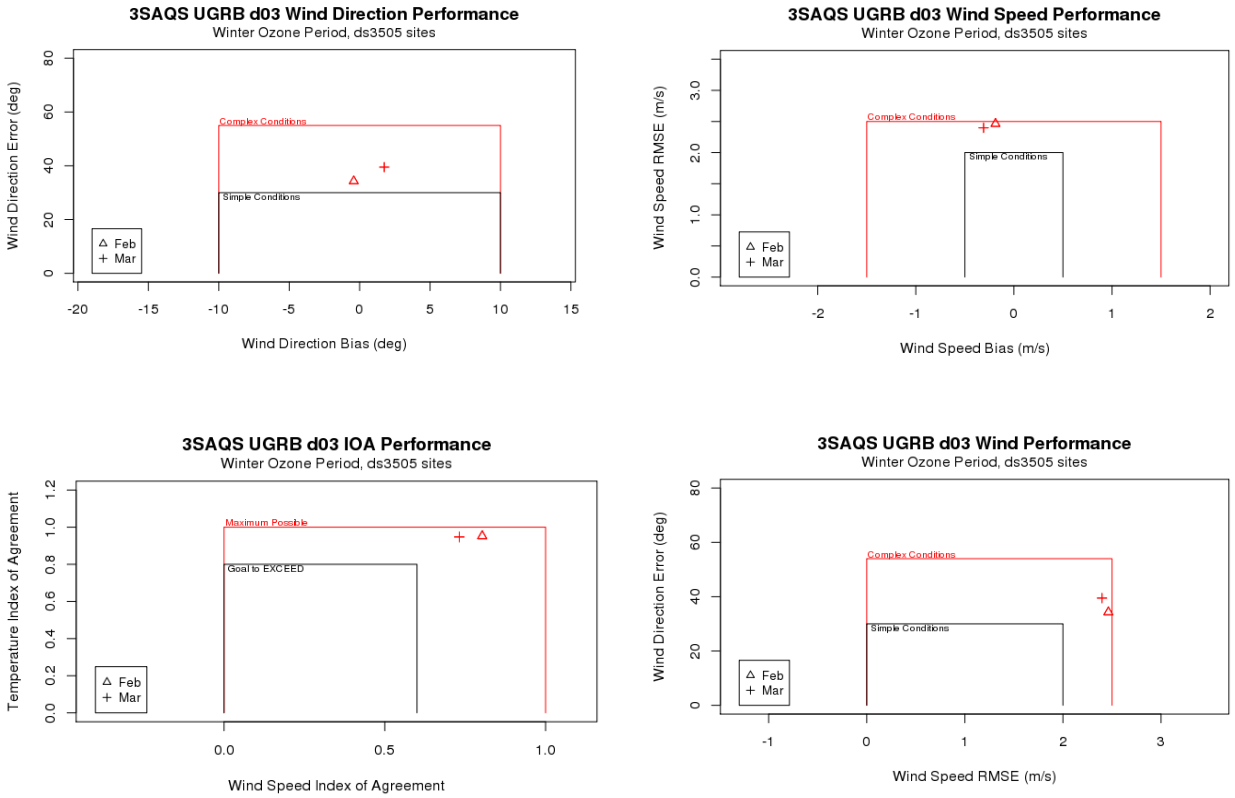

Figure 5-3. Soccer plots of averaged daily statistical performance for winds in the 4 km grid evaluated against ds3505 sites in the UGRB: (top left) wind direction error vs. wind direction bias; (top right) wind speed RMSE vs. wind speed bias; (bottom left) temperature IOA vs. wind speed IOA; (bottom right) wind direction error vs. wind speed RMSE.

5.2 Temperature

Soccerplots of WRF temperature bias and error during February and March 2011 in the UGR area are shown in Figure 5-4 that displays a slight cold bias (0-1.5 K) for the two winter months using both the on-site and ds3505 data. Temperature error varied from 2.0 -4.0 K, only meeting the complex conditions against the ds3505 data. The differences in temperatures depend on the location of the observation sites and potential measurement bias. WRF slightly under predicted the cold pooling conditions in the basin.

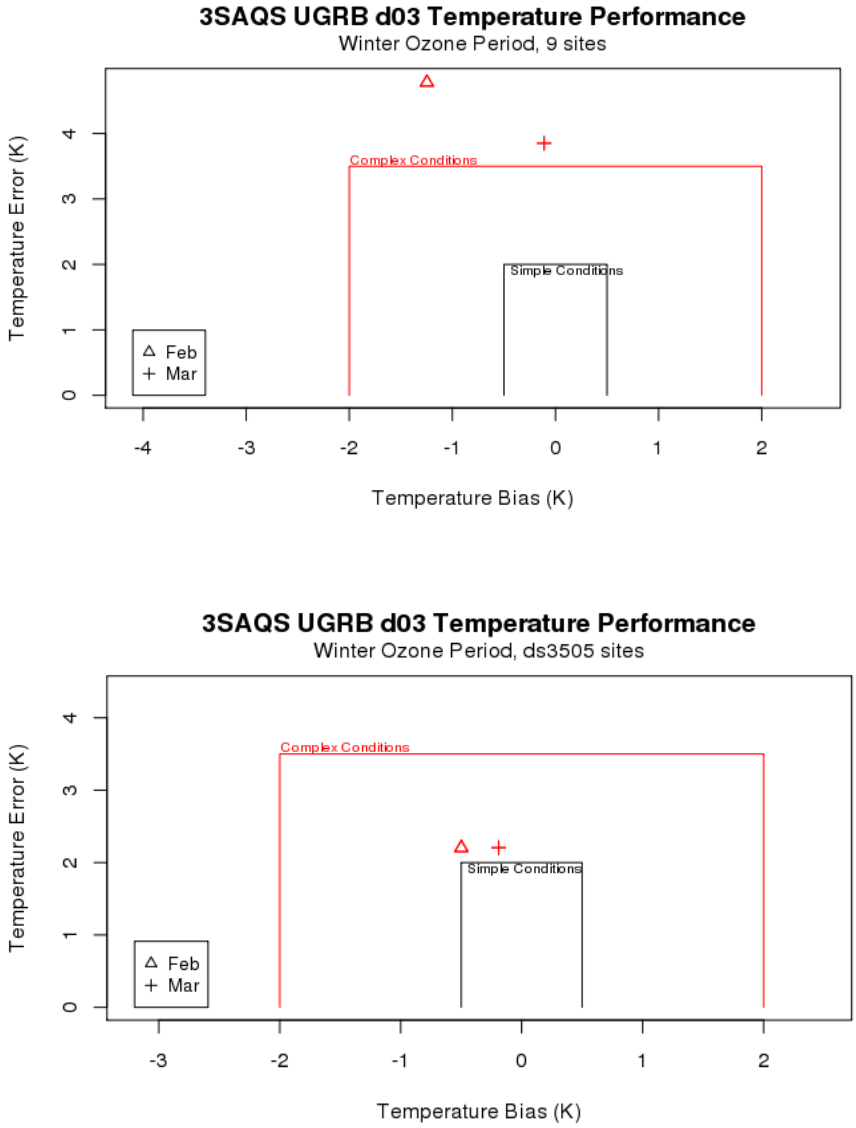

Figure 5-4. Soccer plots of averaged daily statistical performance for temperature in the 4 km grid evaluated against nine local sites in the UGRB (top) and ds3505 sites (bottom).

5.3 Humidity

WRF performed well for humidity for both the on-site and ds3505 data as seen in Figure 5-5. Humidity bias met the stricter benchmark for simple conditions for the on-site data and met the benchmark for complex conditions in February for the ds3505 data. Humidity error was below the benchmark for simple conditions (between 0.5-1.0 g/kg) for both sets of data. Cold wintertime temperatures dictate low humidity values and correspondingly low humidity errors.

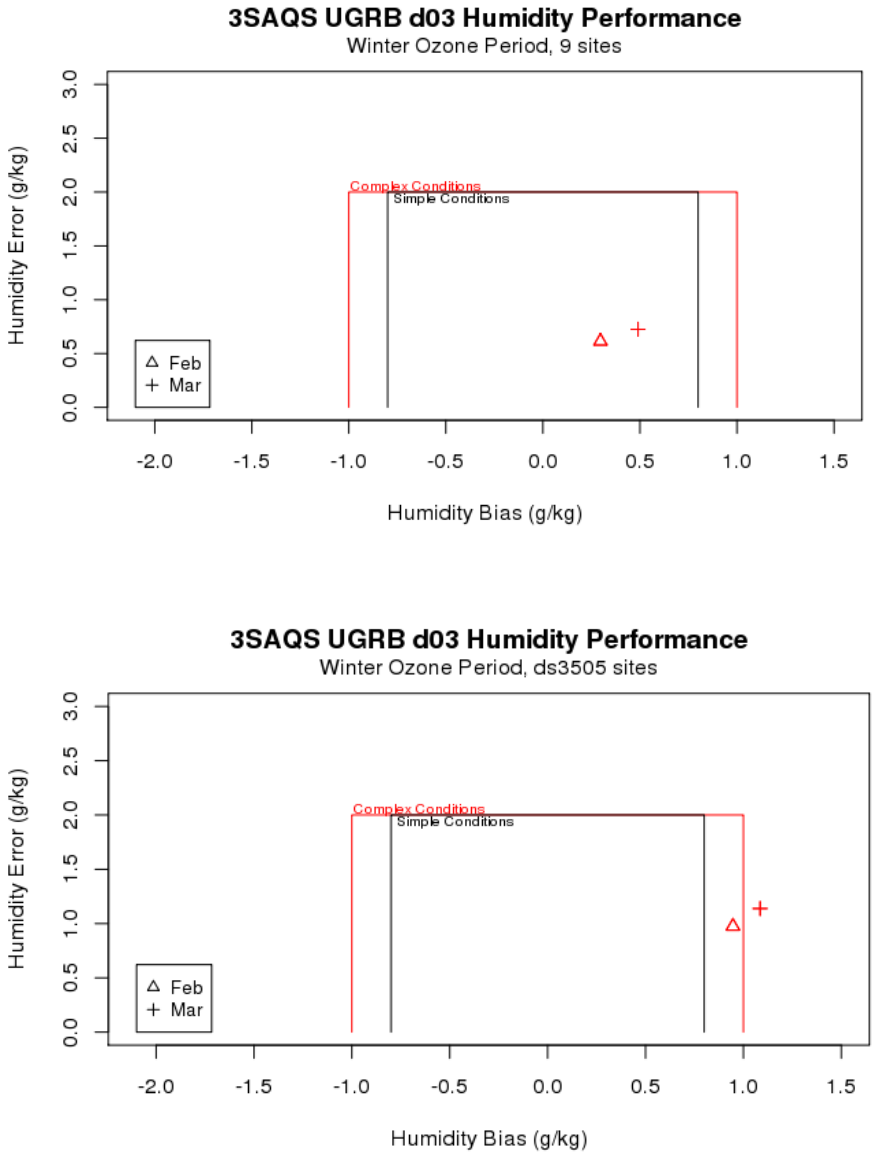

Figure 5-5. Soccer plots of averaged daily statistical performance for humidity in the 4 km grid evaluated against nine local sites in the UGRB (top) and ds3505 sites (bottom).

5.4 Vertical Profiles

Vertical stability and trapping inversions represents one of the most important meteorological phenomena for producing elevated ozone events in the winter. Vertical profiles were available from a tall tower, ozonesondes and a tethered balloon in the UGRB, WY. The 73-meter tall tower was located just off Highway 191 north approximately 20 kilometers south of the junction with Highway 351. Temperature measurements were taken hourly on the tall tower from four levels: 3, 25, 50 and 73 meters. Figure 5-6 depicts early morning (5 AM LST) vertical temperature plots for several elevated ozone events taken from the tall tower in February and March. The ozonesondes were released near the Boulder site in the UGRB 3-4 times per day during elevated ozone events and were equipped with pressure, temperature and humidity sensors. Figure5- 7 depicts morning (8 AM LST) sounding plots for elevated ozone events in March. Temperature and humidity measurements were also taken on a tethered balloon, located near the mobile trailer, from four levels: 4, 33, 67 and 100 meters during daytime hours of elevated ozone events. Figure 5-8 depicts afternoon (12 PM LST) vertical temperature plots during elevated ozone levels from the tethered balloon in the month of March. In both months, WRF predicts the magnitude and height of the inversion reasonably well.

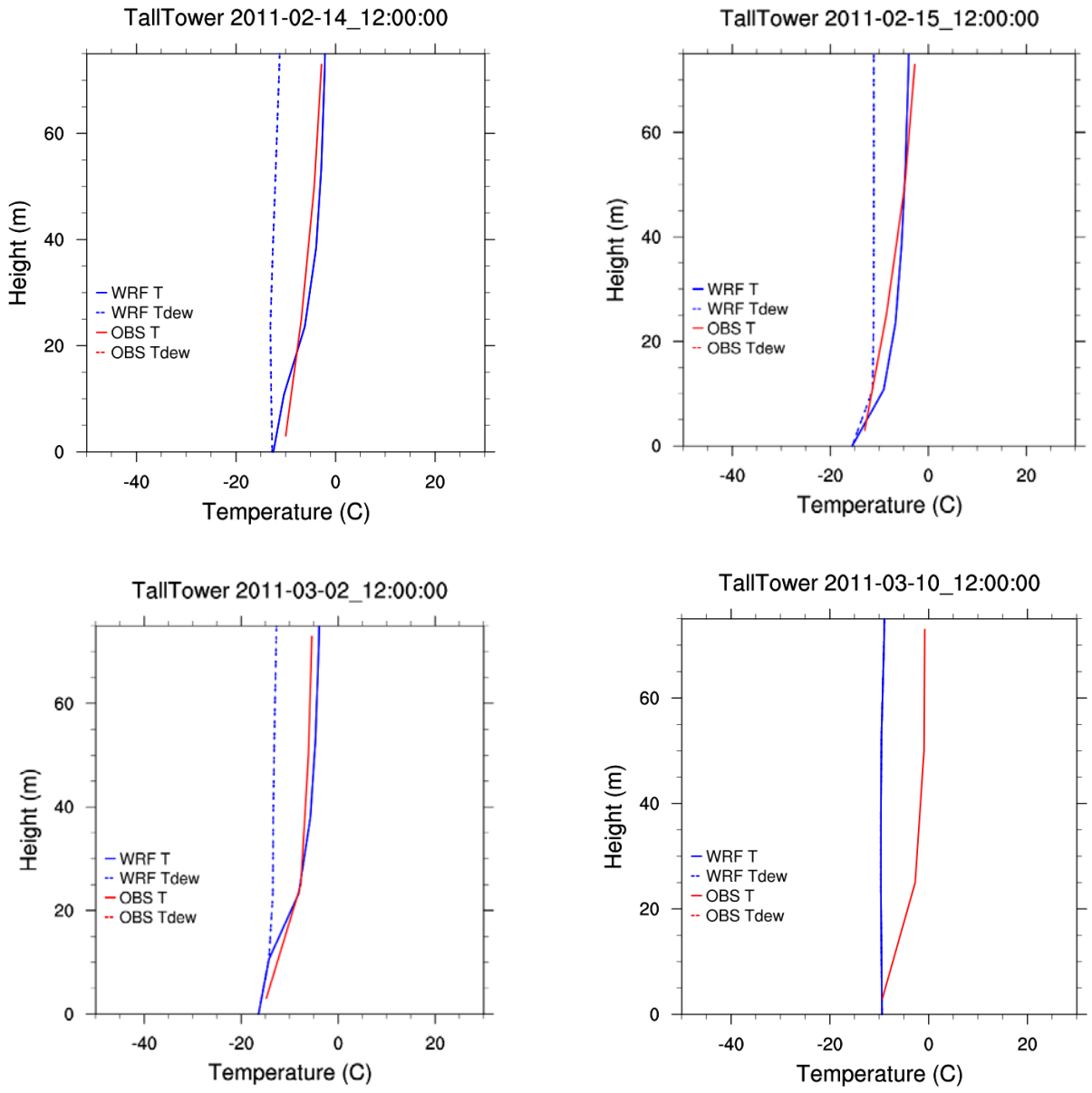

Figure 5-6. Vertical profiles of temperature taken from the tall tower in the UGRB, WY (42.42°N, 109.56°W) at 5am LST on February 14th(top left), February 15th(top right), March 2nd(lower left) and March 10th(lower right).

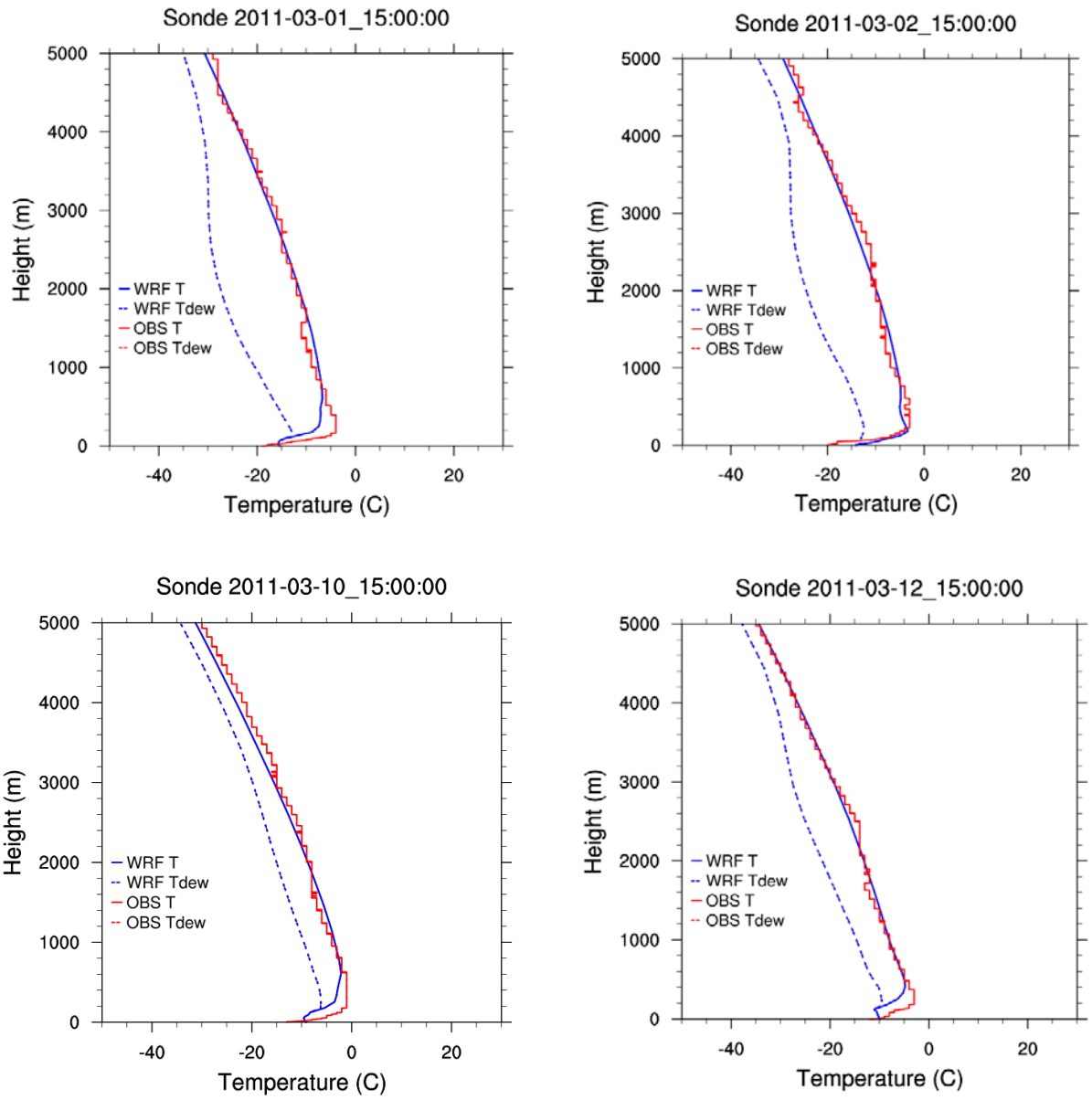

Figure 5-7. Vertical sounding profiles of temperature taken from ozonesondes in the UGRB, WY (42.72°N, 109.75°W) at 8am LST on March 1st(top left), 2nd(top right), 10th(lower left) and 12th(lower right).

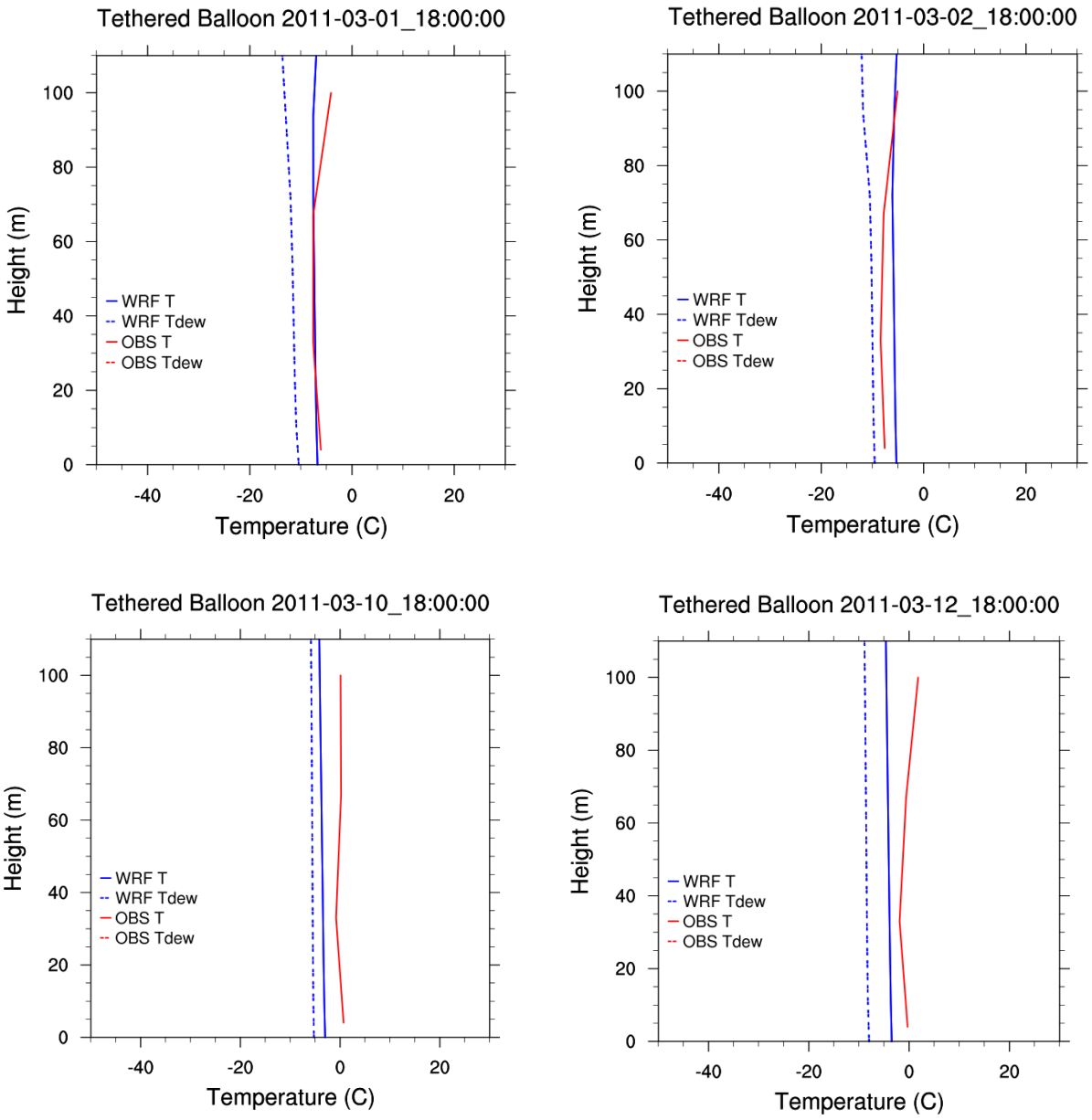

Figure 5-8. Vertical profiles of temperature taken from a tethered balloon in the UGRB, WY (42.68°N, 109.80°W) at 12PM LST on March 1st(top left), 2nd(top right), 10th(lower left) and 12th(lower right).

APPENDIX A

WRF 2011 12 km WESTUS Model Performance Evaluation Statistics by State

Additional Displays can be found at:
ftp://viking.cira.colostate.edu/3SDW/3SAQS/2011/Base11a/plots/MET/

Bias | MAE	Winter	Spring	Summer	Fall	Annual
12km Domain	0.1 | 0.5	0.0 | 0.8	-0.7 | 1.4	-0.3 | 0.9	-0.2 | 0.9
CO	0.4 | 0.5	0.2 | 0.7	-0.6 | 1.4	-0.1 | 0.7	0.0 | 0.8
WY	0.3 | 0.4	0.2 | 0.6	-0.5 | 1.3	0.1 | 0.6	0.0 | 0.7
UT	0.4 | 0.5	-0.1 | 0.7	-0.8 | 1.3	-0.3 | 0.7	-0.2 | 0.8
WA	0.0 | 0.4	0.0 | 0.5	-0.1 | 0.8	-0.4 | 0.7	-0.1 | 0.6
OR	0.0 | 0.5	0.1 | 0.5	0.2 | 0.9	-0.3 | 0.8	0.0 | 0.7
CA	-0.4 | 0.9	-0.3 | 0.9	-0.9 | 1.4	-0.9 | 1.3	-0.6 | 1.1
NV	0.2 | 0.5	0.0 | 0.6	-0.1 | 0.9	-0.1 | 0.6	0.0 | 0.7
ID	0.2 | 0.4	0.0 | 0.6	-0.4 | 1.1	-0.5 | 0.8	-0.2 | 0.7
AZ	0.1 | 0.6	0.0 | 0.6	-0.5 | 1.3	-0.3 | 0.9	-0.2 | 0.8
MT	0.3 | 0.4	0.2 | 0.6	-0.1 | 1.1	0.1 | 0.6	0.1 | 0.6
NM	0.3 | 0.5	0.2 | 0.6	-0.8 | 1.3	-0.3 | 0.8	-0.1 | 0.8
ND	0.2 | 0.3	0.1 | 0.5	-0.5 | 1.2	-0.1 | 0.6	-0.1 | 0.6
SD	0.2 | 0.3	0.2 | 0.6	-0.7 | 1.6	0.0 | 0.6	-0.1 | 0.8
NE	0.3 | 0.4	0.0 | 0.6	-1.0 | 1.8	-0.2 | 0.7	-0.2 | 0.9
KS	0.2 | 0.4	0.1 | 0.8	-1.6 | 2.1	-0.3 | 0.7	-0.4 | 1.0
OK	0.1 | 0.5	-0.3 | 1.0	-2.0 | 2.3	-0.5 | 0.9	-0.7 | 1.1
TX	0.0 | 0.6	-0.3 | 1.1	-1.0 | 1.6	-0.2 | 1.0	-0.4 | 1.1

Table A-5-1 Mixing ratio (kg/kg) bias and mean absolute error over the 12-km domain and individual states for 2011.

Bias | MAE	Winter	Spring	Summer	Fall	Annual
12km Domain	-0.4 | 2.1	-0.3 | 1.9	0.0 | 1.9	-0.2 | 1.8	-0.2 | 1.9
CO	-0.5 | 2.9	-0.4 | 2.5	-0.1 | 2.3	-0.5 | 2.2	-0.4 | 2.5
WY	-0.9 | 3.0	-0.4 | 2.2	0.9 | 2.0	-0.3 | 2.2	-0.2 | 2.3
UT	0.3 | 2.5	-0.6 | 2.0	0.1 | 1.9	0.2 | 1.9	0.0 | 2.1
WA	-0.4 | 1.8	-0.3 | 1.7	-0.8 | 2.0	-0.5 | 1.9	-0.5 | 1.8
OR	-0.1 | 2.1	-0.3 | 1.9	-1.0 | 2.3	-0.5 | 2.2	-0.5 | 2.1
CA	0.0 | 1.9	-0.4 | 1.7	-0.2 | 2.0	0.1 | 1.9	-0.1 | 1.9
NV	-1.3 | 2.7	-1.4 | 2.4	-1.2 | 2.3	-0.8 | 2.3	-1.2 | 2.4
ID	-0.9 | 2.5	-0.5 | 2.2	-0.6 | 2.4	-0.8 | 2.4	-0.7 | 2.4
AZ	-0.6 | 2.1	-1.0 | 2.1	-0.2 | 2.0	-0.5 | 2.0	-0.6 | 2.1
MT	-1.2 | 2.9	-0.5 | 2.1	0.5 | 2.0	-0.4 | 2.4	-0.4 | 2.3
NM	-0.6 | 2.4	-0.8 | 2.1	0.1 | 2.0	-0.1 | 1.8	-0.3 | 2.1
ND	-0.7 | 2.2	0.0 | 1.8	0.7 | 1.8	0.1 | 1.8	0.0 | 1.9
SD	-0.5 | 2.4	0.4 | 1.9	1.0 | 2.1	0.0 | 1.9	0.3 | 2.1
NE	-0.6 | 2.4	0.2 | 2.0	0.8 | 2.0	0.0 | 1.8	0.1 | 2.0
KS	-0.7 | 2.1	0.3 | 2.1	0.9 | 2.0	-0.2 | 1.6	0.1 | 1.9
OK	-0.3 | 2.0	0.4 | 2.0	1.0 | 1.9	0.3 | 1.5	0.3 | 1.9
TX	0.0 | 1.7	-0.3 | 1.9	0.2 | 1.5	-0.1 | 1.6	0.0 | 1.7

Table A-5-2. Temperature (K) bias and mean absolute error over the 12-km domain and individual states for 2011.

Bias | MAE	Winter	Spring	Summer	Fall	Annual
12km Domain	-0.6 | 1.3	-0.6 | 1.4	-0.6 | 1.3	-0.6 | 1.3	-0.6 | 1.3
CO	-0.8 | 1.5	-1.2 | 1.8	-1.2 | 1.7	-0.9 | 1.5	-1.0 | 1.6
WY	-0.7 | 1.8	-1.0 | 1.8	-0.9 | 1.6	-0.8 | 1.7	-0.8 | 1.7
UT	0.1 | 1.5	-0.4 | 1.6	-0.4 | 1.4	-0.3 | 1.3	-0.3 | 1.5
WA	-0.5 | 1.3	-0.5 | 1.3	-0.6 | 1.2	-0.5 | 1.2	-0.5 | 1.2
OR	-0.8 | 1.4	-0.7 | 1.4	-0.7 | 1.2	-0.7 | 1.3	-0.7 | 1.3
CA	-0.4 | 1.3	-0.6 | 1.4	-0.5 | 1.2	-0.5 | 1.2	-0.5 | 1.2
NV	-0.5 | 1.4	-0.3 | 1.6	-0.5 | 1.4	-0.4 | 1.4	-0.4 | 1.4
ID	-0.8 | 1.5	-0.9 | 1.6	-0.6 | 1.3	-0.6 | 1.3	-0.7 | 1.4
AZ	-0.4 | 1.4	-0.4 | 1.5	-0.6 | 1.4	-0.6 | 1.3	-0.5 | 1.4
MT	-1.1 | 1.8	-1.0 | 1.7	-1.0 | 1.5	-0.9 | 1.5	-1.0 | 1.6
NM	-0.8 | 1.5	-1.1 | 1.7	-1.1 | 1.6	-0.9 | 1.4	-1.0 | 1.6
ND	-0.8 | 1.4	-0.8 | 1.4	-0.6 | 1.2	-0.6 | 1.2	-0.7 | 1.3
SD	-0.7 | 1.5	-0.8 | 1.5	-0.6 | 1.3	-0.6 | 1.3	-0.7 | 1.4
NE	-0.6 | 1.3	-0.8 | 1.4	-0.6 | 1.3	-0.7 | 1.3	-0.7 | 1.3
KS	-0.6 | 1.2	-0.7 | 1.4	-0.5 | 1.2	-0.7 | 1.2	-0.6 | 1.3
OK	-0.9 | 1.4	-1.0 | 1.6	-0.8 | 1.4	-0.8 | 1.4	-0.9 | 1.4
TX	-0.6 | 1.2	-0.7 | 1.4	-0.5 | 1.2	-0.6 | 1.2	-0.6 | 1.3

Table A-5-3. Wind speed (m/s) bias and mean absolute error over the 12-km domain and individual states for 2011.